Kainate receptor auxiliary subunits NETO1 and NETO2 in anxiety and fear-related behaviors

Marie Mennesson

Molecular and Integrative Biosciences research program

Faculty of Biological and Environmental Sciences

University of Helsinki

———

Doctoral School in Health Sciences

Doctoral Program Brain and Mind

ACADEMIC DISSERTATION

To be presented for public examination, with permission of the Faculty of Biological and Environmental Sciences of the University of Helsinki in lecture room 1041, Biocenter 2, on the 28th of June 2019 at 12 noon.

Supervisor	Professor Iiris Hovatta University of Helsinki (Finland)
Thesis Committee members	Docent Sari Lauri University of Helsinki (Finland)
	Professor Anna-Elina Lehesjoki University of Helsinki (Finland)
	Professor Juha Voipio University of Helsinki (Finland)
Pre-examiners	Professor Heikki Tanila University of Eastern Finland (Finland)
	Professor Sulev Koks Murdoch University, Perth (Australia)
Opponent	Privatdozent Carsten Wotjak Max Planck Institute, Munich (Germany)
Custos	Professor Juha Partanen University of Helsinki (Finland)

The Faculty of Biological and Environmental Sciences, University of Helsinki, uses the Urkund system (plagiarism recognition) to examine all doctoral dissertations.

ISSN: 2342-3161 (paperback) and 2342-317X (PDF, http://ethesis.helsinki.fi)

ISBN: 978-951-51-5308-1 (paperback) and 978-951-51-5309-8 (PDF, http://ethesis.helsinki.fi)

Printing house: Unigrafia Oy

Printing location: Helsinki, Finland

Printed on: 06.2019

Cover artwork adapted from a picture by: Alina Grubnyak on Unsplash

Table of contents

Original publications

This thesis is based on the following article and manuscript, referred to in the text by their Roman numerals (**I** and **II**). In both publications, the author had a major role in planning and performing the experiments, as well as in the writing of the manuscripts. Additionally, this thesis contains unpublished data. Publication I is reprinted by permission from Springer Nature.

I. **Marie Mennesson,** Emilie Rydgren, Tatiana Lipina, Ewa Sokolowska, Natalia Kulesskaya, Francesca Morello, Evgueni Ivakine, Vootele Voikar, Victoria Risbrough, Juha Partanen, and Iiris Hovatta. *Kainate receptor auxiliary subunit NETO2 is required for normal fear expression and extinction*, 2019, Neuropsychopharmacology, [epub ahead of print].

II. **Marie Mennesson,** Ester Orav, Adrien Gigliotta, Natalia Kuleskaya, Suvi Saarnio, Anna Kirjavainen, Sebnem Kesaf, Frederike Winkel, Maria Llach-Pou, Juzoh Umemori, Vootele Voikar, Victoria Risbrough, Juha Partanen, Eero Castrén, Sari Lauri and Iiris Hovatta. *NETO2 in cued fear conditioning and amygdala maturity and excitability* (manuscript).

Abstract

Anxiety disorders are the most prevalent mental illnesses in Europe, yet, their molecular basis is poorly understood. Unraveling the molecular mechanisms underlying the occurrence and maintenance of anxiety is crucial for effective drug development to treat anxiety disorders. In this thesis work, I focused on the NETO1 and NETO2 auxiliary proteins for kainate receptors (KARs) that tightly modulate the functional properties of the receptor. Because variants in KAR genes have been associated with psychiatric diseases in humans, and with anxiety-like behavior in mice, we hypothesized that NETO1 and NETO2 regulate anxiety through their modulation of KARs. Therefore, the aim of this thesis was to investigate the role of NETO1 and NETO2 in the regulation of anxiety and fear, and to evaluate their potential as novel treatment targets for anxiety disorders.

To test our hypothesis, I first carried out a comprehensive behavioral screen of *Neto1*$^{+/+}$, *Neto1*$^{-/-}$, *Neto2*$^{+/+}$ and *Neto2*$^{-/-}$ mouse anxiety-like and fear-related behaviors. We showed that neither NETO1 nor NETO2 regulated anxiety-like behavior in mice. However, *Neto2*$^{-/-}$ mice had reduced activity in novel environments without effect on locomotor activity in familiar environments, stress physiology or depression-like behaviors. In cued fear conditioning, *Neto2*$^{-/-}$ but not *Neto1*$^{-/-}$ mice had increased fear expression and delayed extinction. To establish the molecular and cellular mechanisms modulating the fear phenotype of the *Neto2*$^{-/-}$ mice, I investigated its expression pattern by in situ hybridization in the core fear network, composed of the medial prefrontal cortex, the amygdala and the hippocampus. *Neto2* was widely expressed in all of these regions and in both excitatory and inhibitory neurons. Accordingly, the NETO2 protein was detectable in the same regions. We next established that in the synapses of these brain regions, the abundance of GLUK2/3 and GLUK5 KAR subunits was reduced 20–40% in the absence of NETO2. By focusing on the amygdala, the central brain region for the processing of fear-inducing stimuli and fear learning, we observed immature features of parvalbumin-expressing inhibitory neurons in *Neto2*$^{-/-}$ mice. Furthermore, we found a higher amplitude and frequency of miniature excitatory post-synaptic currents specifically in the basolateral amygdala, which is a critical brain region for fear memory consolidation. Concurrent with these results, dendritic spine density in thin dendrites was higher in *Neto2*$^{-/-}$ compared to *Neto2*$^{+/+}$ mice. Taken together, these findings imply stronger glutamatergic synapses within the amygdala in the absence of NETO2. Finally, using the c-Fos immediate early gene as a marker for neuronal activation, we found increased activation of amygdala neurons in *Neto2*$^{-/-}$ compared to *Neto2*$^{+/+}$ mice after fear acquisition. Higher activation of the amygdala

may be related to stronger associative learning and be represented behaviorally by higher levels of fear expression during fear conditioning.

To summarize, we showed that in the absence of NETO2, mice demonstrate higher conditioned fear expression and extinction delay suggestive of a higher overall conditionability, which is a symptom of posttraumatic stress disorder (PTSD). Furthermore, we established that neither *Neto1* nor *Neto2* is required for innate anxiety-like behaviors. We propose that the reduced KAR abundance at the synapses of *Neto2*$^{-/-}$ mice, together with the immaturity and increased excitability of the amygdala, and with the stronger activation of local circuits within the amygdala during fear acquisition underlie the higher conditionability and delayed fear extinction phenotype. Our findings suggest directions for future mechanistic studies on the role of NETO2 in fear conditionability. Taken together, this work showed for the first time that *Neto2* is required for normal fear expression and conditioning, and that it modulates amygdala function during associative fear learning, findings with putative therapeutic significance for PTSD.

Abbreviations

Amg	amygdala
AMPAR	α-amino-3-hydroxy-5-methyl-4-isoxazolepropionic acid receptor
ASR	acoustic startle reflex
BLA	basolateral amygdala
CB1	cannabinoid receptor 1
CCK	cholecystokinin
CE	central nucleus of the amygdala
Ceb	cerebellum
Cg1	cingulate cortex 1
CNS	central nervous system
CORT	corticosterone
CS	conditioned stimuli
CUB	complement C1r/C1s, Uegf, Bmp1
DG	dentate gyrus
DOR	displaced object recognition
DSM	the Diagnostic and Statistical Manual of Mental Disorders
EPM	elevated-plus maze
EPSC	excitatory post-synaptic current
EZM	elevated-zero maze
FC	fear conditioning
FST	forced swim test
GABA	γ-aminobutyric acid
GAD	generalized anxiety disorder
GRIP	glutamate receptor interacting protein
HET	heterozygote
Hpc	hippocampus
iGluR	ionotropic glutamate receptor
IHC	immunohistochemistry
IL	infralimbic cortex
IPSC	inhibitory post-synaptic current
ISH	in situ hybridization
ITC	intercalated cell mass
KAR	kainate receptor
KCC2	K-Cl co-transporter 2
KO	knockout
LA	lateral amygdala
LD	light/dark box
LDLa	low-density lipoprotein class a

LTP	long-term potentiation
MB	marble burying
mEPSC	miniature excitatory post-synaptic current
mPFC	medial prefrontal cortex
MWM	Morris water maze
NETO	neuropilin and tolloid-like
NMDAR	N-methyl-D-aspartate receptor
NOR	novel object recognition
NSF	novelty-suppressed feeding
OCD	obsessive-compulsive disorder
OF	open field
OTX2	orthodenticle homeobox 2
PAG	periaqueductal grey
PB	parabrachial nucleus
PKC-δ	protein kinase C delta
PL	prelimbic cortex
PNN	perineuronal net
PSD	post-synaptic density
PSD-95	post-synaptic density protein 95 kDa
PTSD	post-traumatic stress disorder
PV	parvalbumin
RAZ	risk assessment zone
RT-qPCR	reverse transcriptase quantitative polymerase chain reaction
SD	standard deviation
SEM	standard error of the mean
siRNA	silencing RNA
SNRI	serotonin and norepinephrine reuptake inhibitors
SSRI	selective serotonin reuptake inhibitor
SYP	synaptophysin
TH	thalamus
US	unconditioned stimuli
WB	western blot
WT	wild type

Review of the literature

1. Anxiety and fear

1.1. Human anxiety and fear

Anxiety and fear are both normal responses to threatening situations and are distinguished depending on the imminence of the threat. Anxiety corresponds to the ensemble of responses to potential threats that might occur in the future, in the absence of immediate danger. In opposition, fear is produced in reaction to real and imminent threats. In humans, an excess of either can be responsible for the appearance of psychiatric disorders such as anxiety disorders, obsessive-compulsive spectrum disorders or trauma- and stressor-related disorders (the Diagnostic and Statistical Manual of Mental Disorders-V or DSM-V from the American Psychiatric Association, Table 1). These three disorder classes were previously grouped as one (i.e., anxiety disorders from the DSM-IV) and were the most common psychiatric disorders in Europe in 2010 with a prevalence of 14% [205]. In 1990, the economic burden of anxiety disorders to the American society was estimated at approximately US$ 46 billion [159].

Although anxiety disorders share common features such as subjective reports of tension or chronic excess of worry together with physiological somatic symptoms including elevated heart rate or blood pressure [67, 28], they are further identifiable based on their specific symptoms. For instance, the main symptom of panic disorder is panic attack, while social anxiety disorder (SAD or social phobia) is defined by unreasonable anxiety caused by public situations and obsessive-compulsive disorder (OCD) patients demonstrate stereotyped behaviors in order to cope with their obsession [67]. Depending on the origin of the excessive fear, phobias are categorized into social phobia, agoraphobia and specific phobias, including fear of heights (acrophobia), fear of confined spaces (claustrophobia) or fear of certain animals/insects [49]. Post-traumatic stress disorder (PTSD) is a trauma-related disorder commonly observed after experiencing a life-threatening situation, which was affecting approximately 3% of the European population in 2010 [205]. The disorder's main symptom originates from a persistent memory of the frightening event through flashback or nightmare, often triggered by salient and irrelevant cues from the environment [67]. Furthermore, it has been widely established that the sensory, cognitive and autonomic responses vary between PTSD patients and control individuals, including higher conditionability leading to enhanced reaction to trauma reminders and difficulties to extinguish fear caused by the traumatic event [144].

Because anxiety disorders are often co-morbid with other mood disorders or drug abuse, their diagnosis can be challenging. Nevertheless, the main issue in the field results from the lack of performant and specific drug treatment. Since their discovery in the 1950s, benzodiazepines have been widely used to treat anxiety disorders [67]. However, these drugs are responsible for numerous side effects associated with dependence and tolerance. Over the past 50 years, non-benzodiazepine compounds which do not cause dependence or tolerance have emerged, including the anti-depressant selective serotonin reuptake inhibitors (SSRIs) and serotonin and norepinephrine reuptake inhibitors (SNRIs), and are used to treat anxiety disorders [80]. The main caveat of these medications derives from their lack of efficacy on certain patients. Thus, there is a need for the discovery of new compounds to treat these diseases, and unraveling the mechanisms by which these disorders appear is therefore crucial. Although finding new effective medication is critical for the field, recent findings show that only a proper combination of personalized psychotherapy and drug treatment successfully treat anxiety disorders in the long-term [13, 188]. Notably, since the 1960s, therapy using prolonged and chronic exposure to stimuli considered as fear-inducing or with high emotional valence, referred to as exposure therapy, has greatly improved the treatment of anxiety and fear-related disorders such as OCD and PTSD [61].

Table1. Description of the previous human anxiety disorders class from the DSM-IV split into three new classes in the DSM-V.

DSM-V classes	*Disorders*
Anxiety disorders	Separation anxiety disorder, selective mutism, phobia, panic disorder and generalized anxiety disorder (GAD)
Obsessive-compulsive spectrum disorders	Obsessive-compulsive disorder (OCD), body dysmorphic disorder, hoarding disorder, trichotillomania and excoriation disorder
Trauma- and stressor-related disorders	Reactive attachment disorder, disinhibited social engagement disorder, post-traumatic stress disorder (PTSD), acute stress disorder and adjustment disorders

DSM = the Diagnostic and Statistical Manual of Mental Disorders, GAD = generalized anxiety disorder, OCD = obsessive compulsive disorder, PTSD = post-traumatic stress disorder.

1.2. Mouse models of anxiety and fear

Studying anxiety and fear-related disorders in humans has led to great advances in their symptomatology, diagnoses and treatments. However, investigating the precise molecular mechanisms involved in fear and anxiety regulation is not always feasible in humans. Thus, modeling anxiety and fear-related disorders is crucial for a better understanding of their etiology and discovery of new drug compounds. To control for genetic heterogeneity and environmental factors, inbred mice are commonly used as models. Mice present many advantages for the study of human diseases since 80% of their genes are orthologues to human genes (i.e., homology between species) [134]. Moreover, based on similarities between human and mouse brain anatomy and physiology, a multitude of valuable tools, such as transgenic mice, pharmacological injection, brain lesions and inactivation, can be used in mice to assess the role of specific genes, molecules or brain regions related to human diseases [138]. However, the investigation of human psychiatric disorders using mice models represents a challenge since their diagnosis is mostly based on subjective report rather than the presence of biological marker(s). Therefore, the study of psychiatric disorders such as anxiety and fear-related disorders in mice is based on the observation of physiological and behavioral reactions in response to certain stimuli.

1.2.1. *Anxiety-like behaviors*

The word "anxiety" most often refers to its subjective feeling [110, 116]. However, it is also used to define the physiological and behavioral responses from an organism in uncertain situations, referred to as "state" anxiety as opposed to the pathological "trait" anxiety [28]. To adequately model anxiety disorders, the phenotype observed during anxiety-like behavior tests must be representative of the behavioral and physiological anxiety response in humans (face validity), sensitive to anxiolytic drugs used to treat human anxiety disorders (predictive validity) and processed from comparable neurobiological mechanisms as anxiety in humans (construct validity).

Since subjective feelings cannot be assessed in animals, the majority of tests investigating anxiety are based on approach conflict to explore novel environments and avoidance of open, exposed or bright areas that represent a risk for mice. These approach–avoidance assays comprise the elevated-plus or elevated-zero maze (EPM or EZM), the open field (OF) and the light/dark box (LD) tests (Figure 1, Table 2) [59, 28]. These tests have high face and predictive validity since avoidance of situations representing a potential danger is a component of human anxiety disorders and because they are sensitive to anxiolytic drugs, mostly to benzodiazepines [22]. In the EPM or EZM, an anxious mouse will preferably remain in the areas enclosed with walls and avoid the open arms/areas of the maze (Figure 1, Table 2) [72, 151,

175]. In the OF, anxious animals stay in the peripheral zone and avoid crossing the central part [70], while in the LD they will tend to spend more time in the dark compartment than the bright part of the apparatus (Figure 1, Table 2) [39, 7]. Because these tests are based on passive exploration behaviors, defects in locomotor activity can confound the analysis and need to be assessed in a familiar environment [28].

In the absence of motor deficits, increased activity due to novelty seeking is a major drawback of these approach–avoidance assays [28]. Thus, active avoidance behaviors such as the burying of marbles introduced in a familiar environment, representative of an uncertain source of harm, can be assessed in the marble burying test (MB) (Figure 1, Table 2) [192, 140]. Commonly used to study obsessive and repetitive behaviors such as those observed in OCD, this burying behavior is sensitive to anxiolytics [192, 140, 187]. However, because it might mostly represent natural digging behavior in mice, the use of this test to model human anxiety-related disorders is controversial [189]. Hyponeophagia or the novelty-suppressed feeding test (NSF) also offer an alternative to assess anxiety-like behaviors without the passive exploration caveat. NSF is based on the motivation of a food-deprived mouse to feed in a novel environment, depicted by a longer latency to reach for food in anxious mice, and is sensitive to both benzodiazepines and SSRIs (Figure 1, Table 2) [129, 47]. Because stress represents the basis of somatic responses observed in anxiety disorders such as increased heart rate or higher blood pressure, tests measuring stress physiology can be assessed complementarily to anxiety-like behaviors tests. They usually comprise vital sign measurements (e.g., heart rate, respiration), concentration of circulating stress hormones (corticosterone or CORT) and stress-induced hyperthermia (SIH) test [28, 137].

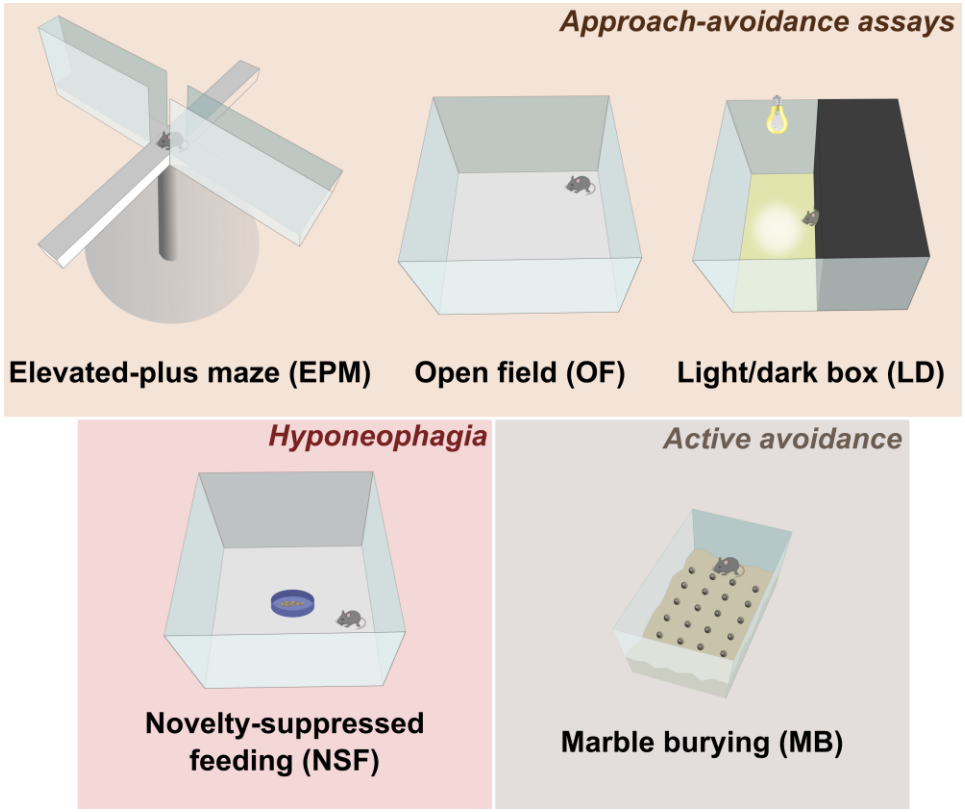

Figure 1. Schematic of anxiety-like behavioral tests generally used to model human anxiety disorders. EPM = elevated-plus maze, LD = light/dark box, MB = marble burying, NSF = novelty-suppressed feeding, OF = open field.

1.2.2. *Fear responses in mice*

Due to its relevance for the survival of a species, fear is a highly conserved emotion and its neurobiological features are comparable between mice and humans [113, 191]. As for anxiety, the word "fear" is defined as the subjective feeling of being afraid [110, 116], but is also used in reference to the ensemble of defensive responses elicited in threatening situations. Fear responses can be triggered by unconditioned stimuli (US) that innately represent a danger such as the presence of predators, pain stimuli or aggressive behaviors [68, 178], and is referred to as innate fear [19]. However, when co-occurring with a US, neutral stimuli such as a smell, a sound or a specific context can elicit defensive behaviors (conditioned stimuli or CS), defined therefore as learned or conditioned fear [53, 56, 112, 202, 55].

Because both innate and acquired fear can be affected in anxiety disorders [130, 120, 20, 121], they are commonly investigated in mouse models of anxiety (Table 2). Innate fear can be assessed by measuring the whole body startle reaction to unexpected loud acoustic stimuli in the acoustic startle reflex test (ASR), and acquired fear is traditionally studied through the fear conditioning (FC) paradigm (Figure 2)

[28]. FC is based on Pavlovian classical conditioning principles [150] where a fear-inducing event such as a footshock (US) is associated with a neutral cue (CS), usually a sound, which then becomes a predictor of the threatening event (Figure 2). In mice, defensive responses during FC are quantified by the duration of freezing behaviors represented by a total absence of movement, except breathing. Freezing is a fear-related behavior observed in many species [112] which occurs innately when an animal is confronted with predators, pain stimuli or simply bright environments and appears instantly after a footshock presentation in rodents [91, 111]. The different components of classical FC are usually assessed as described in Figure 2, referred to as cued FC [191]. However, several alternative protocols have been described [60], including contextual FC, wherein the conditioning context is the only predictor of the US onset [56].

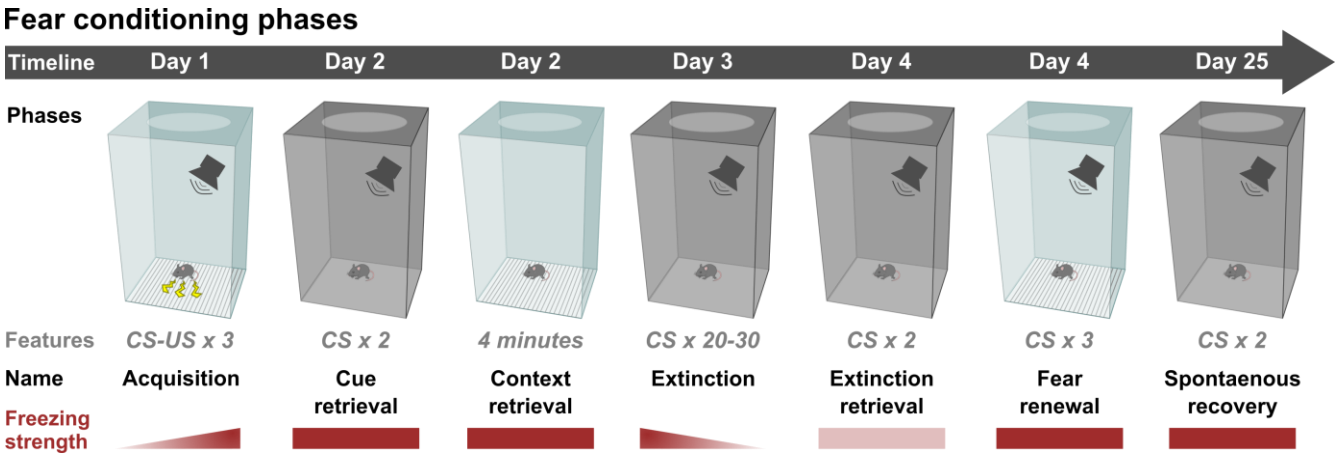

Figure 2. Description of the classical or cued fear conditioning (FC) protocol and its different phases. Fear strength is represented by a color gradient between dark red for high fear level and light red for low fear level. At **Acquisition** = the animal receives a footshock three times (unconditioned stimulus or US) co-terminated with a sound (conditioned stimulus or CS) in the conditioning chamber (context A, transparent wall, footshock grid). **Cue retrieval** = CS presented in a new context elicits fear in the absence of the US (context B, black wall, hidden footshock grid). **Context retrieval** = exposure to context A where the fear-inducing event occurred causes fear expression when presented without any CS. **Extinction** = presenting the CS several times without any footshock causes a decrease in CS-elicited fear expression. **Extinction retrieval** = CS presentation after extinction elicits lower fear expression than during cue retrieval. **Fear renewal** = CS presented in the conditioning chamber where the CS–US association took place still elicits fear (Context A). **Spontaneous recovery** = CS-elicited fear re-appears a few days or weeks after extinction. CS = conditioned stimulus, US = unconditioned stimulus.

Table 2. Behavioral tests used for the modeling of human anxiety and fear-related disorders and their corresponding phenotype in mice. In all these behavioral tests, differences from a control group are used to define the anxiety-like or fear-related phenotype of a tested group.

Test	*Phenotype corresponding to increased anxiety-like behavior*
Elevated-plus or elevated-zero maze (EPM / EZM)	Decreased time or reduced number of entries in the open arms (EPM) or areas (EZM) Increased latency to enter the open arms (EPM) or areas (EZM)
Open field (OF)	Decreased time or reduced number of entries in the center zone Increased latency to enter the center zone
Light/dark box (LD)	Decreased time or reduced number of entries in the light compartment Increased latency to enter the light compartment
Novelty-suppressed feeding (NSF)	Increased latency to reach the food in a novel environment
Marble burying (MB)	Increased number of buried marbles
Fear conditioning (FC)	Increased fear expression and memory retention (i.e., increased conditionability) Impaired extinction

EPM = elevated-plus maze, EZM = elevated-zero maze, FC = fear conditioning, LD = light dark box, MB = marble burying, NSF = novelty-suppressed feeding.

2. Brain network underlying anxiety and fear in mice

Over the past century, the use of lesion and inactivation studies led to the identification of key brain regions involved in anxiety and fear regulation including the amygdala (Amg), medial prefrontal cortex (mPFC) and hippocampus (Hpc) (Figure 3) [66]. However, because they affect the function of a whole brain region, these techniques lack specificity. Recently, the emergence of precise methods based on the manipulation of selected neuronal populations, through their projection targets or via expression of channel rhodopsin in optogenetics, have allowed for the investigation of the network underlying anxiety and fear at the circuit level. These methods have led to the establishment of specific circuits involved in the detection, integration and reaction to an immediate danger [178] and the encoding of fear-inducing

events [89, 208] or simply the maintenance of anxiety levels in the absence of immediate threats [194, 199]. Therefore, although regulation of anxiety and fear have common features, they depend on different brain circuits originating from overlapping brain regions.

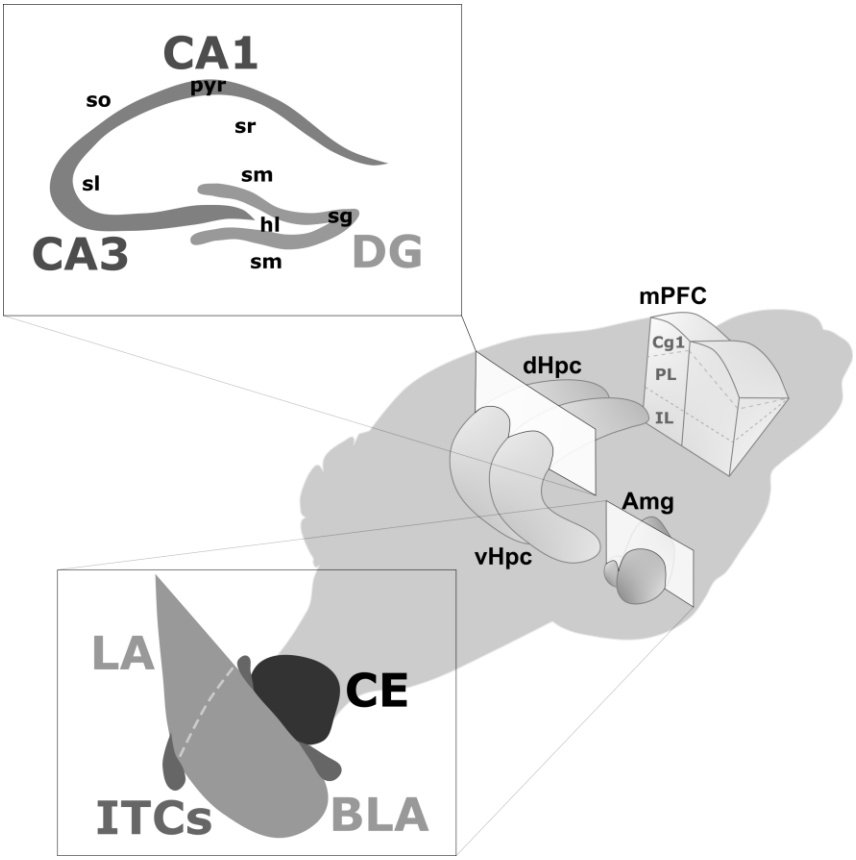

Figure 3. Anxiety and fear key brain regions and their corresponding sub-regions. The medial prefrontal cortex (mPFC) is subdivided in cingulate1 (Cg1), prelimbic (PL) and infralimbic (IL) cortices. The amygdala (Amg) is composed of three main subnuclei: the lateral (LA), basolateral (BLA) and central (CE) nucleus; but also contain intercalated cell masses (ITCs) along the LA/BLA. The hippocampus (Hpc) is divided into dorsal and ventral Hpc (dHpc and vHpc) and is composed of the cornu ammonis area 1 and 3 (CA1 and CA3), and dentate gyrus (DG) subregions further organized in stratum (outer to inner): stratum oriens (so), stratum pyramidal (pyr, only in CA1 and CA3), stratum granulosum (sg, only in DG), stratum radiatum (sr), stratum molecular (sm, only in CA1 and DG), stratum lucidum (sl, only in CA3) and hilus (hl, only in DG). BLA = basolateral amygdala, CA1 = cornu ammonis area 1, CA3 = cornu ammonis area 3, CE = central amygdala, Cg1 = cingulate cortex1, DG = dentate gyrus, dHpc = dorsal hippocampus, hl = hilus, IL = infralimbic cortex, ITCs = intercalated cell masses, LA = lateral amygdala, mPFC = medial prefrontal cortex, pyr = stratum pyramidal, sg = stratum granulosum, sl = stratum lucidum, sm = stratum molecular, so = stratum oriens, sr = stratum radiatum, vHpc = ventral hippocampus.

2.1. Neuronal circuit of anxiety

The emergence of advanced approaches to manipulate neuronal projections such as optogenetics has allowed for studying the circuits involved in the regulation of "state" anxiety more precisely (Figure 4) [28, 191]. The Amg is known to play a central role in the etiology of human anxiety [52] and to contain three main subnuclei: the lateral (LA), basolateral (BLA) and central (CE) amygdala. These subnuclei receive direct projections from the sensory cortices and the thalamus (TH), the central relay region for the sensory pathways [145, 193, 46], and have all been linked to the modulation of anxiety in animal models [194, 199, 27, 62]. In the LA, increased phasic neuronal activity was found in rats expressing generalized fear, a symptom of anxiety disorders [62]. The photoactivation of BLA neurons produces increased innate anxiety [194], and their tonic activation was associated with anxiety-like behavior in EPM and OF tests [199]. Strikingly, the precise activation of glutamatergic neuronal populations from the BLA projecting locally to the CE is responsible for effects comparable to anxiolytic drugs [194]. The CE is the output nucleus of the Amg which connects to the periaqueductal gray (PAG), the main brainstem region for defensive responses. Direct activation of a specific class of inhibitory neurons that express protein kinase C-delta (PKC-δ) from the lateral CE (CEl) produces anxiolytic effects in NSF, EPM, OF and LD tests [27]. Furthermore, BLA projections to the bed nucleus of the stria terminalis (BNST), also called the extended Amg, have been implicated in the regulation of innate anxiety [33, 103]. Inhibition of inputs from the BLA to the anterodorsal BNST increased anxiety-like behaviors [103], while inhibiting projections to the ventrolateral BNST reduced freezing during unpredictable stress and social interactions [33]. The downstream pathways from BNST are believed to be the ventral tegmental area (VTA), hypothalamus (HT) and parabrachial nucleus (PB), known to respectively regulate positive *vs* negative valence, risk avoidance and respiration rate [87, 103]. Recently, LeDoux and Pine (2016), suggested that BNST acts as the relay nucleus in terms of processing uncertain threats in the brain circuit of anxiety [116]. Furthermore, the activation of projections from the BLA to the CA1 regions of the ventral Hpc (vHpc) increased anxiety-like behaviors in the EPM and OF tests [58]. In opposition, stimulation of granule cells of the ventral dentate gyrus (vDG) eliminates anxiety-like behaviors in these tests [97]. Regulation of innate anxiety via vHpc occurs through connections to the lateral septum (LS) and HT, the latter playing a central role in response to stress via the hypothalamic-pituitary-adrenal (HPA) axis [160, 161]. In addition, interconnexions between the Amg, the vHpc and the mPFC are necessary for the evaluation of threats [28], the mPFC being referred to as the main brain regions for the interpretation of dangers. The mPFC receives projections from both the Amg and vHpc as well as the

TH. Notably, reduced anxiety was found as a result of the periodic firing of mPFC neurons, potentially sending safety signals to the BLA [119]. In addition, increased synchrony between the mPFC to vHpc were observed during anxiety-like tests [4, 5].

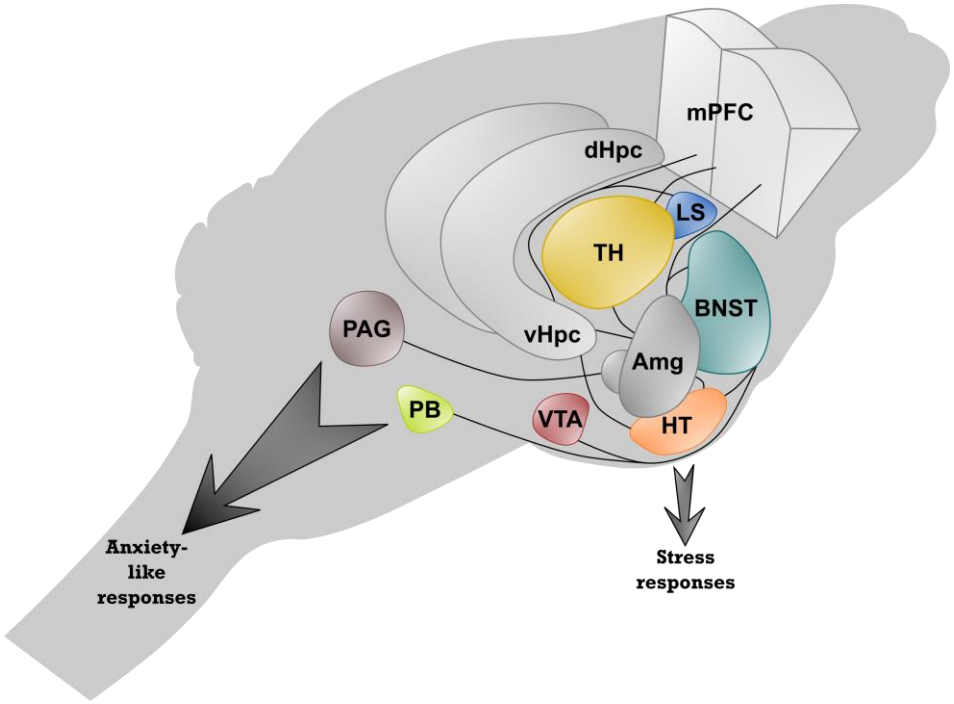

Figure 4. Neuronal circuits involved in anxiety. The established connections between the displayed brain regions were obtained from recent research using optogenetics, neuronal tracing, electrophysiology and behavioral approaches. Figure adapted from [28, 191]. Amg = amygdala, BNST = bed nucleus of the stria terminalis, PB = parabrachial nucleus, dHpc = dorsal hippocampus, HT = hypothalamus, LS = lateral septum, mPFC = medial prefrontal cortex, PAG = periaqueductal grey, TH = thalamus, vHpc = ventral hippocampus, VTA = ventral tegmental area.

2.2. Neuronal circuit of innate fear

In the presence of an imminent threat which is innately considered fearful, the organism needs to integrate information from the environment and respond rapidly for its survival. For many animals including rodents, responses to dangers usually comprise freezing, fighting or fleeing, referred to as the defensive trio by J.E. LeDoux: “freeze first, fight if you can or flight if you must” [114]. The detection of threats inducing innate fear is initiated by olfactory, auditory and visual cues from the environment via primary sensory cortices [19] and their interpretations have been shown to depend on the type of imminent dangers [68, 178] (Figure 5). In the presence of a predator, the olfactory cortex stimulates the posteroventral part of the medial nucleus of the Amg (pvMEA) and both the auditory and visual cortices

activate the LA and subsequently the basomedial Amg (BMA) prior to the recruitment of a predator responsive circuit within the TH [29]. While aggressive behavior from a member of the same species (conspecific) causes rapid activation of the posteromedial MEA (pmMEA), further stimulating a TH conspecific-responsive circuit [133]. Acute pain is also considered a threat inducing innate fear, although controversial due to its additional harmful nature, and is directly detected by the BLA and CE nuclei of the Amg [191]. For these three types of threats, defensive responses emerge from the PAG, the dorsolateral and dorsomedial parts (dlPAG and dmPAG) being responsible for innate defensive responses to predators and aggressive conspecifics, whereas the ventrolateral PAG (vlPAG) controls freezing behaviors [190].

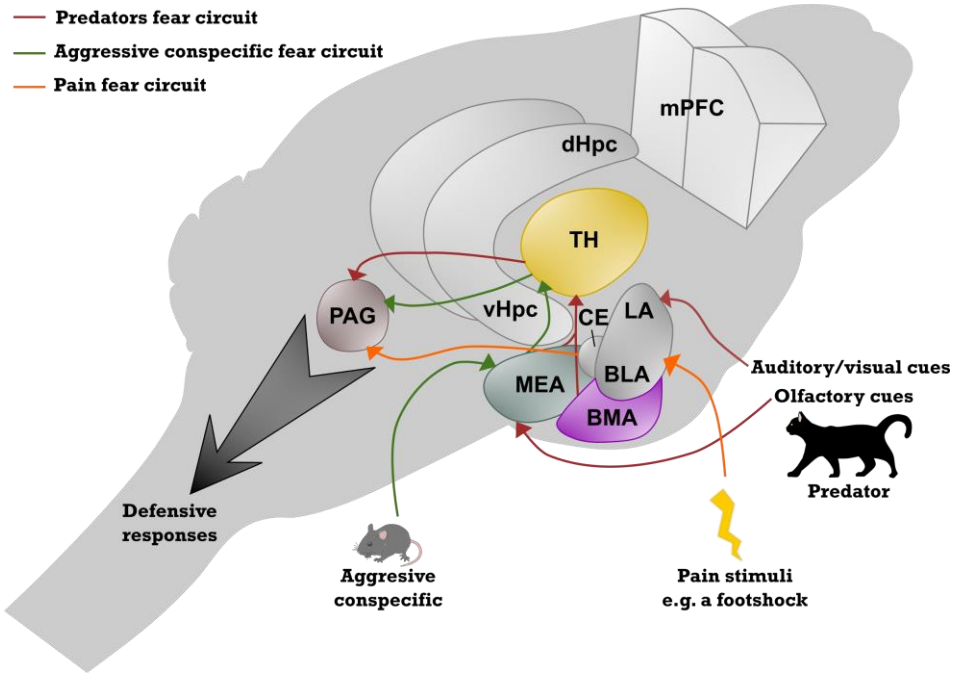

Figure 5. Neuronal circuits involved in innate fear. The established connections between the displayed brain regions were obtained from recent research using optogenetics, neuronal tracing, electrophysiology and behavioral approaches. Figure adapted from [68, 178]. BLA = basolateral nucleus, BMA = basomedial nucleus, CE = central nucleus, dHpc = dorsal hippocampus, LA = lateral nucleus, MEA = medial nucleus, mPFC = medial prefrontal cortex, PAG = periaqueductal grey, TH = thalamus, vHpc = ventral hippocampus.

2.3. Neuronal circuits of acquired fear

In situations that induce innate fear, the organism is able to memorize the distinctive cues of the threatening situation, referred to as fear learning. The FC paradigm (see section 1.2.2) has been widely used to investigate anxiety and fear in both humans and rodents [114]. Because it offers a great tool to

study fear learning and memory, the neuronal circuits underlying acquired fear have been extensively examined in the past decades through FC [53, 56, 111, 112, 54, 55, 76, 77, 191], as opposed to anxiety and innate fear circuits, which were only recently investigated via the emergence of advanced techniques such as optogenetics. Nevertheless, these approaches have also substantially improved our understanding of the neuronal circuits of fear learning and memory [28, 191] (Figure 6). The Amg is the central brain region for fear-inducing stimuli processing, fear memory encoding and initiation of freezing responses [115, 111]. The acquisition of FC is initiated in the LA, which receives input from both the TH and sensory cortices, thus referred to as the fear entrance gate [89]. During cued FC, auditory stimuli information originates from both the auditory cortex and auditory TH, which correspond to the medial division of the medial geniculate body [163]. However, only complex auditory stimuli seem to require the involvement of the auditory cortex [85]. US inputs come from either the somatosensory cortex or posterior intralaminar nuclei of the TH [176]. The information collected through the LA is then transmitted to the BLA where the consolidation of fear memory is believed to take place [54]. The information is conveyed via the CE, wherein fear memories are also known to be gated [203, 216], and is further transferred to motoneurons through midbrain vlPAG and hindbrain relays to produce freezing responses [190]. Additionally, projections from the lateral PB (lPB) to the lateral CE (CEl) are involved in the relay of nociceptive stimuli and in the modulation of fear memory [71, 171].

As previously mentioned, in fearful situations the Amg communicates tightly with the mPFC and vHpc through several reciprocal projections. However, these connections also play an important role for the encoding of the different features of fear memories and have been widely studied in terms of fear learning [28, 191]. Recently, Courtin et al. (2014) identified a class of inhibitory γ-aminobutyric acid (GABA) interneurons from mPFC cingulate1 (Cg1) and prelimbic (PL) cortices which modulate fear expression via regulation of BLA excitatory principal neuron firing synchrony [38]. Moreover, neurons form PL and infralimbic (IL) cortices projecting to BLA principal neurons regulate fear expression and extinction memory, respectively [38]. In return, the PL and IL receive inhibitory input from the CE, acting as a feedback loop which controls fear expression during FC [207]. In the BLA, the PL and IL project onto different populations of principal neurons that are either activated in response to fear (fear neuron) or during extinction (extinction neuron) (Figure 8) [76, 173]. Distinct circuits within the mPFC-Amg-vHpc network are respectively involved in the regulation of fear expression and extinction via these two identified principal neuron classes [76]. During fear learning, projections from the vHpc to the BLA fear neurons and from the BLA fear neurons to the mPFC are stimulated, while reciprocal connections

between BLA extinction neurons and the mPFC are activated during fear extinction [76]. Furthermore, vHpc and BLA reciprocal connectivity have been shown to regulate the contextual encoding of FC [180]. Using optogenetics and viral tracer methods, Xu et al. (2016) showed that two distinct circuits starting from the vCA1 stratum oriens and projecting to either the BLA or CE respectively controlled context retrieval and fear renewal of FC [214]. Finally, although the mPFC, Amg and vHpc represent the main acquired fear network, other brain regions are known to play a role in fear learning. Notably, the nucleus accumbens (NAc) is known to modulate the extinction of FC [82, 162] and play an important role in active avoidance behaviors through connections with the BLA, and PL and IL cortices [24].

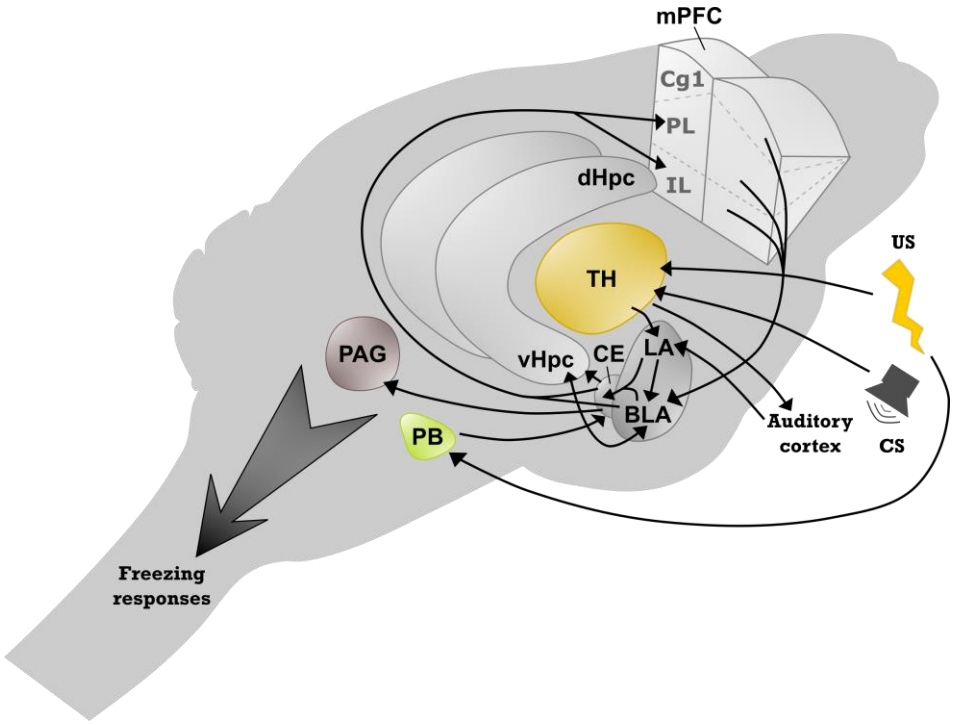

Figure 6. Neuronal circuits involved in acquired fear. The established connections between the displayed brain regions were obtained from recent research using optogenetics, neuronal tracing, electrophysiology and behavioral approaches. Figure adapted from [191]. BLA = basolateral nucleus, CE = central nucleus, Cg1 = cingulate cortex1, CS = conditioned stimulus, dHpc = dorsal hippocampus, IL = infralimbic, LA = lateral nucleus, mPFC = medial prefrontal cortex, PAG = periaqueductal grey, PB = parabrachial nucleus, PL = prelimbic, TH = thalamus, US = unconditioned stimulus, vHpc = ventral hippocampus.

2.4. Amygdala intrinsic micro-circuits and fear conditioning

Considered as the key brain region for the processing and learning of conditioned fear, the function of the Amg has been widely investigated in fear memory [115, 111, 118, 50, 117, 48, 208, 216]. Moreover,

several micro-circuits within this brain region have been recently identified using a combination of advanced methods such as electrophysiology with optogenetics and viral tracers [76, 118, 36, 73, 173, 208, 207]. As previously mentioned, the Amg is composed of three main subnuclei: the LA, BLA and CE, and also contain small intercalated cell masses (ITCs) present along the LA/BLA almond-shaped region (see Figure 3). The Amg can also be subdivided into cortical- (LA and BLA) and striatum-like structures (CE and ITCs). As in the cortex, the LA and BLA are composed of a majority of excitatory glutamatergic neurons, while the CE and ITCs are similar to striatum and contain mostly inhibitory GABAergic neurons [50]. In the central nervous system (CNS), there are different subtypes of GABAergic neurons which play distinct modulatory roles and can be classified using specific markers depending on their gene expression patterns [186].

In the LA, principal neurons receive direct sensory inputs from thalamic and cortical excitatory neurons, stimulating the Amg during fear learning (Figure 7). However, LA principal neuron activity is also modulated by local interneurons, themselves receiving inputs from the TH and sensory cortex (Figure 7) [50]. Using optogenetic techniques, a recent study has shown that two populations of interneurons tightly modulate the activity of LA principal neurons and are crucial for fear learning [208]. The parvalbumin- (PV) expressing interneurons were activated during CS and inhibited during US presentations, while the opposite was found for somatostatin- (SOM) expressing cell populations (Figure 8) [208]. Therefore, these two classes of interneurons are responsible for a dynamic regulation of principal neurons within the LA in a stimulus-specific manner supposedly underlying the mechanism behind the consolidation of fear memory in the Amg [208]. Moreover, in the BLA, a third class of interneuron expressing cholecystokinin (CCK) and cannabinoid receptor 1 (CB1) also control the activity of principal neurons and have been suggested as central mediators of fear extinction (Figure 8) [124, 207]. Furthermore, principal neurons from the LA/BLA project into the CE [50], which due to its striatum-like structure contains mostly GABAergic neurons, including PKC-δ-expressing interneurons [73, 27]. In the CEl, the PKC-δ positive interneurons are inhibited during CS presentation (CEl-OFF), while PKC-δ negative cells are activated (CEl-ON) (Figure 8). These two interneuron populations tightly modulate the activity of the interneuron form the medial CE (CEm), responsible for the initiation of freezing responses [73]. However, only CEl-OFF neurons directly contact CEm interneurons and CEl-ON appears to regulate their activity via the inhibition of CEl-OFF cells. Finally, inhibitory neurons from ITCs communicate with the LA, BLA and CE nuclei via direct projection (Figure 8) [50]. Consequently, they have been implicated in the regulation of fear acquisition, consolidation and extinction memory [26, 117].

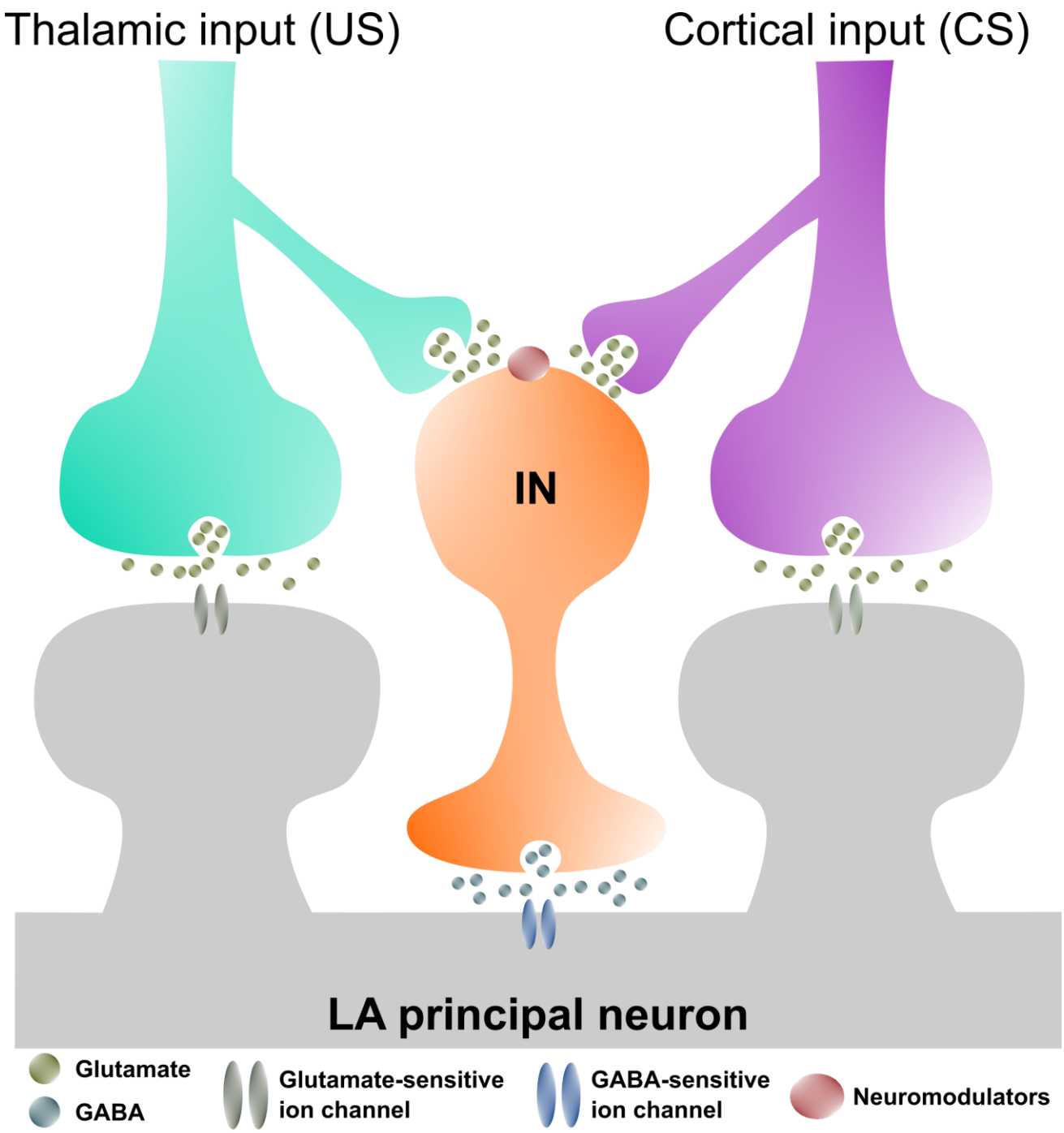

Figure 7. Representative inputs from the sensory cortex and thalamus onto principal neurons from the lateral nucleus (LA) of the Amg gating the CS–US association during fear conditioning. Figure adapted from [50]. CS=conditioned stimulus, GABA = γ-aminobutyric acid, IN=interneuron, LA=lateral nucleus, US=unconditioned stimulus.

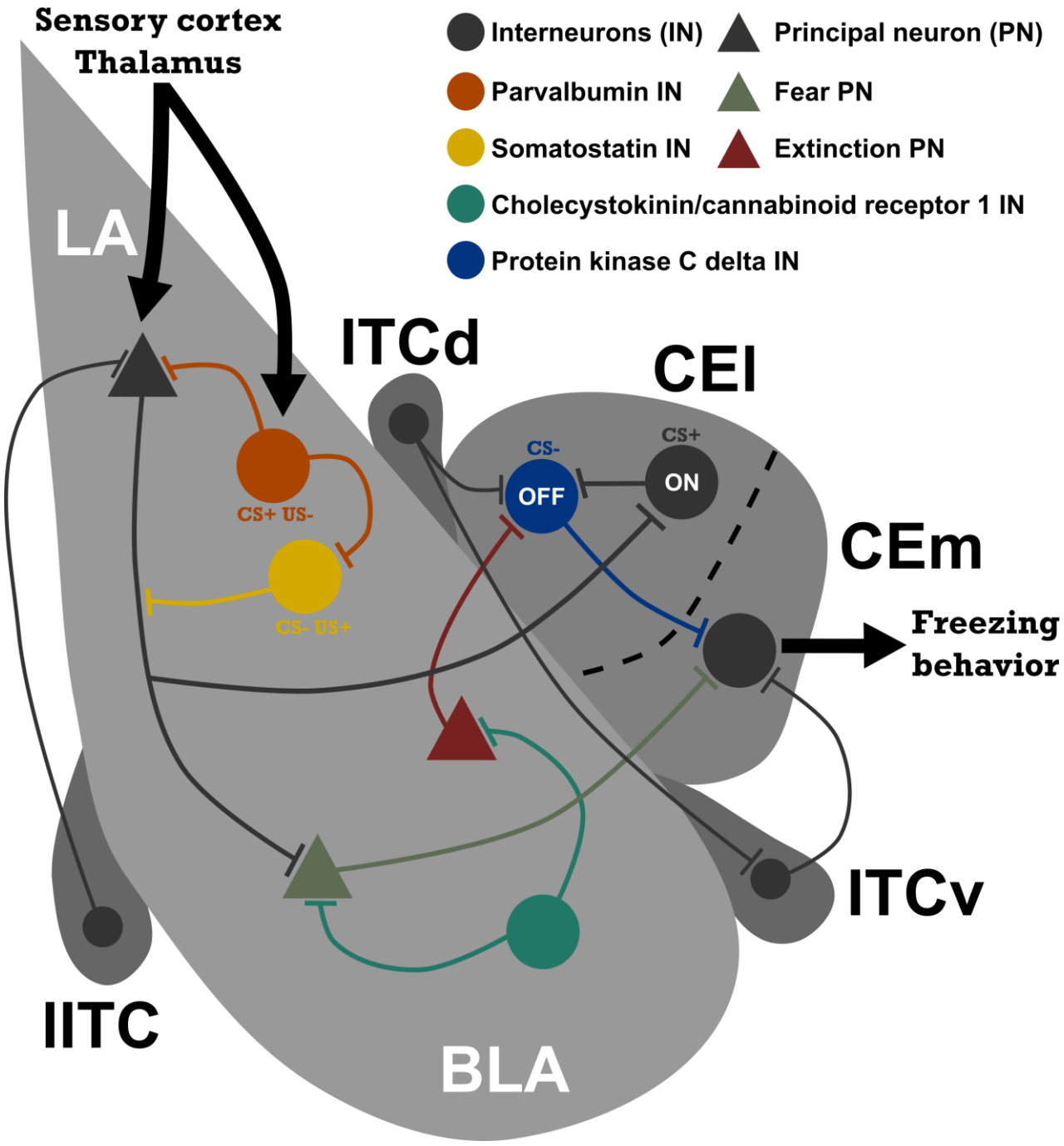

Figure 8. Amg micro-circuits involved in acquired fear and extinction memory. Figure adapted from [50, 48]. BLA = basolateral nucleus, CEl = lateral part of the central nucleus, CEm = medial part of the central nucleus, CS = conditioned stimulus, IN = interneuron, ITCd = dorsal intercalated nucleus, ITCv = ventral intercalated nucleus, LA = lateral nucleus, lITC = lateral intercalated nucleus, PN = principal neuron, US = unconditioned stimulus.

3. Cellular and molecular mechanisms of fear memory

3.1. Molecular mechanisms of fear memory

Fear memory has been widely investigated since the first description of classical conditioning by Pavlov [53, 56, 111, 112, 54, 113, 79, 55, 76, 77, 88, 110, 78, 191]. Moreover, the emergence of advanced techniques such as optogenetics has substantially increased our knowledge on the molecular mechanisms occurring during the different phases of fear conditioning. Considering its central role in fear expression and memory, most of the studies have been focusing on the molecular basis of fear learning and consolidation in the Amg. Fear learning processes are initiated in the LA, the sensory information entrance nucleus, and are described in the literature as activity-dependent or Hebbian synaptic plasticity [88], based on Donald Hebb's theory [74, 172]. This theory can be interpreted as a strengthening effect of the associative learning due to the occurrence of a weak input from the neutral cue (CS) together with a strong input from the fear-inducing event (US) onto the same target, in our case LA principal neurons (Figure 7) [74, 172]. This activity-dependent synaptic plasticity mainly originates from the activation of postsynaptic glutamate N-methyl-D-aspartate receptors (NMDAR) via glutamate release from the presynaptic neurons (Figure 9) [88]. However, the inhibitory GABAergic system also plays an important part in fear learning through disinhibition of the Amg via auditory and thalamic inputs (see section 2.4 and Figure 7 and 8) [208].

The stabilization of acquired fear memory originates from the activation of intracellular cascades such as the mitogen-activated protein kinase (MAPK) pathway that then initiates the machinery for the synthesis of messengers RNA (mRNA) and proteins (Figure 9) [88]. The exact physiological mechanism through which fear memory consolidates is supposedly long-term potentiation (LTP) [146]. This phenomenon consists of specific synapses strengthening, which at the molecular level corresponds to an increased abundance of the glutamatergic α-amino-3-hydroxy-5-methyl-4-isoxazolepropionic acid receptors (AMPAR) at the post-synaptic density (PSD) (Figure 9). Consequently, the activation of synapses that have been selectively strengthened elicits a stronger activation of post-synaptic neurons than previously and underlies the molecular basis of learning and memory [88].

Finally, the molecular mechanisms of fear extinction are similar to those involved in fear learning [136]. However, fear extinction is mainly modulated by inhibitory circuits [117] and would consist of the inhibition of the previously acquired fear memory [136]. This theory is based on the fact that CS-elicited fear expression re-appears a few days or weeks after fear extinction training, referred to as spontaneous

recovery, indicating that extinction is a *de novo* learning, rather than a permanent erasure of acquired fear memory. Moreover, it is known that two distinct populations of principal neurons from the BLA encode fear learning and extinction and involve distinct circuits within the fear-related brain regions [76, 173] (figure 8). Thus, the difference between fear learning and extinction would derive from the circuit involved rather than the molecular mechanisms *per se*.

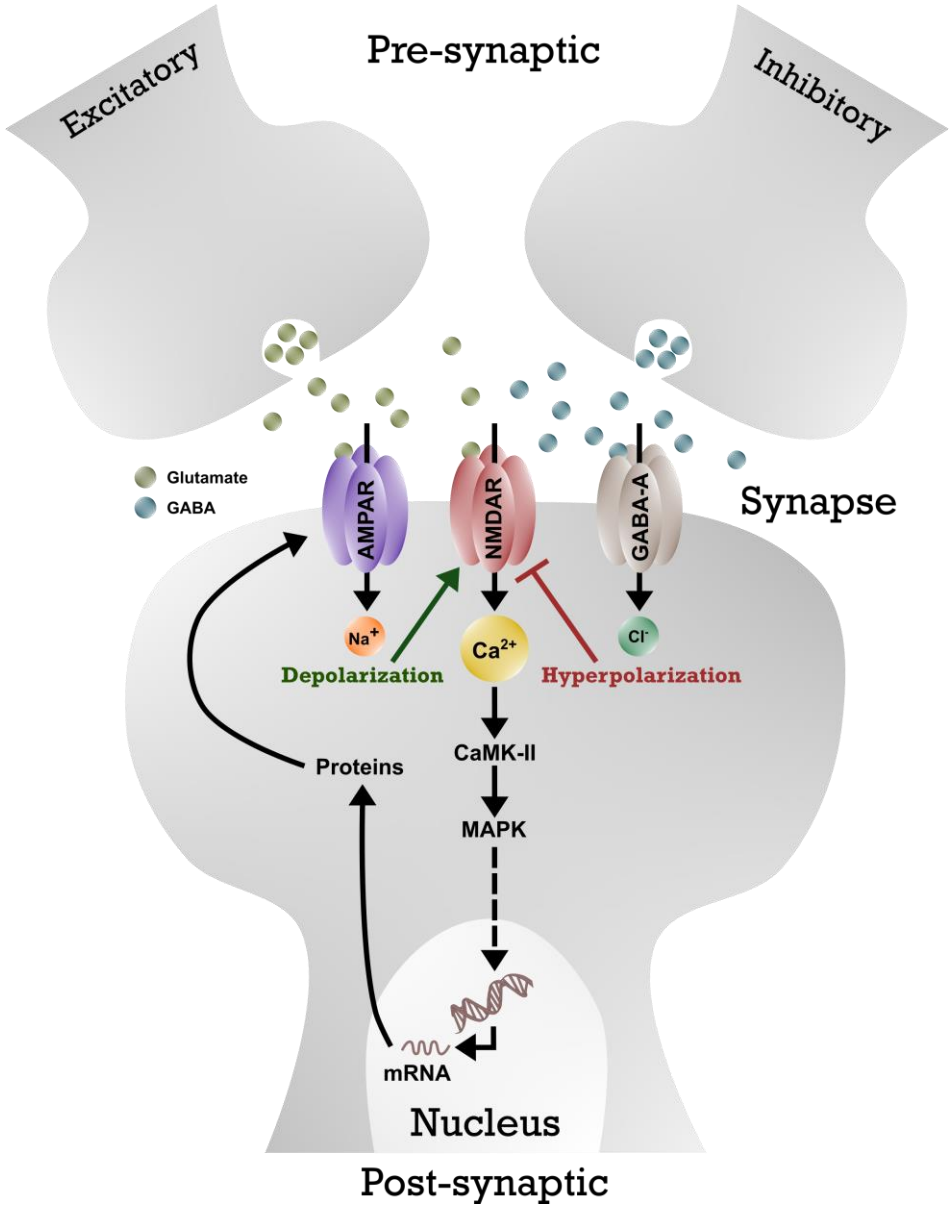

Figure 9. Simplified molecular mechanisms involved in fear learning, consolidation and extinction. Ion channels represented are the glutamatergic receptor AMPAR (α-amino-3-hydroxy-5-methyl-4-isoxazolepropionic acid receptor) and NMDAR (N-methyl-D-aspartate receptor) and the GABAergic GABA-A receptor (γ-aminobutyric acid-A receptor). AMPA = α-amino-3-hydroxy-5-methyl-4-

isoxazolepropionic acid receptor, Ca^{2+} = calcium ions, CaMKII = Ca^{2+}/Calmodulin-dependent protein kinase II, Cl^- = chloride ions, GABA = γ-aminobutyric acid, MAPK = mitogen-activated- protein kinase, mRNA = messenger ribonucleotide acid, Na^+ = sodium ions, NMDA = N-methyl-D-aspartate receptor.

3.2. Dendritic spines and memory formation

In the nervous system, neurons are considered the "functional unit" of brain activity, but the mechanism underlying memory processes occurs at a much smaller level by allowing the strengthening of specific synapses. Synapses are defined as the contact area between pre- and post-synaptic neurons (Figure 9) and can be studied functionally through electrophysiological techniques as well as morphologically via measurement of spine abundance, referred as spine density in the literature [126, 51, 11, 181].

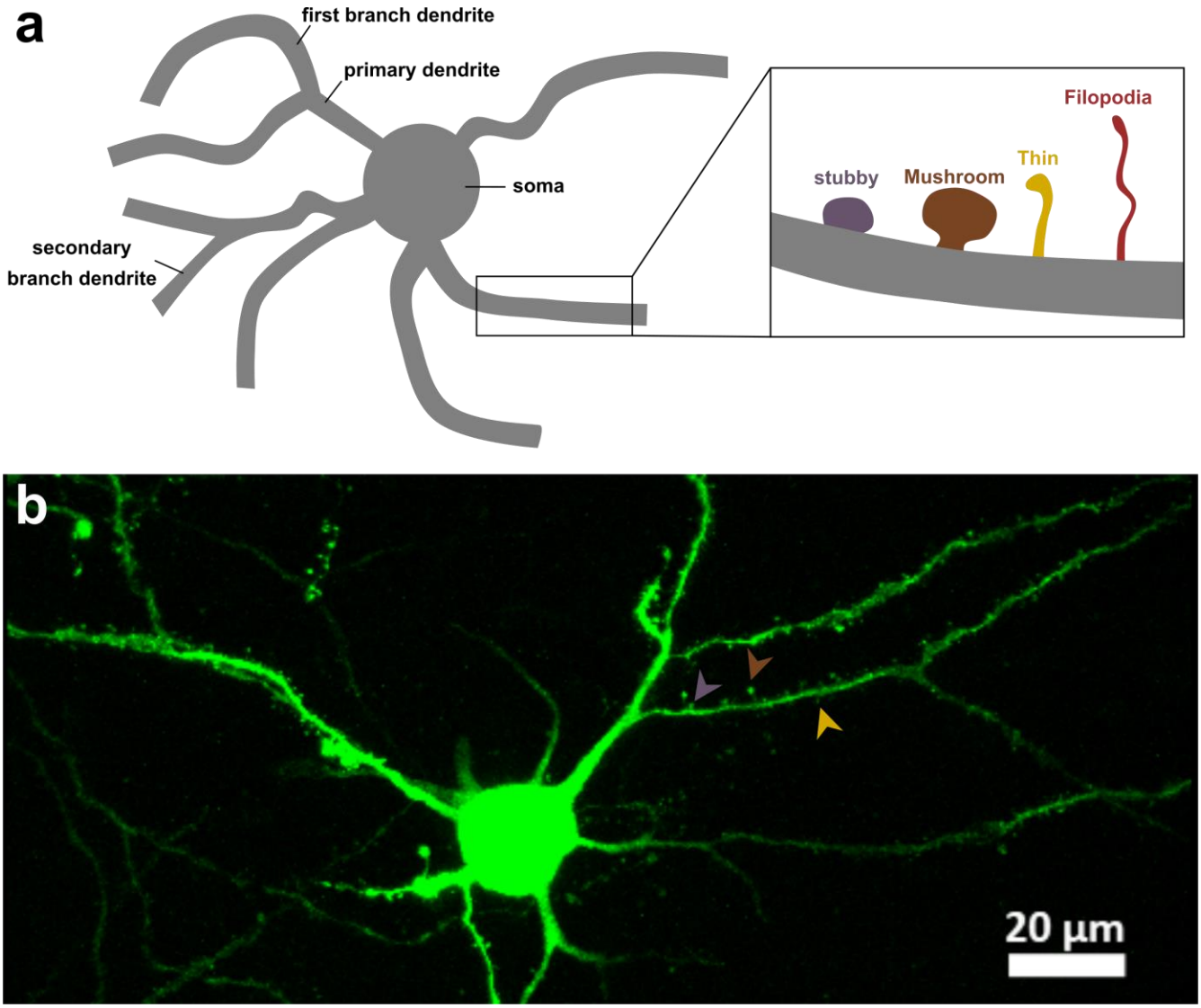

Figure 10. Dendritic spine density and morphology in the mouse brain. (a) Schematic representation of neuronal dendrite branching and dendritic spine morphology. **(b)** Picture of an immunohistochemically stained neuron from mice Amg. Colored arrowheads indicate example of dendritic spines from different morphological classes: yellow = thin spine, brown = mushroom spine and purple = stubby spine.

Spine represent a morphological and functional unit from a specific neuron forming synapses with spines from another neuron, which are mostly, but not exclusively, glutamatergic synapses [181]. Therefore, spine density is considered as an estimation of the amount of excitatory inputs onto a specific neuron [181], which can differ substantially between brain regions [11]. Spines are found all over neuron branches, called dendrites. However, they are usually more abundant after the first subdivision of the primary dendrite (Figure 10.b). In addition, dendritic spines can be of different sizes and shapes (Figure 10.a) [126]. At immature stages, neuron dendrites will contain mainly long and thin spines called filopodia, which are nearly absent from mature neurons (Figure 10.a) [169, 90]. In adults, thin spines characterize recent connections and are supposedly sensitive to new experiences [81], while stable synapses are made through mushroom and stubby spines, marks of established memory (Figure 10) [95, 23]. Crucially, spine abundance is increased in the Amg and reduced in the Hpc in mouse models of stress-related disorders and thus is interesting to study in terms of anxiety and fear regulation [166, 34].

3.3. Perineuronal nets and fear memory

Strengthening of spine connectivity onto specific neurons is believed to be the mechanism behind the consolidation of memory. Recently, perineuronal nets (PNNs) have been shown to play an important role in the stabilization of synapses onto the neuron they surround [31, 198]. PNNs are specialized extracellular matrix surrounding soma and primary dendrites onto selected neuron populations. They are mostly composed of chondroitin sulfate proteoglycan, hyaluronan and tenascin-R molecules and control the composition of the surrounded neuron micro-environment [198]. PNNs appear progressively during development and are linked to the closure of highly plastic periods occurring during early life [155, 198]. In adults, they are involved in memory consolidation [63, 83, 164, 179] and their role in the stabilization and re-arrangement of PV-inhibitory networks is well-established [179, 215, 12, 57]. Moreover, as a mark of consolidated memory, their abundance negatively correlates with fear extinction efficiency in the Amg [63]. Accordingly, Gunduz-Cinar et al. (2017) showed a difference in the abundance of PV surrounded by PNN (PV-PNN) within the Amg of two mouse strains presenting innate differences in

fear extinction efficiency [69]. Therefore, the PV-PNN population from the Amg represents an interesting target for the investigation of fear memory consolidation and extinction.

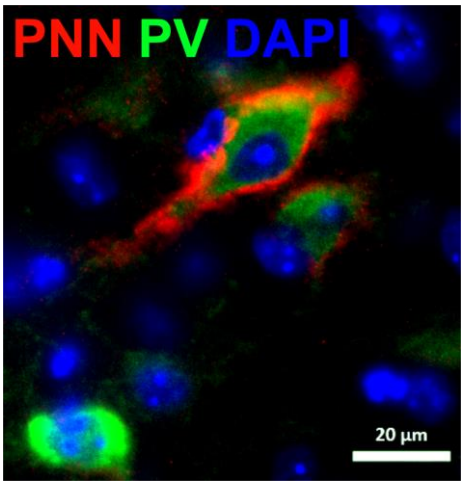

Figure 11. Picture of a perineuronal net surrounding the soma and proximal dendrites of a parvalbumin-expressing interneuron (PV-PNN). The 4′,6-diamidino-2-phenylindole or DAPI molecule binds to DNA and is used as a marker of cell nuclei. DAPI = 4′,6-diamidino-2-phenylindole, PNN = perineuronal nets, PV = parvalbumin.

3.4. Fear memory during development

In adults, fear learning and memory are mediated by reciprocal connections within the mPFC-Amg-vHpc network, where specific circuits modulate different features of fear conditioning (see section 2.3) [28, 191]. At juvenile or pre-adolescent ages, fear conditioning seems to involve the same brain regions as in adult mice [102, 99, 77, 148, 149]. However, very little is known about the specific circuits and molecular mechanisms implicated in fear memory at this early developmental stage. FC is generally performed post-weaning in rodents (~post-natal day 21 or P21) when the fear network is known to be functional [77]. Nevertheless, a few studies have explored FC features at earlier ages, focusing mainly on fear extinction [100-102, 63, 99]. At pre-weaning time points, fear extinction is considered an erasure of acquired memory since no fear renewal or spontaneous recovery are present at P17 in rats or P16 in mice [101, 63]. Notably, after weaning, extinction memory already demonstrates features of an adult-like *de novo* memory [101, 102, 63, 99]. Furthermore, Pattwell et al. (2012) showed strong neuronal activation in the PL and IL during fear learning and extinction respectively in pre-adolescent mice, similarly to adults [149]. However, pre-adolescent mice fear expression levels and extinction efficiency are higher compared to adults, demonstrating dissimilarities in behavioral responses during FC between these two ages (Figure 12) [148, 149].

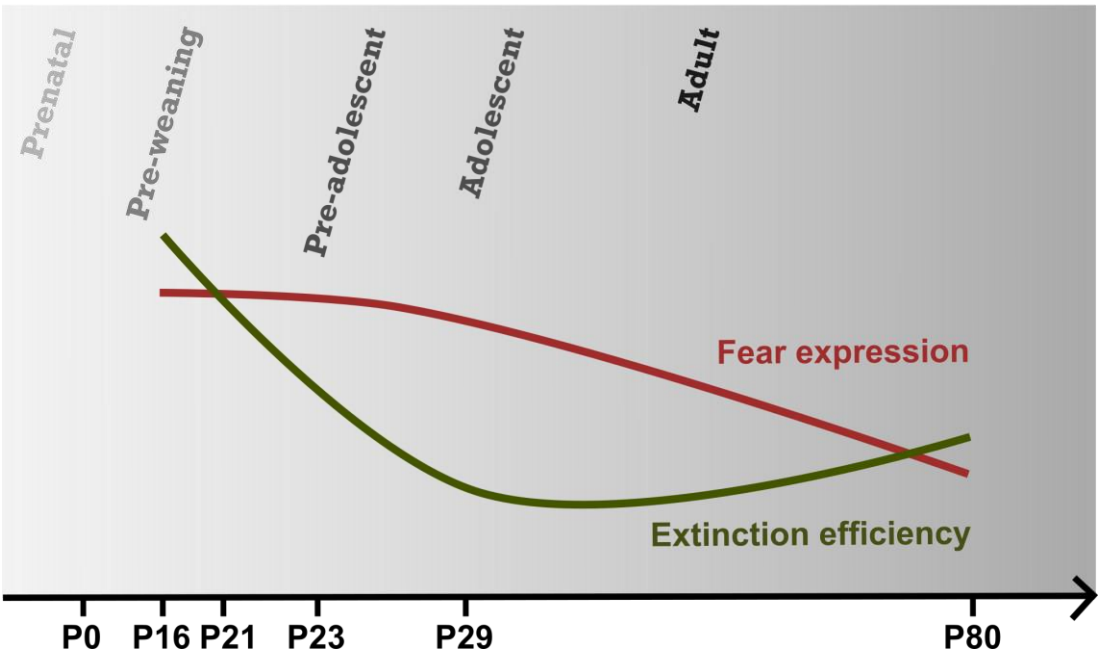

Figure 12. Fear memory features in cued FC during development in mice. Schematic of freezing level and extinction efficiency between postnatal day 16 (P16) and adult age (P80). Adapted from [63, 149].

These developmental differences might derive from an overall higher plasticity of the brain at younger ages. Inhibitory networks composed of PV-expressing interneurons are known to play an important role in the plasticity-permissive period occurring on specific circuits at precise times during development (i.e., critical periods). This type of plasticity has been widely studied in the visual cortex where the closure of one eye is sufficient to produce re-arrangement of cortical neuron networks under the control of PV interneurons [75]. In the Hpc, re-arrangement of the PV interneuron network measured via the intensity of PV staining are observed between juvenile and adult mice [45]. As previously mentioned, PV interneurons are often surrounded by PNNs which also play a central role in brain plasticity during development. PNN abundance increases throughout development and their enzymatic destruction in the Amg causes juvenile-like extinction in adult mice (i.e., permanent extinction) [63]. Thus, in line with their role in memory consolidation, PNNs protect from fear erasure and may partly explain the developmental differences observed in fear expression and extinction.

During the closure of critical periods, PNNs develop around selected PV interneurons and induce their maturation by capturing and distributing transcription factors necessary to cell growth from the micro-environment, such as OTX2 for PV maturation [18]. Moreover, they are responsible for the stabilization of synaptic connectivity onto the neuron they surround [31, 198], which is presumably how memories

are formed and consolidated. Accordingly, PV-PNN cell populations within the Amg could encode memory from fear-inducing events occurring during early stages.

4. NETO proteins & interacting partners

Exactly ten years ago, NETO1 and NETO2 (neuropilin and tolloid-like 1 and 2) proteins were first described as auxiliary subunits for ionotropic glutamate receptors (iGluRs) [139, 217]. Since then numerous studies have investigated their roles in the CNS [182, 185, 184, 84, 212, 141, 213]. NETO1 and NETO2 are homologous (~70% at transcript and ~60% at protein levels) transmembrane CUB (complement C1r/C1s, Uegf, Bmp1) domain-containing proteins that are coded by two different genes in both humans and mice (Figure 13). The NETO proteins (NETOs) are both widely expressed and are highly similar in structure but due to differences in their expression patterns and interacting partners, they play different roles in the mouse brain [139, 217, 182, 185, 184, 84, 212]. NETO1 interacts with native NMDARs and kainate receptors (KARs) and is most abundant in the Hpc [139, 217, 182, 185, 212], while NETO2 is an auxiliary subunit for KARs and potassium/chloride ions (K^+/Cl^-) co-transporter 2 (KCC2) and its expression is the highest in the cerebellum (Ceb) [217, 184, 84, 123]. They both interact with ion channels through their CUB domains [139] and regulate their activity (i.e., desensitization kinetics) via an active domain called LDLa (low-density lipoprotein class a) (Figure 13) [217]. Finally, at their C-terminal they have a PDZ-ligand domain [PDZ is an initialism for post-synaptic density protein 95 kDa (PSD95), drosophila disc large tumor suppressor (Dlg1), and zonula occludens-1 protein (zo-1)], which gives them the ability to bind with various scaffolding proteins at synapses, allowing them to interact with distinct proteins since NETO1 contains a class I and NETO2 a class II PDZ-ligand domain (Figure 13). Therefore, NETOs play an important role in the stabilization of macromolecular complexes at synapses through their multiple interactions with scaffolding proteins and ion channels.

During the past ten years, several studies have demonstrated the importance of NETOs, especially on the KAR-mediated transmission in the developing mouse brain. At early ages, NETO1 regulates KAR-mediated excitatory post-synaptic currents (EPSCs) [185, 212, 213] and axonal targeting of KARs in the Hpc [141], while NETO2 is important for KAR-mediated EPSCs in the Ceb during development [217]. Recently, Wyeth et al. (2017) demonstrated that both NETO1 and NETO2 regulate tonic inhibition from CCK-expressing interneurons in the developing Hpc via modulation of KAR activity [213]. Altogether, these results show the important regulatory role of NETOs on the functions of KARs in the developing mouse brain. Interestingly, *Neto2* expression is down-regulated during development while *Neto1* is up-

regulated [141], showing that these two proteins have distinct dynamics of expression patterns through development.

In the adult brain, NETO1 and NETO2 regulates major KAR subunit abundance at PSDs, in the Hpc and Ceb respectively [185, 184]. Furthermore, to investigate the role of NETO1 in spatial memory, Ng et al. (2009) tested *Neto1* knock-out (KO) adult mice behavior using the Morris water maze (MWM) and the displaced and novel object recognition tests (NOR and DOR) [139]. In accordance with the high abundance of NETO1 in the Hpc, they showed that *Neto1* ablation caused spatial memory impairment in both the MWM and DOR, which are Hpc-dependent tests [139]. They did not find differences between wild type (WT) and mutant mice in the NOR test [139], which is mainly perirhinal cortex-dependent [135, 25, 200], suggesting that *Neto1* ablation mostly affects behaviors that depend principally on the function of the Hpc. However, little is known about the molecular mechanisms through which NETOs modulate adult brain functions and thus on their involvement in other types of behavior and memory.

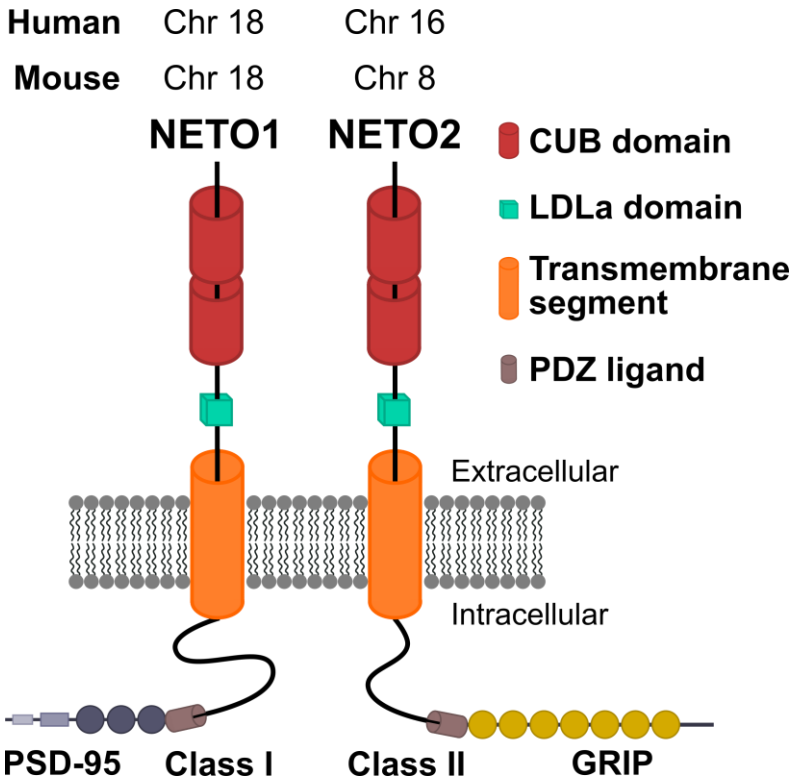

Figure 13. Schematic presentation of NETO1 and NETO2 protein domains and the chromosomes (Chr) their genes reside on in humans and mice. Chr = Chromosome; CUB = complement C1r/C1s, Uegf, Bmp1; GRIP = glutamate receptor interacting protein; LDLa = low-density lipoprotein class a; NETO = neuropilin and tolloid-like; PDZ = initialism for post-synaptic density protein 95 kDa (PSD95), drosophila disc large tumor suppressor (Dlg1), and zonula occludens-1 protein (zo-1); PSD-95 = post-synaptic density protein 95 kDa.

5. Kainate receptors (KARs)

KARs are members of the iGluR family, together with NMDARs and AMPARs, which mediate fast excitatory neurotransmission in the CNS. They are tetrameric ligand-gated ion channels composed of five subunits (GLUK1–5) coded by five genes (*GRIK1–5* in humans and *Grik1–5* in mice). Their ion channels are usually heteromeric, containing two low affinity subunits (GLUK1–3) together with two high-affinity subunits (GLUK4 and 5). However, GLUK1–3 subunits are able to form homomers and heteromers, while GLUK4 and 5 can only form heteromers with low-affinity subunits. In the mouse brain, KAR subunits show distinct temporal and spatial expression patterns and are present in various brain regions, cell types or subcellular compartments [204, 147, 209, 201, 213].

Similarly to NMDARs and AMPARs, KARs are activated by glutamate binding at postsynaptic compartments which mediate excitatory neurotransmission. However, in opposition to the other iGluR family members, they are not predominantly found at excitatory postsynaptic compartments. Additionally, they presynaptically regulate neurotransmitter release at both excitatory [108, 109, 154] and inhibitory synapses [42, 98]. Consequently they are referred as "modulators of synaptic transmission and neuronal excitability" [37]. Therefore, dysregulations of the KAR-mediated transduction system may be involved in the etiology of various brain diseases. Indeed, variation in the *GRIK2* gene has been associated with OCD [125] and variation in *GRIK5* with bipolar disorders [65]. Moreover, decreases in *GRIK1* and *GRIK2* expression levels were reported in the medial temporal lobe from bipolar disorder, major depression and schizophrenia patients [15]. Furthermore, *Grik1* KO mice demonstrated higher anxiety-like behavior [211], while *Grik2* and *Grik4* KO mice showed reduced anxiety-like behaviors compared to WT mice [174, 30]. As mentioned in the previous section, both NETO1 and NETO2 regulate KAR abundance and function in the adult and developing mouse brain. Therefore, they represent attractive candidates to investigate their potential role in anxiety and fear regulation via their modulation of KAR functionality.

Hypotheses and aims of the study

We hypothesized that NETO1 and NETO2 regulate anxiety-like and/or fear-related behaviors via modulation of KAR function in the CNS (**I**). Based on our initial findings, we further hypothesized that NETO2 is required for normal fear expression and extinction by influencing the function of the Amg (**I** and **II**).

The specific aims of this study were:

1) To characterize anxiety- and fear-related behaviors of *Neto1* and *Neto2* KO mice (**I**).

2) To determine the mRNA expression pattern and synaptic protein abundance of *Neto2* in the brain regions regulating anxiety and fear in juvenile and adult mice (**I** and **II**).

3) To further investigate the molecular mechanisms underlying the *Neto2* KO mouse higher fear expression and delayed extinction phenotype by focusing on the Amg maturity and excitability using both juvenile and adult mice (**II**).

Materials and methods

The materials and methods used in this thesis are described in detail in the original publications (**I** and **II**) and summarized here. Methods from unpublished data are presented in more detail.

1. Ethical statement

Animal procedures presented in this thesis were approved by the project authorization board of the Animal Experiment Board in Finland and carried out in accordance to directive 2010/63/EU of the European Parliament and of the Council and the Finnish Act on the Protection of Animals Used for Science or Educational Purposes (497/2013). Behavioral experiments from this thesis were performed under the external licenses ESAVI/2766/04.10.07/2014 and ESAVI/3119/04.10.07/2017, and the author has the competence to carry-out and design animal behavior experiments (animal experimentation level 2, granted at the University of Bordeaux II, France).

2. Mouse models

2.1. Housing

Animals were housed under the standard condition applied by the laboratory animal center (LAC) at the University of Helsinki (Viikki Campus) with food ad libitum and 12h light/dark cycles (light ON from 6 am to 6 pm). Animals used for behavioral testing were single-housed one week prior to the first test. Wild type (WT) and knockout (KO) animals used in this thesis were obtained from heterozygote (HET) breeding pairs, and both males and females were used in the study.

2.1.1. *Neto1*$^{-/-}$ mice

Neto1 KOs and WTs, referred to as *Neto1*$^{-/-}$ and *Neto1*$^{+/+}$ in this thesis, were littermates from HET (*Neto1*$^{+/-}$) breeding pairs, obtained as a gift from Dr. R.R. McInnes from McGill University, Montreal, Canada and were created as described [139]. Briefly, embryonic stem cells (ES) from 129S1Sv/J strain carrying a mutated *Neto1* gene were injected into blastocysts. Obtained chimeric males were then mated with C57Bl/6J females. The *Neto1* mouse line was maintained in C57Bl/6J and C57Bl/6NCrI backgrounds (mixed B6J/B6N background). The remaining background from the ES strain around the transgene was characterized using chip DNA sequencing (Illumina Speed Congenic) at the institute for molecular medicine Finland (FIMM, medicum, University of Helsinki) and estimated at around 10 Mb. To avoid genetic drift, the line has been backcrossed 12 times since the establishment of the model.

2.1.2. *Neto2*$^{-/-}$ mice

Neto2 KOs and WTs, referred as *Neto2*$^{-/-}$ and *Neto2*$^{+/+}$ in this thesis, were littermates from HET (*Neto2*$^{+/-}$) breeding pairs, obtained as a gift from Dr. R.R. McInnes from McGill University, Montreal, Canada and were created as described for the *Neto1* line [185]. The background from the ES 129S1Sv/J strain around the transgene was genotyped using Chip DNA sequencing (Illumina Speed Congenic) at FIMM and estimated at around 40 Mb. To reduce the size of the original 129S1Sv/J strain around the transgene and avoid genetic drift, the line has been backcrossed 13 times since the establishment of the model. Additionally, single nucleotide polymorphisms (SNPs) around the transgene were genotyped using high resolution melting (HRM) analysis to select HET mice with the lowest 129S1Sv/J background around the transgene. Primer pairs were designed to amplify 100 bp fragments containing a SNP that is polymorphic between 129S1Sv/J and C57Bl/6 strain using the Jax SNPs database [2]. Using this method, DNA from the original 129S1Sv/J strain was reduced to approximately 10 Mb (Figure 14).

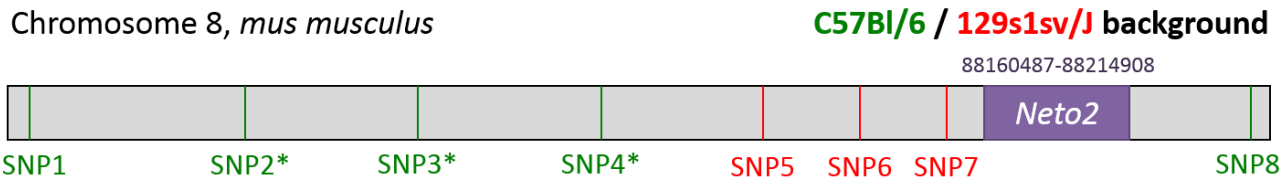

ID	SNP Number	*Neto2*$^{+/+}$	*Neto2*$^{+/-}$	*Neto2*$^{-/-}$	C57Bl/6	129
SNP1	rs13479768	C/C	C/C	C/C	C/C	A/A
SNP2	rs3656875	A/A	A/A	A/A	A/A	G/G
SNP3	rs4227253	A/A	A/A	A/A	A/A	G/G
SNP4	rs32729998	A/A	A/A	A/A	A/A	G/G
SNP5	rs6257357	A/A	A/G	G/G	A/A	G/G
SNP6	rs13479880	A/A	A/C	C/C	A/A	C/C
SNP7	rs13479884	C/C	C/A	A/A	C/C	A/A
SNP8	rs13479922	G/G	G/G	G/G	G/G	A/A

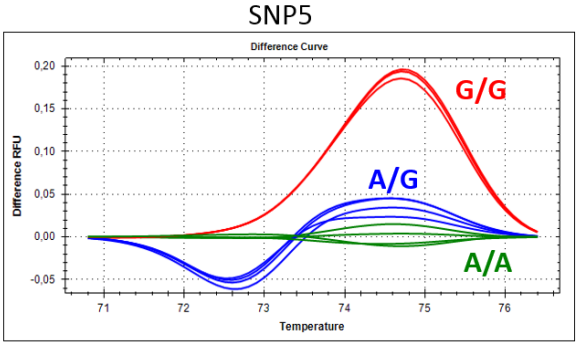

Figure 14. Selected SNPs around the *Neto2* transgene in the *Neto2* line and an example of HRM output results. *shows SNPs from the DNA region that switched from the 129S1Sv/J to C57Bl/6 background by homologous recombination using backcrossing and HET animal selection. Melting curve example from SNP5 genotyping: y axis represents the difference in relative fluorescence units (RFU) and x axis the temperature in Celsius (°C). A = adenine, C = cytosine, G = guanine, HET = heterozygote, HRM = high resolution melt analysis, RFU = relative fluorescence unit, SNP = single nucleotide polymorphism.

2.1.3. *Genotyping*

Animals used in this thesis were genotyped from ear samples using Direct PCR Phire kit (Thermo Fisher Scientific, Waltham, MA, USA). The sequences for *Neto1* and *Neto2* primer pairs were obtained from

Jax laboratory resources [2]. Mice were genotyped after weaning and at the end of the experiment if used in behavioral testing or molecular analyses such as western blot (WB), in situ hybridization (ISH) or immunohistochemistry (IHC). In the *Neto2* line, to ensure stabilization of the original 129S1Sv/J strain region around the transgene to 10 Mb, SNP4 and 5 from HET animals selected for breeding were controlled using HRM analysis (Figure 14).

3. Behavioral testing

For all tests performed in this thesis, mice were brought to the testing room at least 30 min before the beginning of the test. Methods from unpublished results are described in this thesis methods section. For the other tests, refer to the methods section from the corresponding original publication. The table below presents behavioral tests used in this thesis:

Table 3. Behavioral testing used in this thesis for the assessment of *Neto1* and *Neto2* mice line behavior and, if published, the corresponding original publication.

Group of test	*Test*	*Line tested*	*Publication*
Anxiety-like behavior	Elevated plus maze (EPM)	Neto1 & Neto2	**I**
	Elevated zero maze (EPM)	Neto2	**I**
	Open field (OF)	Neto1 & Neto2	**I**
	Light/dark box (LD)	Neto1 & Neto2	**I**
	Novelty-suppressed feeding (NSF)	Neto1 & Neto2	**unpublished**
OCD-like behavior	Marble burying (MB)	Neto1 & Neto2	**unpublished**
Depression-like behavior	Saccharin preference (SP)	Neto2	**I**
	Forced swim test (FST)	Neto2	**I**
Stress physiology	Stress-induced hyperthermia (SIH)	Neto2	**I**
Fear-related behavior	Contextual fear conditioning	Neto1 & Neto2	**I**
	Cued fear conditioning, long version	Neto1 & Neto2	**I**
	Cued fear conditioning, short version	Neto2	**II**
Locomotor activity	Home cage activity (HCA)	Neto1 & Neto2	**I**
Hearing and pain sensitivity	Acoustic startle reflex (ASR)	Neto1 & Neto2	**I**
	Hot plate (HP)	Neto1 & Neto2	**I**
Working memory	Spontaneous alternation in T-maze	Neto2	**I**

ASR = acoustic startle reflex, EPM = elevated-plus maze, EZM = elevated-zero maze, FST = forced swim test, HCA = home cage activity, HP = hot plate, LD = light/dark box, MB = marble burying, NSF = novelty-suppressed feeding, OF = open field, SP = saccharin preference, SIH = stress-induced hyperthermia.

3.1. Novelty-suppressed feeding (NSF)

To perform the NSF test, animals were food-deprived overnight (4 pm to 8 am). The next day they were placed in an acrylic box with white walls (30 x 30 cm) which contained small pieces of food pellets placed in a blue flacon tube cap in the center of the arena (Figure 1). Latency to reach for food in this novel environment was scored (maximum 5 min) and mice were placed back into their home cage. To control for feeding behaviors related to appetite, we also measured latency to reach food and food consumption (g) over 5 min in a familiar environment (home cage), and found no appetite deficit in KO mice.

3.2. Marble burying (MB)

MB testing was performed in a novel Makrolon III open top cage (15 x 30 cm) containing 20 marbles positioned in a 4 x 5 formation on the top of approximately 4.5 cm of fresh bedding material, as previously described (Figure 1) [41]. The test was done with a dim light setting (50 lux) to reduce baseline anxiety levels. The number of marbles more than 50% covered after 30 minutes was scored. This test assesses digging behavior commonly observed in mice and is thought to represent repetitive or obsessive-like behavior, as well as anxiety-like behavior.

4. Blood analysis

Blood samples were collected from the submandibular vein 30 minutes after the end of the forced swim test (FST), which was used as a stressor. Samples were left to clot for 15–30 minutes at +4°C, centrifuged at 1,000-2,000 g for 10 minutes and stored at -20°C. CORT level was measured in the serum using an ELISA kit (Immunodiagnostic System, the Boldons, UK) (**I**).

5. RNA analysis

5.1. In situ hybridization (ISH)

ISHs were performed on *Neto2*$^{+/+}$ mouse brains to characterize *Neto2* expression patterns in fear-related brain regions. I designed a *Neto2* probe conjugated with digoxin and a *Vglut1* probe conjugated with fluorescein. Specificity of the antisense probes were tested by comparison to sense probes for both and with WT vs KO tissue for the *Neto2* antisense probe. We obtained a *Gad1* probe conjugated with fluorescein as a gift from Professor Juha Partanen [Molecular and Integrative Biosciences research program (MIBS), University of Helsinki]. We performed simple and double ISH on juvenile (post-natal day 23 or P23) (**II**) and adult (**I**) mice, using 10 µm paraffin slices as previously described [106].

5.2. Reverse transcriptase quantitative polymerase chain reaction (RT-qPCR)

Neto2 mRNA quantitative analyses were done by RT-qPCR using micro-punch dissected brain regions (Amg, mPFC and vHpc) from four developmental time points: P10 (pre-weaning), P23, P42 and P84 (post-weaning). The P23 time point corresponds to the age of the juvenile mice group and P84 approximately corresponds to the age of the adult mice group (**II**). Quantification was performed on technical triplicates using a SYBR green qPCR kit (Bio-Rad, Hercules, CA, USA) on a Bio-Rad CFX396 thermal cycler, and the level of expression was normalized by a mean between *ppib* and *gapdh* housekeeper genes expression levels.

6. Protein analysis

6.1. Western blot (WB)

Amg, Ceb, mPFC and vHpc brain regions were dissected on ice and snap frozen instantly at -80°C. Amg and mPFC were dissected using micro-punch. Total protein from lysates were extracted using RIPA buffer and synaptosomal fractionation was performed as previously [122]. Protein level to load in the gel were characterized using colorimetric methods such as Bradford on a plate or Coomassie blue on a gel. Proteins were size-separated by electrophoresis and transferred on a nitrocellulose membrane. Our proteins of interest — NETO2, PSD-95, synaptophysin (SYP), GLUK2/3 and GLUK5 — were detected using selected primary antibodies (Table 4). Peroxidase-conjugated secondary antibodies directed against the species of primary antibodies were used to detect the proteins of interest. Protein level was characterized by optic density of bands observed via chemiluminescence detection method (Pierce ECL Western Blotting Substrate) and normalized using ubiquitously expressed protein β-actin (**I**).

6.2. Immunohistochemistry (IHC)

Paraffin sections (10 µm) were used to detect PNN, PV, and c-Fos positive cells in the Amg. Staining was performed using selected primary antibodies (Table 4), except PNN staining which was achieved using a biotinylated Wisteria Floribunda Agglutinin (WFA) that naturally binds to PNNs. Fluorescent staining of the proteins of interest was achieved using alexa fluor-conjugated secondary antibodies directed against the species of primary antibodies, except for biotinylated WFA which was recognized by alexa fluor-conjugated streptavidin (**II**).

Table 4. List of primary antibodies used in this thesis.

Antigen	*Species*	*Catalogue n°*	*Application*	*References*	*Publication*
Neto2	Rabbit	none	WB	[184]	**I**
PSD-95	Mouse	Sc-32290	WB	[93]	**I**
SYP	Mouse	S5768	WB	[156]	**I**
GLUK2/3	Rabbit	04-921	WB	[217]	**I**
GLUK5	Rabbit	06-315	WB	[185]	**I**
β-actin	Mouse	A1978	WB	[92]	**I**
PV	Mouse	235	IHC	[45]	**II**
c-Fos	Rabbit	Sc-52	IHC	[45]	**II**

IHC = immunohistochemistry, PSD-95 = post synaptic density 95 kDa, PV = parvalbumin, SYP = synaptophysin, WB = western blot.

7. Imaging

Microscope imaging was performed using the Zeiss Apotome Axio Imager 2 microscope (Carl Zeiss AG, Oberkochen, Germany), processed and exported with Zeiss Zen Lite Software (Carl Zeiss AG, Oberkochen, Germany), and adjusted with Photoshop software (Adobe, San Jose, CA, USA). Imaging of electrophoresis gels (genotyping) and nitrocellulose membranes (WB) were respectively achieved using a UV or chemiluminescence Syngene apparatus (Syngene, Frederick, MD, USA) or UVP detection system (Analytic Jena US LLC, Upland, CA, USA). Pictures obtained were then annotated with Paint (Microsoft, Redmond, WA, USA) and analyzed with ImageJ version 1.47v software (National Institute of Health, Bethesda, MD, USA).

8. Dendritic spine analysis

Our collaborators Sari Lauri and Ester Orav (MIBS, University of Helsinki) performed *ex vivo* electrophysiological recordings in the Amg of *Neto2*$^{+/+}$ and *Neto2*$^{-/-}$ mice from acute brain slices. At the end of the experiment, recorded cells were filled with biocytin and later on stained by incubation with an alexa fluor-conjugated streptavidin. First, the recorded cell location was validated at the Zeiss Apotome Axio Imager 2 microscope (Carl Zeiss AG, Oberkochen, Germany) and z-stack pictures of first branch dendrites were taken to quantify the abundance of spines onto recorded cells at the Zeiss LSM 700 confocal microscope (Carl Zeiss AG, Oberkochen, Germany). Quantification and classification of spines

was achieved manually using NeuronStudio's spines classifier threshold (Computational Neurobiology and Imaging Center, Mount Sinai School of Medicine, NY, USA).

9. Statistical analysis

Results presented in this thesis were analyzed using SPSS (IBM, Armonk, NY, USA), GraphPad Prism 8 (GraphPad software, San Diego, CA, USA) and R-studio (R-studio Inc, Boston, MA, USA) programs. Normality of dependent variables was checked using the Shapiro–Wilk test and further analyzed depending on their distribution. Normally distributed variables (Shapiro–Wilk > 0.05) were processed using parametric tests (Student t-test, one-way ANOVA, mixed ANOVA, ANCOVA, repeated measures ANOVA, Generalized Estimated Equation and log rank Kaplan–Meier survival analysis), while non-normally distributed data (Shapiro–Wilk < 0.05) were analyzed by non-parametric tests (Wilcoxon and Mann–Whitney tests). Dependent variables repeatedly collected from the same animals were analyzed with mixed ANOVA (genotype or age effect) or repeated measures ANOVA (time effect). Dependent variables that could derive from the same cell, animal or picture were analyzed using Generalized Estimated Equation (GEE) analysis as previously described [107]. Chi-square ($\chi 2$) tests were performed to determine whether significant differences were present between expected (control group) and observed frequencies. Data points were considered outliers if greater than ± three standard deviations (3SD) and were excluded from the analysis. In the original publications this thesis is based on, the burden of multiple testing from the numerous behavioral tests performed was considered using Benjamini–Hockberg (BH) multiple correction testing [17, 16]. However, considering the fact that adjusted p-values will vary from the original publications if a novel BH correction is applied to the behavioral tests which compose this thesis, the author chose to present and discuss here only the nominal p-values (for adjusted p-values, see original publication **I** and **II**).

Results

1. NETO1 and NETO2 do not influence anxiety-like behavior in mice (I)

NETO1 and NETO2 both interact with native KAR subunits and regulate their function in the CNS. According to the involvement of KARs in psychiatric disorders in humans [15, 65, 125] and anxiety-like behavior in mice [105, 211, 30], we hypothesized that NETOs could regulate anxiety through their modulations on KAR functions. We carried out a comprehensive behavioral analysis of anxiety-like behaviors among *Neto1*$^{+/+}$, *Neto1*$^{-/-}$, *Neto2*$^{+/+}$ and *Neto2*$^{-/-}$ mice using tests based on approach–avoidance conflicts (EPM, EZM, OF and LD) (Table 5). In the EPM, there were no differences in the time spent in the open arms, considered as anxiogenic zones, between *Neto1*$^{+/+}$ and *Neto1*$^{-/-}$ or *Neto2*$^{+/+}$ and *Neto2*$^{-/-}$ mice. However, *Neto2*$^{-/-}$ females spent significantly less time in the closed arms (p=0.012) (Table 5), potentially indicating an anxiety-like phenotype. However, this result might also reflect an increased time spent in the central zone of the plus-shaped EPM, which can confound the analysis [28]. Thus, we tested the behaviors of *Neto2*$^{+/+}$ and *Neto2*$^{-/-}$ mice in the EZM, which in opposition to the EPM does not contain a central zone since it has a zero shape. There were no differences in the time spent in open or closed areas between genotype in the EZM, but in *Neto2*$^{-/-}$ females we observed a trend for reduced time spent in the risk assessment zones (RAZ), which represent anxiogenic zones at the edges of open and closed areas of the zero shaped maze (p=0.069) (Table 5). We did not detect differences between either *Neto1*$^{+/+}$ and *Neto1*$^{-/-}$ or *Neto2*$^{+/+}$ and *Neto2*$^{-/-}$ mice anxiety-like behaviors in the OF test. There were no differences between *Neto1*$^{+/+}$ and *Neto1*$^{-/-}$ in the LD, while *Neto2*$^{-/-}$ males spent more time in the anxiogenic light zone (p=0.040) and *Neto2*$^{-/-}$ females showed a trend for decreased latency to enter the light compartment (p=0.050) (Table 5). However, since these findings did not survive multiple testing correction (**I**), we exclude the possibility of a reduced anxiety-like behavior in LD in the absence of NETO2. Altogether, these findings showed that neither NETO1 nor NETO2 seem to regulate anxiety-like behavior in mice in tests based on approach–avoidance conflicts.

The activity phenotype of a mutant mouse can confound the analysis of behavioral measurements [28]. In addition, in the EPM, EZM and OF tests, we observed a reduced activity among *Neto2*$^{-/-}$ mice in their respective non-anxiogenic zones: closed arms (female p=0.012), closed areas (female p=0.001) and peripheral zones (male p=0.019 and female p=0.003) (Table 5). Therefore, we tested the locomotor activity of *Neto1*$^{+/+}$, *Neto1*$^{-/-}$, *Neto2*$^{+/+}$ and *Neto2*$^{-/-}$ mice in their home cage environment (HCA). We did not observe differences in their activity during either light or dark phases, the latter representing the

active phase in rodents (Table 5). Thus, *Neto2*$^{-/-}$ mice demonstrate a decreased explorative activity phenotype in novel environments, such as the EPM, EZM and OF paradigms. A novel environment represents a stressful situation in rodents. Therefore, we hypothesized that stress-related functions are impaired in the absence of NETO2 and measured stress-physiology indicators (SIH and CORT level) and depressive-like behaviors (FST and SP) in *Neto2*$^{+/+}$ and *Neto2*$^{-/-}$ mice, but did not detect differences between genotype in any of these tests (Table 5).

Approach–avoidance conflict tests are based on the analysis of passive exploration behaviors in anxious *vs* non-anxious zones, thus, a novelty-induced activity phenotype can confound the analysis [28]. Goal-oriented and active avoidance behaviors such as feeding in a novel environment during NSF or burying a potentially harmful object in the MB test are commonly performed in association with approach–avoidance assays. In the NSF test, there were no differences in the latency to reach food in a novel environment between *Neto1*$^{+/+}$ and *Neto1*$^{-/-}$ or *Neto2*$^{+/+}$ and *Neto2*$^{-/-}$ mice (Figure 15.a, Table 5). However, most of the animals did not reach the food after the five minute test period, creating a "plateau" effect. Although, it might be challenging to observe increased anxiety-like behavior effects of *Neto1* or *Neto2* ablation from NSF results due to this "plateau" effect, our results indicate that ablation of neither of them reduces hyponeophagia in mice. We also performed the MB test, in which higher burying scores are believed to demonstrate obsessive- or repetitive-like behaviors as well as, to some extent, increased anxiety-like behaviors [30]. We did not find differences in the percentage of buried marbles for either *Neto1*$^{+/+}$ *vs Neto1*$^{-/-}$ or *Neto2*$^{+/+}$ *vs Neto2*$^{-/-}$ mice (Figure 15.b, Table 5). However, the WT control groups already had high marble burying scores in this test, and it would be difficult to observe higher scores in the KO groups. Because we did not observe a reduction of marble burying score between genotype, we can conclude that neither *Neto1* nor *Neto2* ablation decreases anxiety-like behaviors in the MB test. Proper achievement of these two tests might require more appropriate settings such as increasing the NSF test length to 10–15 minutes [129, 47, 27] and measuring marbles buried in time frames shorter than 30 minutes [189]. However, neither *Neto1* nor *Neto2* ablation seems to reduce anxiety-like behaviors in NSF or MB tests. To conclude, taken together, our findings suggest that neither *Neto1* nor *Neto2* genes regulate anxiety-like behavior in mice, while *Neto2* seems to regulate novelty-induced activity.

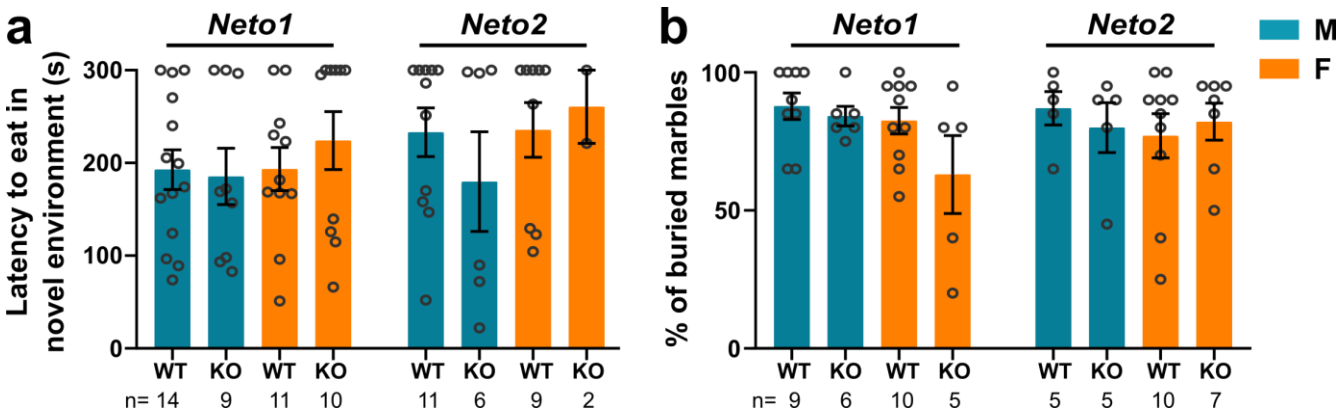

Figure 15. Behavioral results of *Neto1* and *Neto2* mouse lines in NSF and MB tests. (a) Latency to eat in a novel environment using a five-minute test (300 seconds maximum). **(b)** Percentage (%) of buried marbles after 30 minutes. Genotype effect calculated by non-parametrical Mann–Whitney test. Mean ± standard error of the mean is shown and each dot represents one animal. M=male, F=female, WT=wild type, KO=knockout.

2. NETO2 is required for normal fear expression and extinction (I)

2.1. *Neto1*$^{+/+}$, *Neto1*$^{-/-}$, *Neto2*$^{+/+}$ and *Neto2*$^{-/-}$ mice in contextual fear conditioning

We next tested *Neto1* and *Neto2* KO and WT mice in contextual FC which is a simple FC paradigm where a footshock (US) is given in the testing chamber, referred to as the context, becoming a predictor of the onset of the US. The memory of the context is referred to as multimodal because it contains several distinctive cues such as the grid or the wall and is mainly dependent on the function of the Hpc [153]. However, conditioning to the footshock (US) during contextual FC depends on the function of the Amg [153]. During the acquisition phase, we observed an increased percentage of time spent freezing throughout the process for *Neto1*$^{+/+}$, *Neto1*$^{-/-}$, *Neto2*$^{+/+}$ and *Neto2*$^{-/-}$ male and female mice, showing a proper learning of the contextual FC test. Notably, *Neto2*$^{-/-}$ male mice expressed more fear during acquisition compared to their *Neto2*$^{+/+}$ control group (p=0.013) (Table 5). On the next day, we tested context memory retrieval by placing the animals back in the conditioning chamber without presenting any footshock. *Neto1*$^{-/-}$ females froze more to the context during retrieval than *Neto1*$^{+/+}$ mice (p=0.006), suggesting a stronger memory of the context in the absence of NETO1 among female mice (Table 5). We did not observe differences between *Neto2*$^{+/+}$ and *Neto2*$^{-/-}$ mice during context retrieval of contextual FC (Table 5). Therefore, although *Neto2* ablation increases fear expression in males during acquisition, it does not influence fear recall during context presentation and thus does not affect consolidation of contextual FC memory.

2.2. *Neto1*$^{+/+}$, *Neto1*$^{-/-}$, *Neto2*$^{+/+}$ and *Neto2*$^{-/-}$ mice in cued fear conditioning

To further investigate fear-related behaviors, we used a paradigm called cued or classical FC, where a sound cue is always co-terminated by a footshock (see review of literature, section 1.2.2). Cued FC is widely used to evaluate fear-related behaviors and is mostly dependent on the function of the Amg [153]. Remarkably, *Neto2*$^{-/-}$ mice, but not *Neto1*$^{-/-}$, demonstrated higher fear expression throughout cued FC compared to *Neto2*$^{+/+}$ mice, shown by a higher percentage of time spent freezing (acquisition, males $p<0.001$, females $p=0.001$; context retrieval, males $p=0.004$, females $p=0.009$; cue retrieval, males $p=0.002$, females $p=0.002$; extinction, males $p=0.012$, females $p=0.004$; extinction retrieval, males $p=0.33$, females $p=0.010$) (Table 5).

During extinction of acquired fear, the percentage of time spent freezing was averaged by four CS presentations further referred to as blocks. We found that *Neto2*$^{-/-}$ male mice were not able to extinguish the previously acquired fear memory because their freezing level was not significantly different between the first and last block of extinction ($p=0.22$), while *Neto1*$^{+/+}$ (males $p=0.001$, females $p=0.048$), *Neto1*$^{-/-}$ (males $p=0.002$, females $p<0.001$), *Neto2*$^{+/+}$ (males $p=0.003$, females $p=0.003$), and *Neto2*$^{-/-}$ females ($p=0.005$) showed significant reductions of fear expression (Table 5). The analysis of extinction can be confounded by differences in freezing levels such as the observed *Neto2*$^{-/-}$ mice's higher fear expression levels. Therefore, to normalize fear expression levels during extinction, we performed Kaplan–Meier survival analysis. This method is commonly used to evaluate survival rates in epidemiology studies but is a useful tool to study any decreasing parameters, such as fear expression during extinction. Briefly, for each mouse we used the mean percentage of freezing during the first block of extinction as a 100% fear expression value. Then for each CS presentation a mouse was coded as either non-extinguished or extinguished when the freezing level was respectively above or below 50% of this value. We considered the obtained result as a ratio of extinguished mice. Using this analysis, we confirmed that both *Neto2*$^{-/-}$ male ($p<0.01$) and female mice ($p<0.01$) presented a delayed fear extinction in cued FC (Table 5). Female *Neto1*$^{-/-}$ mice showed a more efficient fear extinction compared to their WT littermates ($p=0.035$) (Table 5). These results suggest that *Neto1* ablation facilitates extinction of acquired memory in female mice, while *Neto2* ablation causes extinction impairment in both male and female mice.

To ensure that the increased fear expression observed in *Neto2*$^{-/-}$ *vs* *Neto2*$^{+/+}$ mice does not derive from an overall higher hearing or pain sensitivity, we performed acoustic startle reflex (ASR) and hotplate (HP) tests on *Neto2* WT and KO mice. *Neto2*$^{-/-}$ males presented lower ASR levels compared to their WT littermates, confirming that they do not exhibit a higher hearing sensitivity since they showed a reduced

reaction to acoustic stimuli. Finally, we did not observe differences between genotypes in pain sensitivity during the HP test, demonstrating that the higher fear expression of *Neto2*$^{-/-}$ mice does not derive from an overall stronger pain sensitivity.

2.3. *Neto2*$^{+/+}$ and *Neto2*$^{-/-}$ mice in spatial memory, novel object recognition and spontaneous alternation tests

Brain regions implicated in fear learning during cued FC are well-known (see review of literature section 2.3), including the Amg, mPFC and Hpc, and can be investigated individually through behavioral tests depending on brain regions of interest. Therefore, to identify the brain region(s) involved in the higher fear expression and delayed extinction observed in the absence of NETO2, our collaborator Tatiana Lipina, performed the MWM, DOR and NOR tests on *Neto2*$^{+/+}$ and *Neto2*$^{-/-}$ male mice (included in **I**). The MWM and DOR tests involve memory of spatial cues and are mainly Hpc-dependent [206]; whereas the NOR test assesses the ability to distinguish between familiar and novel objects, which mostly relies on the function of the perirhinal cortex [135, 25, 200] but might also involve the Amg and Hpc [132, 131, 165, 152]. In the MWM and DOR tests, *Neto2*$^{-/-}$ and *Neto2*$^{+/+}$ mice were both able to correctly memorize spatial cues. However, *Neto2*$^{-/-}$ mice were unable to differentiate between novel and familiar objects ($p=0.195$), while *Neto2*$^{+/+}$ mice could ($p=0.001$), demonstrating an impairment in the perirhinal cortex, Amg or Hpc functions, the brain regions involved in novel object recognition. At the LAC, we also performed the spontaneous alternation in a T-maze test that measures working memory in mice and is mostly dependent on the functions of the mPFC and Hpc [104, 43]. In this test, both WT and KO mice were able to alternate above chance levels (i.e., 50%), and there were no differences between genotype ($p=0.42$) (Table 5). To conclude, *Neto2* ablation does not affect spatial and working memory functions but is important for novel object recognition in mice. Altogether, our results demonstrate that NETO2 is required for normal fear expression and extinction, baseline startle reflex and novel object recognition in mice, while the absence of NETO1 appeared to facilitate fear recall in contextual FC and extinction in cued FC in female mice.

Table 5. Statistical analysis of genotype effect (WT *vs* KO) from the comprehensive behavioral screen performed on *Neto1* and *Neto2* mice lines **(I)**. **Significant nominal p-value p<0.05 in bold,** *trend p<0.1 in italics*. ↓ represents a reduction and ↑ an increase in KO *vs* WT of the parameters analyzed. Observed reduced anxiety-like behavior is marked in green, increased anxiety-like behavior in red and phenotypes related to a reduced activity in novel environments in purple. Fear-related phenotypes showing higher fear expression are presented in blue and delayed extinction in orange.

Test	*Analyzed parameter*	*Neto1 M*	*Neto1 F*	*Neto2 M*	*Neto2 F*
EPM	Time in open arms	0.119	0.812	0.917	0.181
	Time in closed arms	0.345	0.343	0.441	**0.012** ↓
	Distance moved in closed arms	0.565	0.141	0.135	**0.020** ↓
EZM	Time in open areas			0.253	0.331
	Time in RAZ		NT	0.485	*0.069* ↓
	Distance moved in closed areas			0.171	**0.001**↓
LD	Time in light	0.100	0.658	**0.040** ↑	0.251
	Latency to enter light	0.637	0.799	0.559	*0.050* ↓
	Distance moved in dark	0.311	0.868	0.212	0.151
OF	Time in center	0.451	0.478	0.367	0.721
	Distance in periphery	0.768	0.447	**0.019** ↓	**0.003** ↓
NSF	Latency to reach food	0.817	0.459	0.307	>0.999
MB	% of buried marbles	0.342	0.265	0.571	0.719
HCA	Activity in light	0.838	0.525	0.710	0.255
	Activity in dark	0.665	0.948	0.496	0.610
SIH	Delta temperature			0.247	0.833
CORT	CORT level in plasma		NT	0.742	0.373
SP	Saccharin preference			0.214	0.787
FST	Immobility time			0.876	0.685
Contextual FC	Freezing % during acquisition	0.142	0.807	**0.013** ↑	0.816
	Freezing % during context test	0.431	**0.006** ↑	0.290	0.821
Cued FC	Freezing % during acquisition	0.728	0.715	**<0.001** ↑	**0.002** ↑
	Freezing % during context retrieval	0.632	0.977	**0.004** ↑	**0.009** ↑
	Freezing % during cue retrieval	0.126	0.346	**0.002** ↑	**0.002** ↑
	Freezing % during extinction (ex)	0.685	0.533	**0.012** ↑	**0.004** ↑
	Freezing % during ex retrieval	0.424	0.569	0.334	**0.010** ↑
	Survival analysis	0.753	**0.035**↑	**<0.001** ↓	**<0.001** ↓
T-maze	Alternation %			0.416	0.323
ASR	Startle reflex		NT	**0.004** ↓	*0.075* ↓
Hot plate	Paw withdrawal latency			0.496	0.205

ASR = acoustic startle reflex, CORT = corticosterone, FC = fear conditioning, FST = forced swim test, HCA = home cage activity, EPM = elevated plus maze, EZM = elevated zero maze, RAZ = risk assessment zone, LD = light/dark box, MB = marble burying, NFS = novelty-suppressed feeding, NT = not tested, OF = open field, SIH = stress-induced hyperthermia, SP = saccharin preference.

2.4. NETO2 is important for fear expression and extinction already at juvenile ages (II)

Neto2 expression is down-regulated during development in rats [141]. In mice, higher fear expression levels and extinction efficiency are observed at post-weaning P23 compared to adult age [148, 149]. Therefore, we tested whether NETO2 was important for FC already at P23 juvenile age. Using cued FC with a shorter version than previously, designed to focus on fear extinction by performing it the day after fear acquisition [60], we assessed fear learning and extinction memory in *Neto2*$^{-/-}$ and *Neto2*$^{+/+}$ juvenile P23 and adult mice that were approximately 12 weeks old. By comparing WT juveniles and adults, we could validate the previous finding from the literature showing higher fear expression [148] and stronger extinction efficiency [149] at P23 compared to adult age. Notably, we demonstrated that juvenile mice already showed higher fear expression (acquisition p=0.004, extinction p=0.009) and delayed extinction (p=0.001) in the absence of NETO2 (Table 6). We also validated our previous findings showing higher fear expression (acquisition p<0.001, extinction p<0.001) and delayed extinction (p=0.0003) in *Neto2*$^{-/-}$ compared to *Neto2*$^{+/+}$ adult mice. Still, the difference in percentage of freezing between KO and WT in adult compared to juvenile mice was approximately two times larger at the end of the acquisition phase (16% *vs* 9%), during extinction habituation (20% *vs* 9%) and first extinction block (15% *vs* 6%). In addition, during fear extinction, the difference in freezing between genotypes was abolished during the last two blocks of fear extinction in juvenile mice (p=0.90 and p=0.88), while it was still significantly higher in adult *Neto2* KO compared to WT mice (p=0.007 and p=0.022). To conclude, we showed that NETO2 is needed for normal fear expression and extinction in both juvenile and adult mice.

Table 6. Statistical analysis of genotype effect (WT *vs* KO) from the behavioral analysis of juvenile and adult *Neto2*$^{+/+}$ *vs Neto2*$^{-/-}$ in cued FC **(II)**. **Significant nominal p-value p<0.05 in bold.** ↓ represents a reduction and ↑ an increase in KO *vs* WT of the parameters analyzed.

Test	*Analyzed parameter*	*P23*	*Adult*
Cued FC (short test version)	Freezing % during acquisition	**0.004** ↑	**<0.001** ↑
	Freezing % during extinction	**0.009** ↑	**<0.001** ↑
	Survival analysis	**0.001** ↓	**0.003** ↓
	Freezing % during acquisition - Hab	0.448 – 4%	0.617 – 2%
	Freezing % during acquisition - End	**0.058** ↑ **– 9%**	**<0.001** ↑ **– 16%**
	Freezing % during extinction - Hab	**0.012** ↑ **– 9%**	**<0.001** ↑ **– 20%**
	Freezing % during extinction – Block 1	0.348 – 6%	**0.021** ↑ **– 15%**
	Freezing % during extinction – Block 6	0.859 – 1%	**0.007** ↑ **– 13%**
	Freezing % during extinction – Block 7	0.881 – 0.9%	**0.022** ↑ **–9%**

Hab = habituation, End = end of training phase, Block = represents mean freezing during four CS presentations.

3. NETO2 is widely expressed in fear-related brain regions at both juvenile (II) and adult ages (I)

Due to a poor signal from the probe in the Allen Brain Atlas database [1], the *Neto2* mRNA expression pattern in fear-related brain regions was not well-established. Therefore, we investigated *Neto2* mRNA localization in both juvenile and adult mouse brains using simple and double ISH methods. First, we demonstrated that *Neto2* was widely expressed in the mPFC, Amg, dHpc and vHpc, the fear-related brain regions, in both excitatory and inhibitory neurons (Figure 16), and presented a similar pattern of expression in juveniles and adults. Interestingly at both ages, *Neto2* expression was restricted to some subregions of the fear-related brain regions. In mPFC, we could observe a few cells expressing *Neto2* in both PL and IL cortices, while several were expressing it in the Cg1 cortex. A quantification of the percentage of double positive *Neto2* cells for either *Vglut1* (vesicular glutamate transporter 1; excitatory marker) or *Gad1* (glutamate decarboxylase 1; inhibitory marker) showed that *Neto2* was equally expressed in both neuronal subtypes in the mPFC. In the Hpc, *Neto2* mRNA was found mainly in the stratum pyramidale (pyr) of CA1 and CA3. However, a few inhibitory cells were also found in other layers, such as stratum oriens (so), stratum lucidum (sl), stratum radiatum (sr) and stratum moleculare (sm) also expressed *Neto2*. In the DG, the hilus regions (hl) demonstrated the highest signal level. Interestingly, most of the cells expressing *Neto2* in the DG were excitatory while *Neto2* was equally present in both excitatory and inhibitory neurons in the CA1 and CA3 regions. Finally, in the Amg, we found *Neto2*-expressing cells in both the LA and BLA, while no signal was observed in the CE nucleus. Most of the positive cells in the LA/BLA were excitatory neurons. Also, the ITCs contained only a few cells expressing *Neto2* within their inhibitory neuron population.

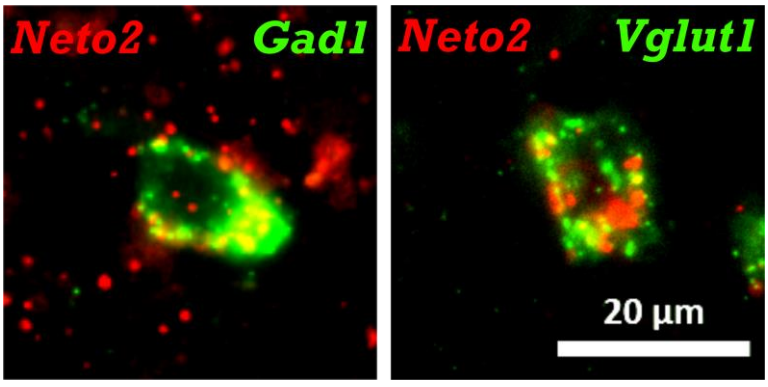

Figure 16. Representative picture showing *Neto2* signal co-localization with GABAergic (*Gad1*) and glutamatergic (*Vglut1*) neuron markers from the double ISH experiment. Gad1 = glutamate decarboxylase 1, ISH = in situ hybridization, Vglut1 = vesicular glutamate transporter 1.

In the rat Hpc, *Neto2* expression is downregulated between postnatal day 4 and 14 (P4 and P14) and is stable after P14 until P50 [141]. However, in mice little is known about the changes in *Neto2* mRNA expression between juvenile (P23) and adult ages in the fear-related brain regions (approximately P84). Therefore, we quantified *Neto2* mRNA levels at pre-weaning (P10) and post-weaning time points (P23, P42 and P84) using RT-qPCR. We selected P23 because it corresponded to the age of the juvenile group used in the cued FC and P84 as it is approximately the age of the adult group. We also chose P42 in order to have a time point between P23 and P84. In the mPFC, Amg and vHpc, there was a significant decrease in mRNA levels between pre- and post-weaning time points (mPFC $p<0.0001$, Amg $p=0.0004$ and vHpc $p<0.0001$) (Table 7). However, we did not observe differences in *Neto2* levels of expression between P23 and P42 (mPFC $p=0.30$, Amg $p=0.51$ and vHpc $p=0.41$) or between P23 and P84 time points (mPFC $p=0.37$, Amg $p=0.72$ and vHpc $p=0.12$), showing that the *Neto2* expression level is stable after P23 in the fear-related brain regions in mice (Table 7). Altogether, these results demonstrate that *Neto2* expression patterns and levels are similar at juvenile and adult ages.

Table 7. *Neto2* RT-qPCR results in WT mouse tissue from fear-related brain regions (II). The mRNA relative expression level of *Neto2* was normalized to cyclophilin and GADPH housekeeping genes expression. **Significant nominal p-value p<0.05 in bold.** *Trend p<0.1 in italics*. ↓ represents a downregulation and ↑ an upregulation through development. Pre-weaning time point P10 and post-weaning time points P23, P42 and P84.

Brain regions	*Age effect*	*Post-weaning only*	*P23 vs P42*	*P23 vs P84*
mPFC	**<0.0001** ↓	*0.05* ↑	0.30	0.37
Amg	**0.0004** ↓	0.41	0.51	0.72
vHpc	**<0.0001** ↓	0.22	0.41	0.12

Amg = amygdala, mPFC = medial prefrontal cortex, vHpc = ventral hippocampus.

4. KAR subunits GLUK2/3 and GLUK5 are reduced 20–40% at synapses in fear-related brain regions of *Neto2*$^{-/-}$ mice (I)

Because NETO2 is known to regulate GLUK2 subunit abundance at cerebellar PSDs [184], we hypothesized that its gene ablation could be responsible for changes in KAR subunit abundance in the fear-related brain regions. Consequently, we investigated GLUK2/3 and GLUK5 major KAR subunit protein levels in the mPFC, Amg and vHpc. In addition, we included the Ceb as a control brain region because it exhibits the highest level of NETO2 protein in the mouse brain [182]. We performed WB

analysis using commercially available antibodies for the major KAR subunits GLUK2/3 and GLUK5, whose specificities were previously validated on KO tissues [168, 182, 183]. First, we measured their protein level in lysates containing proteins from all cellular compartments, but did not find differences between *Neto2*$^{-/-}$ and *Neto2*$^{+/+}$ mouse samples, as previously shown in the Hpc and Ceb [185, 184]. In line with NETO and KAR protein locations being mostly synaptic [185, 184], we then investigated the effects of *Neto2* on GLUK2/3 and GLUK5 abundances at synapses. Together with M.Sc. student Emilie Rydgren, I performed synaptosomal fractionation to obtain enrichment from both pre- and post-synaptic compartments. In the absence of NETO2, we observed a significant reduction of GLUK2/3 in the vHpc (p=0.053, 20.8%) and the mPFC (p=0.026, 36.5%), while GLUK5 was significantly reduced in the vHpc (p=0.038, 23.8%) and the Amg (p=0.001, 16.9%) in the synaptosomal fraction (Table 8). Furthermore, we observed trends for a decrease of GLUK2/3 in the Amg (p=0.075, 29%) and of GLUK5 in the mPFC (p=0.059, 39.5%) (Table 8). Finally, there were no differences in either GLUK2/3 or GLUK5 abundances in the synaptosomes from Ceb of *Neto2*$^{-/-}$ *vs Neto2*$^{+/+}$ (Table 8). Taken together, our findings showed that *Neto2* ablation does reduce KAR abundance at synapses of fear-related brain regions. To conclude, the fear phenotype observed in the absence of NETO2 might derive from a reduction of synaptic GLUK2/3 and GLUK5 KAR subunits in fear-related brain regions.

5. NETO2 modulates amygdala maturity and excitability in adults (II)

5.1. Perineuronal nets and parvalbumin-expressing interneuron abundances in *Neto2*$^{+/+}$ and *Neto2*$^{-/-}$ mice

In the adult Amg, PNNs play a central role in the protection of fear memory from erasure [63], and PV interneurons are crucial for fear memory learning and consolidation [208]. In addition, PNN and PV are both considered as markers of neuronal plasticity [197]. We hypothesized that neuronal plasticity was affected in the *Neto2*$^{-/-}$ mice Amg and therefore we looked at the numbers of PNN positive cells and PV interneurons in *Neto2*$^{-/-}$ compared to WT mice. Together with M.Sc. student Adrien Gigliotta, I quantified the abundance of PNN^{+}, PV^{+} and double positive cells (PV^{+}PNN^{+}) from LA/BLA nuclei in juvenile and adult mice (Figure 17). We first showed that adult mice had a larger number of PNN^{+} ($p<0.001$), PV^{+} ($p=0.013$) and PV^{+}PNN^{+} ($p=0.0001$) cells compared to juvenile mice, as previously described [63, 215, 195]. We then compared *Neto2*$^{+/+}$ vs *Neto2*$^{-/-}$ in juveniles and adults and found no significant differences, but observed a trend for a reduced PV^{+}PNN^{+} abundance in the LA/BLA of *Neto2*$^{-/-}$ adult mice (p=0.054) (Table 8). Based on our observations in the LA/BLA, there were three times more PNN^{+} than PV^{+} cells,

and PNN-surrounding PV cells (PV^+PNN^+) represent approximately half of the PV^+ population. However, the number of PNN^+, PV^+ and PV^+/PNN^+ cells can be variable between individuals. Thus, to normalize the abundance of PV^+PNN^+ to the size of a specific cell population from each individual, we next computed the percentage of PV^+PNN^+ from both PNN and PV populations. We found a significantly reduced fraction of PV^+PNN^+ from the PNN population in the Amg of adult *Neto2*$^{-/-}$ compared to *Neto2*$^{+/+}$ mice (p=0.003) (Table 8).

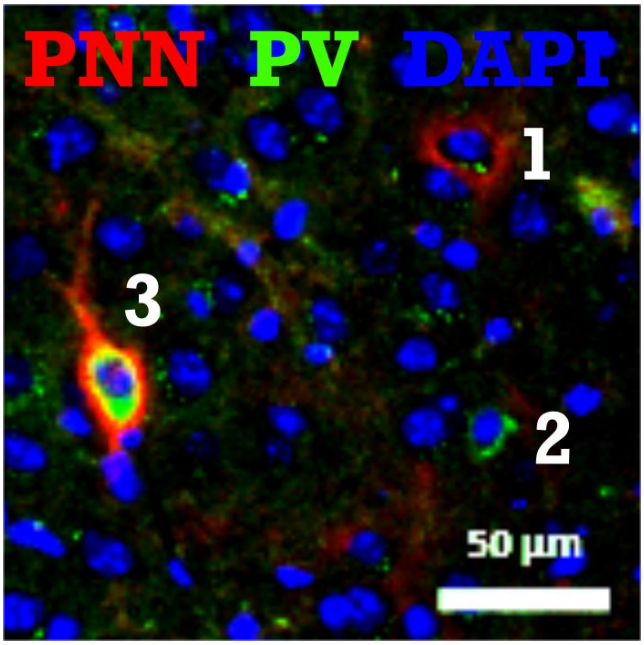

Figure 17. Representative picture showing the three classes of cells quantified in the Amg of juvenile and adult mice. **1:** PNN^+PV^-, **2:** PV^+PNN^- and **3:** PV^+PNN^+. Amg = amygdala, PNN = perineuronal nets, PV = parvalbumin, DAPI = 4′, 6-diamidino-2-phenylindole.

5.2. *Neto2*$^{-/-}$ mice present immature parvalbumin-expressing interneuron network features in the Amg

As previously described by Donato et al. (2013), the intensity of PV staining reflects the maturity of PV-inhibitory networks within the Hpc, low staining intensity being a sign of immaturity [45, 44]. Accordingly, the intensity of PV staining increases between P17 and P24 in the Amg, suggested to be the time window for the critical period in this brain region [196]. Because the reduction in $\%PV^+PNN^+$ of all PNN^+ neurons observed in the absence of NETO2 in adult mice is a potential sign of immaturity, we tested whether its gene ablation was responsible for reduced PV staining intensity in the Amg of adult mice. Thus, we measured PV staining intensity in the LA/BLA of *Neto2*$^{+/+}$ and *Neto2*$^{-/-}$ juvenile and adult mice. We first validated that the overall intensity of PV staining increases between juvenile

and adult time points by comparing WT mice results at both ages ($p<0.001$). We then showed that PV staining intensity was reduced in *Neto2*$^{-/-}$ compared to *Neto2*$^{+/+}$ in adult mice ($p=0.002$) (Table 8), indicating an immature phenotype of the Amg. However, the intensity of PV staining in the LA/BLA of *Neto2*$^{-/-}$ mice was still higher than in juveniles ($p=0.005$), suggesting that their PV-inhibitory network corresponds to an intermediate stage between juvenile and adults.

Donato et al. (2013) also suggested that the maturity of the network is reflected in the PV staining intensity when cells are divided into low-PV, intermediate-low-PV, intermediate-high-PV and high-PV intensity groups [45]. They found a higher fraction of PV cells with low-PV staining intensity at P15 *vs* adult age in mice [45]. To assess the size of different PV intensity fractions between *Neto2*$^{-/-}$ and *Neto2*$^{+/+}$ mice, using adult WT as a reference group, we divided the PV$^+$ cells into four equal fractions according to their intensity (25% of low-PV, 25% of intermediate-low-PV, 25% of intermediate-high-PV and 25% of high-PV). We then compared them with the fraction size obtained in juvenile *Neto2*$^{+/+}$, juvenile *Neto2*$^{-/-}$ and adult *Neto2*$^{-/-}$ mice using the same cut-off values. Juvenile *Neto2*$^{+/+}$ mice showed a larger percentage of low-PV (56%) than high-PV (8%) intensities and their profile was significantly different from adult *Neto2*$^{+/+}$ mice (χ^2 $p<0.0001$). As for the overall PV$^+$ intensity, there were no significant differences in the repartition of PV$^+$ within these four fractions between juvenile *Neto2*$^{+/+}$ and *Neto2*$^{-/-}$ mice (χ^2 $p=0.78$) (Table 8). Notably, in accordance with a reduced PV staining intensity, adult *Neto2*$^{-/-}$ mice showed a more immature profile than *Neto2*$^{+/+}$ mice (low-PV=36% *vs* 25% and high-PV=11% *vs* 25%, χ^2 $p=0.0023$) (Table 8). However, the adult *Neto2*$^{-/-}$ profile was still significantly different from juvenile *Neto2*$^{+/+}$ (χ^2 $p= 0.0006$) and *Neto2*$^{-/-}$ mice (χ^2 $p= 0.0001$), and as for PV staining intensity, their profile corresponded to an intermediate state between juvenile and adult ages.

5.3. NETO2 regulates excitability of the Amg

To test whether NETO2 regulates functional properties of KAR in the Amg, the key brain regions for cued FC, our collaborators Sari Lauri and Ester Orav (MIBS, University of Helsinki) recorded spontaneous activity of neurons from adult BLA subnuclei (included in **II**) (Figure 15). They first recorded spontaneous excitatory and inhibitory post-synaptic currents (sEPSC and sIPSC) and found no differences between genotype in either their amplitude or frequency. However, action potential, which occurs spontaneously during sEPSC recording, can confound the analysis of local network activity. Thus, they also measured action potential-independent glutamatergic events (miniEPSCs or mEPSCs) in the BLA and observed a significant increase in both amplitude ($p=0.013$) and frequency ($p=0.039$) of mEPSCs in *Neto2*$^{-/-}$ compared to *Neto2*$^{+/+}$ mice. This result suggests a higher excitability of local BLA

micro-circuits in the absence of NETO2. We next measured the density of dendritic spines from recorded cells and classified them as mushroom, thin or stubby spines depending on their morphological characteristics. We observed a higher spine density restricted to thin diameter dendrites in *Neto2*$^{-/-}$ compared to *Neto2*$^{+/+}$ mice (p=0.003) (Table 8). Thus, in the absence of NETO2, mEPSCs and spine density analysis point to an increased local glutamatergic synaptic transmission and connectivity, indicating stronger glutamatergic synapses in the BLA nucleus. Taken together with data collected on the PV-inhibitory network, these results demonstrate that NETO2 modulates the maturity and excitability of the Amg in adult mice. To conclude, a reduced maturity of PV-inhibitory networks tightly modulating the activity of local principal neurons via disinhibition within the Amg [208] could be at the origin of the increased glutamatergic transmission observed in *Neto2*$^{-/-}$ mice.

6. *Neto2*$^{-/-}$ mice present an increased activation of the amygdala after fear acquisition (II)

We lastly investigated the number of c-Fos positive (c-Fos^{+}) cells after fear acquisition and extinction in the Amg of adult mice. C-Fos is an immediate early gene used as a marker of neuronal activation [35], the corresponding protein appearing 60 to 120 minutes after the occurrence of many types of stimuli. We measured the abundance of c-Fos^{+} cells in the LA/BLA and CE nuclei 90 minutes after the end of acquisition or extinction of cued FC, and observed a significant increase in c-Fos^{+}/mm^{2} after fear acquisition (LA/BLA p<0.0001 and CE p=0.005), but not extinction, in the Amg of *Neto2*$^{-/-}$ compared to *Neto2*$^{+/+}$ mice (Table 8). Thus, in line with the higher excitability and lower PV-inhibitory network found in naïve mice, *Neto2*$^{-/-}$ mice that underwent fear learning showed a stronger neuronal activation in the Amg compared to their WT littermates.

The intensity of c-Fos staining in the Hpc was previously used as marker of memory strength after contextual FC [167]. We also found it increased in the CE nucleus of *Neto2*$^{-/-}$ mice after fear acquisition, compared to *Neto2*$^{+/+}$ mice (p=0.039, Table 8). This result suggests a stronger memory of the CS–US association in the CE of *Neto2*$^{-/-}$ compared to *Neto2*$^{+/+}$ mice. The CE is considered the main output nucleus for the regulation of freezing behavior [115, 190] and has recently been implicated in the formation of fear memories [170, 216]. Therefore, stronger memory of the associative learning in the CE could be responsible for a stronger fear consolidation, represented by a higher fear expression during cued FC, as is observed in the absence of NETO2. To conclude, a larger neuronal activation might derive

from immature PV-inhibitory networks and higher excitability of the Amg and is potentially responsible for better retention of fear memory in the absence of NETO2.

In naïve adult animals, we found an immature PV-inhibitory network together with higher excitability of the Amg in *Neto2*$^{-/-}$ mice. An increased disinhibition of Amg principal neurons during FC could underlie the larger neuronal recruitment we observed in the absence of NETO2. Thus, we also measured PV staining intensity after fear acquisition and extinction and found a significantly reduced intensity after acquisition of FC in the *Neto2*$^{-/-}$ compared to *Neto2*$^{+/+}$ mice ($p=0.011$), but not after fear extinction (Table 8). Similarly to Donato et al. (2013), we observed re-arrangement of PV-inhibitory networks after fear acquisition, demonstrated by a more plastic network composed of a higher proportion of low-PV intensity cells than in naïve animals (WT, χ^2 $p<0.0001$)(Table 8). In opposition, after fear extinction, PV-inhibitory networks were less plastic and contained a higher percentage of high-PV cells than naïve mice (WT, χ^2 $p=0.0041$) (Table 8). Finally, the *Neto2*$^{-/-}$ profile was significantly different from *Neto2*$^{+/+}$ mice after fear acquisition (χ^2 $p=0.031$), but not extinction.

Table 8. Statistical analysis of genotype effect (WT *vs* KO) from the analysis of cellular and molecular mechanisms underlying the *Neto2*$^{-/-}$ fear phenotype **(II)**. **Significant nominal p-value p<0.05 in bold,** *trend p<0.1 in italics*. ↓ represents a reduction and ↑ an increase in KO *vs* WT of analyzed parameters.

Experiment	*Analyzed parameter*	*Adult*	*P23*
Synaptosomal fractionation	GLUK2/3 Ratio *Neto2*$^{-/-}$ / *Neto2*$^{+/+}$ Ceb	0.41 – 3.3%	NT
	GLUK5 Ratio *Neto2*$^{-/-}$ / *Neto2*$^{+/+}$ Ceb	0.54 – 3.8%	
	GLUK2/3 Ratio *Neto2*$^{-/-}$ / *Neto2*$^{+/+}$ vHpc	**0.005** ↓ – **20.8%**	
	GLUK5 Ratio *Neto2*$^{-/-}$ / *Neto2*$^{+/+}$ vHpc	**0.026** ↓ – **23.8%**	
	GLUK2/3 Ratio *Neto2*$^{-/-}$ / *Neto2*$^{+/+}$ mPFC	**0.038** ↓ – **36.5%**	
	GLUK5 Ratio *Neto2*$^{-/-}$ / *Neto2*$^{+/+}$ mPFC	**0.059** ↓ – **39.5%**	
	GLUK2/3 Ratio *Neto2*$^{-/-}$ / *Neto2*$^{+/+}$ Amg	**0.001** ↓ – **16.9%**	
	GLUK5 Ratio *Neto2*$^{-/-}$ / *Neto2*$^{+/+}$ Amg	**0.075** ↓ – **29.0%**	
PNN and PV in the LA/BLA	PNN^{+} / mm^2	0.393	0.194
	PV^{+} / mm^2	0.108	0.993
	PV^{+}/PNN+ / mm^2	*0.054* ↓	0.679
	%PV^{+}PNN^{+} from PNN population	**0.003** ↓	0.778
	% PV^{+}PNN^{+} from PV population	0.501	0.401
	PV intensity	**0.002** ↓	0.523
	Fraction from PV intensity group	**<0.0001**	0.777
Spine density onto BLA recorded neurons	Total spine density in thin dendrites	**0.003** ↑	NT
	Thin spine density in thin dendrites	**0.041** ↑	
	Mushroom spine density in thin dendrites	**0.006** ↑	
	Stubby spine density in thin dendrites	0.695	
	Total spine density in thick dendrites	0.929	
	Thin spine density in thick dendrites	0.432	
	Mushroom spine density in thick dendrites	0.815	
	Stubby spine density in thick dendrites	0.711	
c-Fos immediate early gene after fear acquisition and extinction in the Amg	c-Fos^{+} / mm^2 in LA/BLA after acquisition	**<0.0001** ↑	NT
	c-Fos^{+} / mm^2 in CE after acquisition	**0.005** ↑	
	c-Fos^{+} / mm^2 in LA/BLA after extinction	0.641	
	c-Fos^{+} / mm^2 in CE after extinction	0.499	
	c-Fos intensity in LA/BLA after acquisition	0.943	
	c-Fos intensity in CE after acquisition	**0.035** ↑	
	c-Fos intensity in LA/BLA after extinction	0.750	
	c-Fos intensity in CE after extinction	0.212	
PV staining intensity after fear acquisition and extinction in the LA/BLA	PV intensity after acquisition	**0.011** ↓	NT
	Fraction from PV intensity group after acquisition	**0.007**	
	PV intensity after extinction	0.141	
	Fraction from PV intensity group after extinction	0.382	

Amg = amygdala, BLA = basolateral amygdala, Ceb = cerebellum, CE = central amygdala, LA = laterla amygdala, mPFC = medial prefrontal cortex, NT=not tested, PNN = perineuronal net, PV = parvalbumin, vHpc = ventral hippocampus.

Discussion

Prior to this work, the functions of NETO1 and NETO2 proteins in the regulation of anxiety and fear had not yet been investigated and very little was known about their roles in complex behaviors in mice. Only Ng et al. (2009) reported on behavioral characterization of the *Neto1*$^{-/-}$ mouse phenotype using spatial memory tests, showing the importance of NETO1 for spatial learning and memory [139]. In this thesis, I performed a comprehensive analysis of anxiety-like and fear-related behavior in *Neto1*$^{+/+}$, *Neto1*$^{-/-}$, *Neto2*$^{+/+}$ and *Neto2*$^{-/-}$ mice. Based on this broad behavioral analysis, this work sheds light on the central role of NETO2 for normal fear expression and extinction. Notably, this study shows that the phenotype of mice lacking the *Neto2* gene is reminiscent of symptoms from PTSD patients, such as higher fear expression and impaired extinction [143, 20], offering *Neto2*$^{-/-}$ mice as a PTSD-like model to further investigate molecular mechanisms of fear-related disorders in humans.

We first characterized *Neto1*$^{+/+}$, *Neto1*$^{-/-}$, *Neto2*$^{+/+}$ and *Neto2*$^{-/-}$ mice phenotypes by performing anxiety-like tests based on approach–avoidance conflicts with high face and predictive validity [67, 28, 191]. In the approach–avoidance assays, we did not find differences in anxiety-like behaviors between *Neto1*$^{+/+}$ and *Neto1*$^{-/-}$ or *Neto2*$^{+/+}$ and *Neto2*$^{-/-}$ mice, while *Neto2*$^{-/-}$ mice presented a reduced activity phenotype in EPM, EZM and OF tests. A reduced locomotor activity in tests based on exploration behavior may appear as an increased anxiety-like behavior and therefore confound the analysis [28]. However, during HCA measurements *Neto2*$^{-/-}$ did not show differences in activity compared to their WT littermates, suggesting that their reduced activity in approach–avoidance assays is induced by novelty rather than by reduced overall locomotor activity. Due to the novelty aspect of approach–avoidance conflict tests together with the fact that they are based on passive exploration behaviors, increased spontaneous motor activity represents a confounder in these tests [28]. This drawback can be avoided using alternative tests based on active avoidance or goal-oriented behaviors such as spontaneous marble burying during the MB test or reaching for food pellets in the NSF test [28]. In MB and NSF tests, we did not find effects of *Neto2* ablation on the percentage of marbles buried or latency to reach for food. Because a novel environment can represent a stressful situation, we tested whether NETO2 influences stress physiology and depression-like behaviors in mice, but did not observe differences between *Neto2*$^{+/+}$ and *Neto2*$^{-/-}$ mice. Altogether, these results suggest that neither *Neto1* nor *Neto2* regulate anxiety-like behavior in mice, while *Neto2* seems to affect activity in novel environments in mice without influencing locomotor activity, stress physiology or depression-like behaviors.

To investigate the potential roles of NETOs in the regulation of fear learning, we performed FC on *Neto1*$^{+/+}$, *Neto1*$^{-/-}$, *Neto2*$^{+/+}$ and *Neto2*$^{-/-}$ mice. In cued FC, *Neto2*$^{-/-}$, but not *Neto1*$^{-/-}$, demonstrated a clear phenotype when compared to their WT littermates: higher fear expression and delayed extinction. Notably, we were able to replicate these results using a different cohort of animals in a shorter cued FC test version [60], demonstrating the high reproducibility of the fear phenotype observed in the absence of NETO2. Because footshock nociception and hearing sensitivity to a CS auditory cue can affect fear expression during FC, we measured *Neto2*$^{+/+}$ and *Neto2*$^{-/-}$ mice latency for paw withdrawal or licking behaviors on an HP and whole body startle reflex induced by loud acoustic stimulus presentation in ASR test. We found that *Neto2*$^{-/-}$ mice were not differently sensitive to pain compared to their WT littermates. Notably, male mice lacking *Neto2* demonstrated lower startle responses to acoustic stimuli during the ASR test, confirming that they do not have higher hearing sensitivity. In stressful situations, the Amg is the relay nucleus for sensory stimulus processing, receiving information from both the TH and sensory cortex [113, 110]. In the Amg, acoustic stimuli are processed in the LA [191] and defensive responses originate from the CE [190]. Both FC and ASR can be considered stressful events and freezing and startling are defensive responses. Therefore, during both FC and ASR, sensory information processing and defensive response pathways converge in the Amg. Because we observed differences between genotypes during these two behavioral tests, the Amg might play a central role in the *Neto2*$^{-/-}$ mice fear and startle phenotypes.

To test whether NETO2 is involved in the regulation of other types of memory, our collaborator Tatiana Lipina performed supplementary behavioral testing (MWM, NOR and DOR tests), and we measured spontaneous alternation using a T-maze test. These tests established that differentiation between novel and familiar objects was affected by *Neto2* ablation during the NOR test, whereas no differences between genotypes were observed during spatial memory in MWM and DOR tests or working memory in the T-maze. With MWM and DOR tests being Hpc-dependent [206, 210] and T-maze mPFC- and Hpc-dependent [104, 43], *Neto2*$^{-/-}$ mice do not seem to present gross abnormalities in these two brain regions. These results indicate that NETO2 might be involved in the circuit underlying novel object recognition, including mostly the perirhinal cortex [135, 25, 200] but also possibly the Amg and Hpc [132, 131, 165, 152] . However, in rats the involvement of the Amg and Hpc in novel object recognition is controversial [6, 135, 10, 25, 14, 200, 9], and very little is known about the neuronal circuits underlying the recognition of novel objects in mice. In addition to fear expression level, fear extinction and acoustic startle reflex, the recognition of novel objects was affected in the absence of NETO2. The Amg is required for acoustic

stimuli processing during fear-inducing situations [113, 110], defensive responses [115, 190], fear memory [113, 50, 36, 73, 88, 78, 191], and might play a role in novel object recognition [132, 131]. Therefore, this brain region is likely to play a part in *Neto2*$^{-/-}$ higher fear expression and delayed extinction, lower acoustic startle reflex and defects in recognition between novel and familiar objects compare to *Neto2*$^{+/+}$ mice.

The *Neto2*$^{-/-}$ mice had significantly higher fear expression and delayed extinction in cued FC compared to WT mice. Higher fear expression after acquired fear learning potentially indicates a stronger memory of the CS–US association, evocative of the enhanced conditionability trait observed in humans [143]. Notably, both higher conditionability and impaired extinction are symptoms of PTSD [143, 20], and correspond to the *Neto2*$^{-/-}$ mice phenotype in cued FC. In addition, while anxiety and fear-related disorders, including PTSD, usually associate with exaggerated baseline startle reflex [144, 157], PSTD patients sometimes demonstrate reduced startle responses [142, 128], comparable to the *Neto2*$^{-/-}$ mice startle phenotype. Imaging studies from PTSD patients compared to control individuals showed that the Amg presented higher responsivity in both neutral and fear-inducing situations [177]. Furthermore, impairments in Amg-dependent tests have been previously associated with fear-related phenotypes in mice and humans [166]. Therefore, focusing on the function of the Amg might reveal the molecular and cellular mechanisms behind the higher fear expression and extinction phenotype observed in the absence of NETO2.

Regarding the role of NETO1 in anxiety and fear, we did not observe any effect of *Neto1* ablation in anxiety-like behaviors and detected few differences between *Neto1*$^{+/+}$ and *Neto1*$^{-/-}$ mice during FC. Interestingly, *Neto1* ablation seemed to facilitate fear recall during contextual FC and fear extinction during cued FC. Although NETO1 and NETO2 are homologous proteins, our results from the comprehensive behavioral screen performed on *Neto1*$^{+/+}$, *Neto1*$^{-/-}$, *Neto2*$^{+/+}$ and *Neto2*$^{-/-}$ mice suggest that they play divergent roles in the adult mouse brain. An earlier study focusing on the phenotype of *Neto1*$^{-/-}$ mice in spatial memory tests showed impaired retention of spatial cues in the absence of NETO1 during MWM and DOR tests [139]. The MWM and DOR are mainly dependent on the function of the Hpc, thus these findings are in the line with the highest levels of NETO1 protein being found in this brain region [182]. By performing the same tests on *Neto2*$^{-/-}$ and *Neto2*$^{+/+}$ mice, our collaborator Tatiana Lipina showed that there was no spatial memory deficit in MWM and DOR tests in the absence of NETO2, confirming the distinct roles of NETO1 and NETO2 in mice. Notably, in the NOR test, *Neto1*$^{-/-}$ mice were able to differentiate between novel and familiar objects [139], while *Neto2*$^{-/-}$ mice failed. In

addition, previous studies showed that NETO1, but not NETO2, modulates major KAR subunit abundance at PSDs in the Hpc [182, 185]; whereas NETO2 regulated GLUK2 abundance at cerebellar PSDs [184], where its protein level is the highest [182]. However, in the Amg, mPFC and vHpc, we showed that both GLUK2/3 and GLUK5 KAR subunits were reduced at synaptosomes, including both pre- and post-synaptic compartments, in the absence of NETO2. In addition, in the Ceb we did not detect differences in GLUK2/3 and GLUK5 abundances at synapses between *Neto2*$^{+/+}$ and *Neto2*$^{-/-}$ mice. Although it is not known whether *Neto1* ablation affects KAR abundance at synapses in the Amg, mPFC and Ceb regions, these results indicate distinct modulation of NETO1 and NETO2 on KAR subunit abundances depending on the brain region and subcellular compartment. Taken together, these findings demonstrate that these two homologous proteins play very distinct roles, in association with their different interaction partners and spatially-restricted expression patterns in the adult mouse brain.

To assess the molecular mechanisms underlying the higher fear expression and delayed extinction due to *Neto2* ablation, we further investigated the abundance of KARs in fear-related brain regions. Based on the study by Tang et al. (2012) showing a reduced abundance of GLUK2 subunits at cerebellar PSDs of *Neto2*$^{-/-}$ mice [184], we tested whether *Neto2* ablation affects abundances of major KAR subunits at synapses of fear-related brain regions. We analyzed protein levels in synaptosomal fractions from the mPFC, Amg and vHpc, composing the main fear network. We found a 20–40% reduction of GLUK2/3 and GLUK5 abundances at synapses of *Neto2*$^{-/-}$ mice compared to their WT littermates in these brain regions. The lower abundance might derive from deficits in trafficking, delivery or stability of KAR subunits to the synapses in the absence of NETO2 [185, 184, 213]. Notably, *Neto1* ablation reduced major KAR subunits in hippocampal PSDs together with lower EPSCs mediated by both KARs and NMDARs [185]. Therefore, NETO2 absence may affect KAR synaptic transmission in fear-related brain regions via a reduction of major subunit abundances at synapses, resulting in higher fear expression and delayed extinction. We did not observe differences in GLUK2/3 and GLUK5 abundances in the synaptosomal fraction from Ceb, which is surprising based on previous findings showing a 40% reduction of GLUK2 at *Neto2*$^{-/-}$ cerebellar PSDs [184]. However, this discrepancy might arise from the dissimilarities between investigating post-synaptic density (PSD) only [184] compared to synaptosomal fractions which are composed of both pre- and post-synaptic compartments. This difference might also originate from the specificity of the primary antibody since Tang et al. (2009) used an antibody directed only against GLUK2 subunits [184], while we selected an antibody recognizing GLUK2 and 3 subunits. To conclude, our results established a reduction of major KAR subunits at synapses of fear-related brain

regions in *Neto2* KO mice, potentially underlying the higher fear expression and delayed extinction observed in the absence of NETO2.

Fear expression is stronger and extinction efficiency better in P23 juvenile mice compared to adults [148, 149]. Thus, we tested whether NETO2 influenced fear already at this younger age. Although we found higher fear expression and delayed extinction in both juvenile and adult mice, the increased fear expression due to *Neto2* ablation was twofold higher amongst adults. Another major difference observed in the absence of NETO2 between these two time points concerns extinction, during which both juveniles and adults demonstrated delays but with distinct efficiencies. Juvenile $Neto2^{-/-}$ mice fear expression levels were not significantly different from the $Neto2^{+/+}$ mice in the two last blocks of extinction, while adult $Neto2^{-/-}$ mice remained significantly different from $Neto2^{+/+}$ mice at the end of extinction. Notably, *Neto2* expression levels and patterns were the same at these two ages. In adults, fear learning and memory are mediated by reciprocal connections within the mPFC-Amg-vHpc network, where specific circuits modulate different features of FC [28, 191]. Although FC appears to involve the same brain regions at juvenile and adult ages [102, 99, 77, 148, 149], little is known about the specific circuits or molecular mechanisms implicated at P23. By measuring the activity of neurons from mPFC PL and IL cortices after fear acquisition and extinction, Pattwell et al. (2012) showed that these regions are activated during fear learning and extinction at both juvenile and adult ages [149]. However, the higher fear expression and extinction efficiency at P23 compared to adult age [148, 149] demonstrate dissimilarities in fear memory features between these two time points in mice. On the one hand, we can speculate that differences in the effect of *Neto2* ablation observed between these two ages derives from distinction in the molecular mechanisms involved in FC. On the other hand, brain maturation processes are still ongoing at P23 [40], considered a pre-adolescent stage in mice [149]. Thus, at P23 the strength of the connections and the plasticity of the fear network might differ from adults [40], potentially explaining the higher fear expression and extinction efficiency of juvenile mice compared to adults.

To investigate cellular mechanisms behind the higher fear expression and delayed extinction of $Neto2^{-/-}$ mice, we further focused on the Amg, the central brain region for fear-inducing stimulus processing and fear memory consolidation. Because PV and PNN populations are known to regulate fear memory consolidation and extinction efficiency, and can be used as markers of neuronal plasticity [63, 208, 69], we measured their abundances in both juvenile and adult $Neto2^{-/-}$ and $Neto2^{+/+}$ mice. We found a significantly reduced percentage of $PV^{+}PNN^{+}$ from the PNN population in the Amg of adult $Neto2^{-/-}$ compared to $Neto2^{+/+}$ mice. Similarly to *Neto2* ablation, chronic fluoxetine treatment, known to re-open

critical period-like states in the adult brain, also causes a reduction of percentage of PV^+PNN^+ relative to the PNN population, thus interpreted as an immature state of the Amg [94].

A reduction in this specific fraction without changes in PNN abundances could indicate that the ablation of *Neto2* causes PNNs to surround a smaller proportion of PV^+ neurons (Figure 18, hypothesis 1). However, the enzymatic degradation of PNNs in the Amg of adult mice does not affect fear expression after acquisition [63]. Therefore, PNNs do not seem required for correct fear processing and learning in the mature Amg, and their presence around another neuronal population seems unlikely to underlie the *Neto2*$^{-/-}$ fear phenotype. Another plausible interpretation for the reduced percentage of PV^+PNN^+ relative to the PNN population could originate from a reduction in PV protein levels under the threshold of detection by immunohistochemistry method in the absence of NETO2 (Figure 18, hypothesis 2). Because this method is based on protein detection via an antibody recognizing PV proteins specifically, the staining intensity can be used as an indicator of protein levels. Therefore, we assessed PV^+ staining intensity in the Amg. In adult *Neto2*$^{-/-}$ mice, the overall PV staining intensity was reduced compared to *Neto2*$^{+/+}$ mice, further strengthening our second hypothesis (Figure18, hypothesis 2).

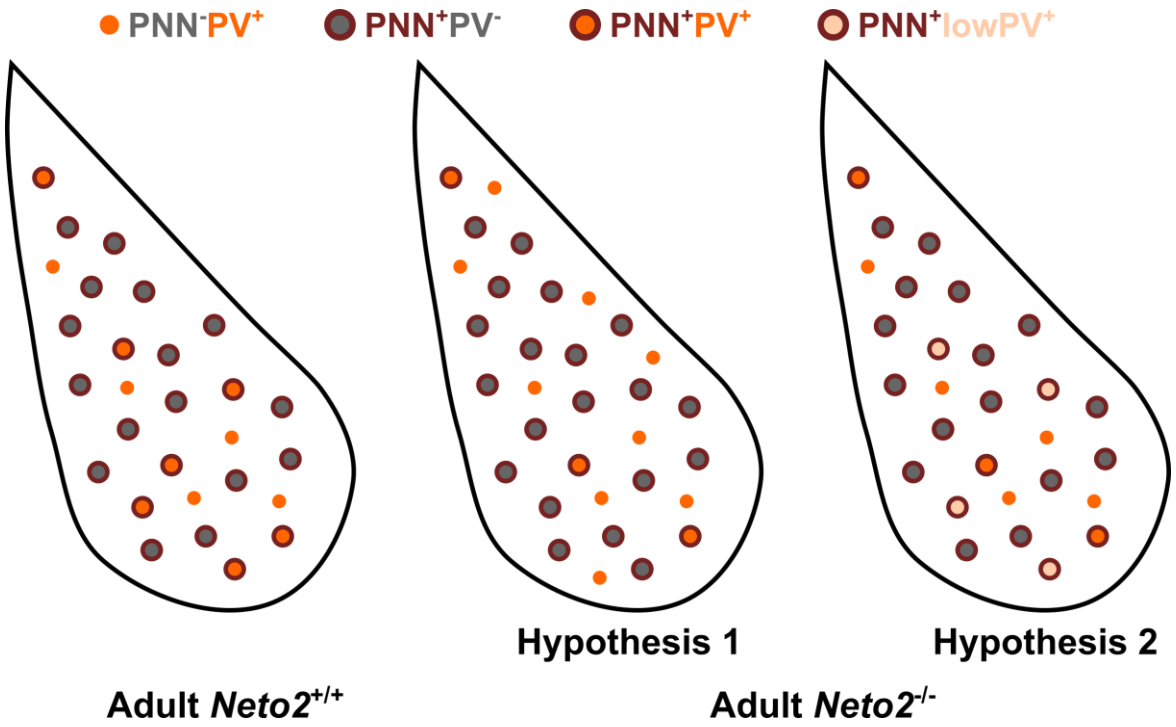

Figure 18. Graphical representation of PNN and PV cellular populations from the LA/BLA of *Neto2*$^{+/+}$ and *Neto2*$^{-/-}$ mice describing two possible theories for the reduced % of PV^+PNN^+ relative to PNN populations. BLA = basolateral amygdala, LA = lateral amygdala, PNN = perineuronal net, PV = parvalbumin.

The intensity of PV staining is believed to reflect the maturity of PV-inhibitory networks within the Hpc, low staining intensity being a sign of immaturity [45]. By comparing PV intensity between *Neto2*$^{-/-}$ and *Neto2*$^{+/+}$ adult mice, we found that PV-inhibitory networks within the Amg presented an immature state in the absence of NETO2, representative of an intermediate state between juvenile and adult time points. Because a PV neuron level of maturity negatively correlates with its level of plasticity [45, 44, 197], the immature-like PV staining intensity found in adult *Neto2*$^{-/-}$ mice suggests higher plasticity of PV cells within the Amg, which corresponds to a plastic state between those of juvenile and adult mice. To further investigate the PV cell population, we divided them in low-PV, int-low-PV, int-high-PV and high-PV fractions depending on their staining intensity, respectively representing high, int-high, int-low and low plasticity groups [45], and confirmed that PV-inhibitory networks of adult *Neto2*$^{-/-}$ mice had an intermediate profile between juvenile and adult *Neto2*$^{+/+}$ mice (Figure 19). In summary, the reduced percentage of PV^{+}PNN^{+} from the PNN population together with the lower PV intensity found in the absence of NETO2 suggests immature features of the Amg at adult age corresponding to an intermediate state between juveniles and adults in WT mice. Notably, fear expression levels of adult *Neto2*$^{-/-}$ mice, but not their extinction efficiency, correspond to an intermediate level between juvenile and adult *Neto2*$^{+/+}$ mice (Figure 19). Disinhibition of Amg micro-circuits by PV neurons is required for the processing and consolidation of fear memory [208], while their role in fear extinction memory remains poorly understood. Although, it is unclear whether the immature feature of PV networks within the Amg modulates fear extinction, the immaturity of PV-inhibitory networks present in adult mice in the absence of NETO2 could be at the origin of the higher fear expression phenotype through a reduced disinhibition of Amg micro-circuits.

Figure 19. Graphical representation of PV neuron staining intensity from the LA/BLA nucleus of juvenile and adult *Neto2*$^{+/+}$ and adult *Neto2*$^{-/-}$ mice and their corresponding level of fear expression and extinction efficiency in cued FC. BLA = basolateral amygdala, FC = fear conditioning, int = intermediate, LA = lateral amygdala, PV = parvalbumin.

Because a reduced disinhibition of Amg micro-circuits would most likely affect the excitability of the neurons within this brain region, our collaborators Sari Lauri and Ester Orav investigated spontaneous activity of neurons from the BLA in adult *Neto2*$^{+/+}$ and *Neto2*$^{-/-}$ mice. They did not find differences in spontaneous glutamatergic or GABAergic currents between genotype, but showed stronger glutamatergic synapses in the Amg of *Neto2*$^{-/-}$ compared to *Neto2*$^{+/+}$ mice, as both mEPSC amplitude and frequency were increased. The higher mEPSC features in the BLA of *Neto2*$^{-/-}$ mice can be interpreted as an increased local excitability, which based on the absence of differences in sEPSC/sIPSC features

between genotype seem to be compensated for at the network level. To test whether spine density could be affected by *Neto2* ablation, we measured their abundances onto dendrites from recorded neurons and reported that thin diameter dendrites have a higher spine density in *Neto2*$^{-/-}$ compared to *Neto2*$^{+/+}$ mice. Because the organization of the dendritic tree of Amg neurons displays heterogeneous morphological features [126], the restriction of this finding to a certain size of dendrites is difficult to interpret. Dendritic branching and spine analysis have been investigated more often from pyramidal neurons of the Hpc, which, as opposed to neurons from the Amg, present highly homogeneous morphological features, such as their diameter within similar levels of branching [181]. Diameter of dendrites might reflect their capacity for anterograde and retrograde trafficking of proteins and organelles, which correlates with strength of activation and neuronal plasticity [96, 64]. Thus, because increased spine density was restricted to thin dendrites, it suggests that pre-synaptic neurons make more synapses with weakly activated dendrites in the absence of NETO2. Weak dendrite activation is observed at early developmental stage, when pruning did not occur yet [32], thus, this finding correlates with the immature and more plastic PV-inhibitory network within BLA micro-circuit. To conclude, an increased local excitability of BLA neurons is coherent with a reduced disinhibition of the Amg micro-circuit due to the immature PV-inhibitory network of *Neto2*$^{-/-}$ mice. Because PV neurons within the BLA play a central part in associative fear learning [208], we can hypothesize that they critically contribute to the *Neto2* higher fear expression phenotype. However, confirming this hypothesis would require demonstration of a causal link between NETO2, PV maturity networks, BLA micro-circuit excitability and connectivity, and fear memory.

To test whether a difference in neuronal recruitment occurs during FC in the absence of NETO2, we examined the abundance of the c-Fos immediate early gene in the Amg of *Neto2*$^{-/-}$mice after fear acquisition and extinction. The staining of c-Fos protein has been widely used as a marker for neuronal activation [35]. In addition, c-Fos^{+} neurons within the BLA increase with fear expression levels after associative learning [79, 158]. In the absence of NETO2, we found a higher c-Fos abundance after fear acquisition, but not extinction, suggestive of an enhanced neuronal activation after fear learning. Thus, immature features of PV-inhibitory networks together with stronger glutamatergic synapses observed in the Amg prior to FC could be responsible for a higher recruitment of neurons during fear acquisition, possibly underlying stronger fear expression in *Neto2*$^{-/-}$ mice. Ruediger et al. (2011) have suggested that the intensity of c-Fos staining after FC is an indicator of the strength of acquired fear memory [167]. To test whether the higher fear expression phenotype in *Neto2*$^{-/-}$ mice, potentially demonstrating a higher

memory of the CS–US associative learning, is associated with an increase in c-Fos staining intensity, we analyzed the intensity of the staining in the Amg after fear acquisition and extinction. After fear acquisition, we found a stronger intensity of c-Fos staining within the CE, the relay nucleus for fear expression [115, 36, 190], also involved in the consolidation of fear memory [170, 203, 216]. These results strengthen the hypothesis according to which higher *Neto2*$^{-/-}$ fear expression corresponds to a stronger memory of the CS–US associative learning and suggest that the enhanced fear memory could originate from stable changes occurring in the CE nucleus after fear acquisition, but this would require further validation such as recording the activity of neurons within this nucleus in the absence of NETO2.

Interestingly, our ISH analysis demonstrated that *Neto2* is not expressed in the CE. However, during the acquisition of fear, projections from the LA and BLA tightly regulate the activity of output neurons from the CEm responsible for freezing behavior [166, 117]. Therefore, we can hypothesize that the immaturity and higher excitability from the BLA found in the absence of NETO2 may affect CEm neuron activity. Recently, Arora et al. (2018) demonstrated that similarly to *Neto2* ablation, *Grik4* over-expression was associated with an increase in mEPSC amplitude and frequency in the BLA [8]. By measuring the input from BLA to CEl nuclei, they further showed that this increased local excitability from the BLA is associated with enhanced or reduced EPSC features from the two distinct populations of neurons from the CEl [8], commonly referred to as CEl-OFF and CEl-ON neurons [73]. CEl-OFF neurons project onto CEm output neurons that regulate fear expression, while CEl-ON neurons locally inhibit CEl-OFF to modulate the activity of CEm interneurons. Accordingly, Wu et al. (2002) showed that GLUK1-containing KARs, which usually contain either GRIK4 or GRIK5 [8], are involved in the regulation of local inhibitory networks and modulate excitatory inputs from the BLA to the CE via increased excitability of Amg interneurons [211]. Thus, in *Neto2*$^{-/-}$ adult mice, higher excitability of BLA neurons could underlie comparable modulation in the CE neurons and thus the increased neuronal activation observed in this nucleus after fear acquisition. Notably, in the Amg of *Neto2*$^{-/-}$ mice, we demonstrated a significant reduction of GLUK2/3 and GLUK5 KAR subunit abundances at synapses. In the mouse brain, the restriction of KAR subunit expression and localization to different brain regions, cell types and subcellular compartments allows for distinct functions of KARs, depending on their subunit composition [204, 147, 86, 209, 201]. Therefore, depending on the restricted GLUK2/3 and GLUK5 localization and KAR assembling patterns in the Amg, a reduction of these subunits at the synapses might be at the origin of the increased excitability of BLA neurons and consequently the neuronal activation in *Neto2*$^{-/-}$ after fear acquisition in these two subnuclei.

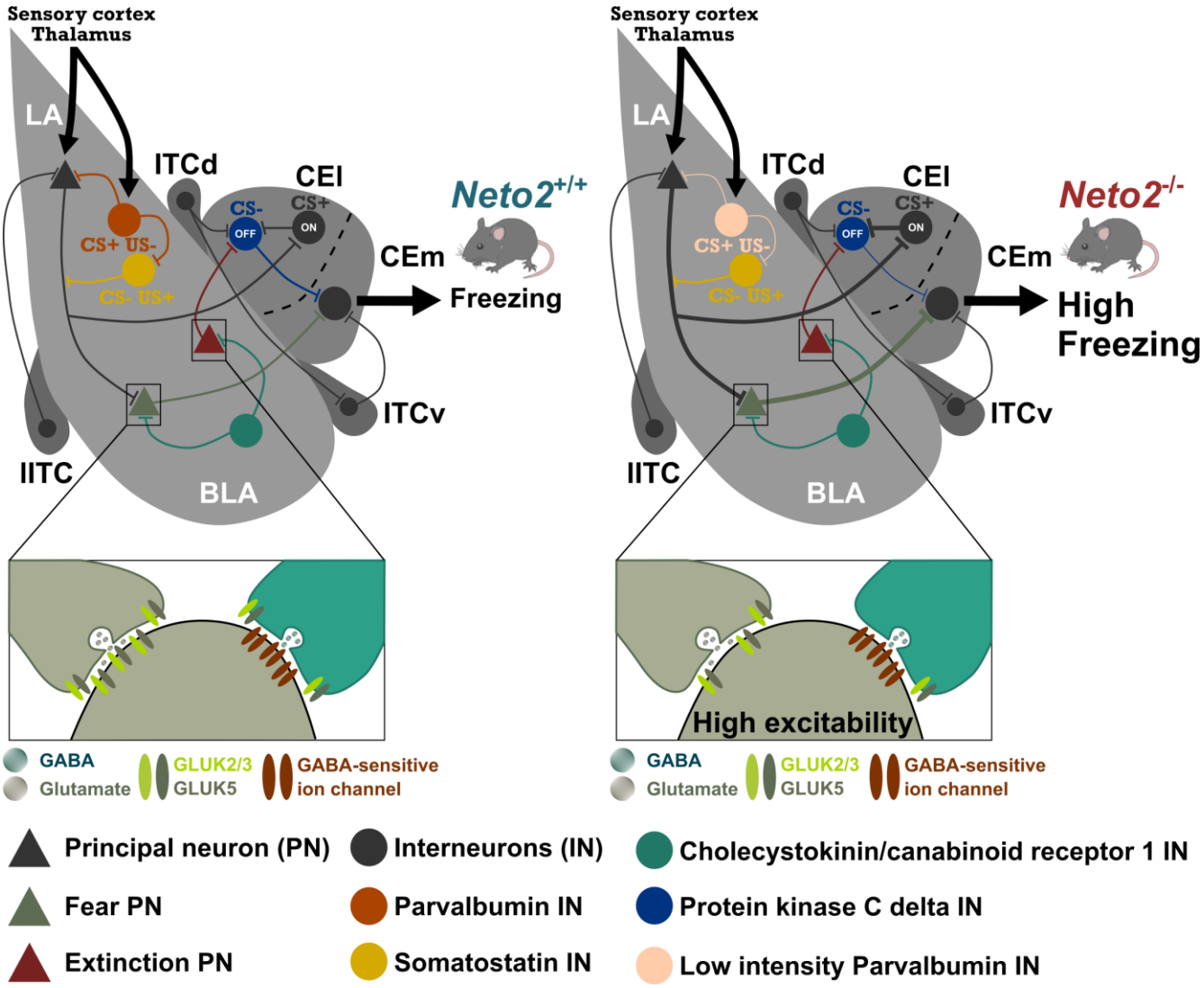

Figure 20. Summary figure representing the hypothetical cellular and molecular mechanisms underlying the higher fear expression observed in the absence of NETO2 in mice. BLA = basolateral amygdala, CEl = lateral central amygdala, CEm = medial central amygdala, CS = conditioned stimulus, GABA = γ-aminobutyric acid, IN = interneuron, ITCd = dorsal intercalated cells, ITCv = ventral intercalated cells, LA = lateral amygdala, lITC = lateral intercalated cells, PN = principal neuron, PV = parvalbumin-expressing interneuron, US = unconditioned stimulus.

In the juvenile mouse Amg, we did not find a difference between genotypes for PNN^+, PV^+ and PV^+PNN^+ abundances or PV staining intensity, indicating that the higher fear expression and delayed extinction observed in *Neto2*$^{-/-}$ mice at this age does not originate from an immaturity of PV-inhibitory networks in the Amg. Because little is known about the cellular and molecular mechanisms involved in FC at P23, further investigation of cell subsets other than PV or PNN from the Amg or of the mPFC or vHpc brain regions, which are also part of the main fear network, would be required to fully understand the *Neto2*$^{-/-}$

mice fear phenotype. Finally, although there was still a significant difference in freezing level between *Neto2*$^{-/-}$ and *Neto2*$^{+/+}$ adult mice at the end of fear extinction, we did not see differences in either c-Fos^{+} cell abundance or staining intensity between genotypes in the group of mice that underwent fear extinction. This result suggests that some of the features of the fear expression and delayed extinction phenotypes among *Neto2*$^{-/-}$ adult mice might derive from changes occurring in other brain regions. Within the main fear network, extinction is mainly dependent on the function of the IL area of the mPFC [76, 77, 173, 21] through reciprocal connections with the Amg, which involves equivalent numbers of input *vs* output projections [76]. Thus, the increased neuronal activation observed in the Amg of *Neto2*$^{-/-}$ mice after fear learning could be responsible for the input/output imbalance in this Amg-mPFC circuit and subsequently underlie the difference in fear expression still present at the end of extinction between *Neto2*$^{-/-}$ and *Neto2*$^{+/+}$ mice.

Concluding remarks and future prospects

In this thesis work, we demonstrated for the first time that NETO2 is required for normal fear expression and extinction in mice at both juvenile and adult ages. In adults, we showed that NETO2 modulates KAR subunit abundances at synapses of the mPFC, Amg and vHpc, the brain regions composing the main fear network. Notably, *Neto2* gene ablation was associated with immature features and stronger glutamatergic synapses in the adult Amg. Neuronal activation in the Amg was increased after fear acquisition in the absence of NETO2. Therefore, we hypothesized that the enhanced activation of the Amg could be at the origin of the higher fear expression of *Neto2*$^{-/-}$ mice after cued FC, which we suggested as a mark of higher conditionability.

Altogether, this work has allowed for an advanced understanding of *Neto2* functions in the adult mouse brain by studying its precise role in fear learning and in the maturation and excitability of the Amg, the key brain region for fear memory processing. However, a complete understanding of the molecular mechanisms behind the higher fear expression and delayed extinction as a consequence of *Neto2* ablation may require additional investigations. Notably, mechanisms through which the higher fear phenotype is established in juveniles or remains after fear extinction in adult *Neto2*$^{-/-}$ mice are yet to be established. In addition, manipulation of the different cell subsets within the Amg to demonstrate a causal link between NETO2, PV networks, local excitability and fear memory would allow for better understanding of the role of NETO2 in fear learning and extinction.

The *Neto2*$^{-/-}$ mouse used in this study is a full KO model, meaning that NETO2 is absent from all the brain regions as well as peripheral tissues. Because, *Neto2* is expressed in several peripheral tissues [3], its ablation is potentially responsible for physiological changes that could affect mouse behavior. In addition, in full KO models, the gene is absent throughout development and compensating mechanisms might have occurred at the two time points studied in this thesis work. Therefore, the use of precise techniques to KO or knock down (KD) a gene in only a specific brain region or subset of cells represents an interesting tool to further study the role of NETO2 in fear memory. As an example, performing FC on mice with a KD of *Neto2* precisely in the PV population of the Amg by stereotaxic injection of cell type–specific short interfering RNA (siRNA) [127] may allow us to establish a causal link between PV-inhibitory networks and the role of NETO2 in fear expression and extinction. In addition, we demonstrated that the adult Amg presented immature features in the absence of NETO2, mostly based on the observed reduced PV-inhibitory networks. One mechanism through which PV cells mature is by

capturing OTX2 transcription factor from the environment via their surrounding PNN [18]. Therefore, OTX2 and PV protein levels could be examined in the Amg of *Neto2*$^{-/-}$ *vs Neto2*$^{+/+}$ mice using the WB method.

We established that local excitability of BLA neurons was modulated by NETO2 at a naive state. However, investigating their physiology after fear acquisition and extinction [148, 149] might unravel the functional mechanisms through which the fear phenotype is established in adult *Neto2* KO mice. Although the recording of local neuronal activity could highlight some excitability changes in the BLA after fear acquisition, studying the physiology of the Amg micro-circuit within BLA-CE connectivity as previously studied on a *Grik4* over-expression model [8] might shed light on the precise cell subsets from the CE involved in the *Neto2*$^{-/-}$ fear expression phenotype after fear acquisition. Finally, we could strengthen the link between higher fear expression and higher conditionability by studying LTP, the molecular mechanisms through which memory is believed to consolidate [74, 172, 88], in the Amg of *Neto2*$^{-/-}$ mice.

Taken together, findings from this thesis work have shed light on NETO1 and NETO2 involvement in complex behaviors related to anxiety and fear in mice. Notably, this work has provided an advanced understanding of the role of the NETO2 protein in the regulation of fear expression and extinction memory through the modulation of Amg maturity and excitability. Finally, the *Neto2*$^{-/-}$ fear phenotype in mice being evocative of symptoms of PTSD in humans, the molecular and cellular mechanisms described in this thesis represent attractive candidates to further investigate fear-related disorders in humans and to potentially discover new effective compounds to treat these diseases.

Acknowledgments

The current study was carried out in the neurogenomics laboratory at the Faculty of Biological and Environmental Sciences, University of Helsinki, Finland and was supported by Jane and Aatos Erkko Foundation, Oskar Öflund Foundation, Finnish Cultural Foundation and Jalmari and Rauha ahokas Foundation. I express my gratitude to Professor Juha Partanen, head of the division of genetics and director of the molecular and integrative biosciences research program for the use of the department facilities.

I would like to warmly thank my supervisor, Professor Iiris Hovatta, for giving me the chance to perform my PhD in her group and for guiding me during these five years. I am deeply grateful for all the knowledge I have learned under her supervision. I also thank Dr. Carsten Wotjak for accepting the invitation to act as Opponent for my doctoral defense, Professor Heikki Tanilla and Professor Sulev Koks for their great feedback on my thesis and Professor Juha Voipio who kindly accepted to be the third member of my thesis committee. I am highly grateful to Docent Sari Lauri and Professor Anna-Elina Lehesjoki for their help and support during my five years of doctoral work as members of my thesis committee. I would also like to thank Professor Juha Partanen for his valuable help on my project, great collaboration and for accepting to act as my Custos.

Thank you to all my colleagues and collaborators without whom this study would not have been possible: Emilie Rydgren, Dr. Ewa Sokolwska, Dr. Natalia Kulesskaya, Adrien Gigliotta, Suvi Saarnio, Professor Juha Partanen, Dr. Francesca Morello, Dr. Anna Kirjavainen, Dr. Vootele Voikar, Ester Orav, Sebnem Kesaf, Docent Sari Lauri, Frederike Winkel, Maria Llach Pou, Dr. Juzoh Umemori, Professor Eero Castren, Professor Victoria Risbrough, Dr. Tatiana Lipina and Dr. Evgueni Ivakine. Particular thoughts to Dr. Ewa Sokolowska and Dr. Ingrid Balcells for taking me under their wings and all the fun we had together, but also to the current and past members from the Hovatta group for their help and support: Lea Urpa, Juho Väänänen, Dr. Zuzanna Misiewicz, Suvi Saarnio, Dr. Natalia Kulesskaya, Dr. Ari Rouhiainen, Dr. Kalevi Trontti, Mikaela Laine, Sarah Steffens, Sarah Journée and Adrien Gigliotta.

This adventure would not have been possible without the support of my family and my precious friends from France. Moreover, my stay would not have been so pleasant without all the great people I had the

chance to meet during the five past years. Particular thanks to my lovely roommate, Eeva Hotta, for her kindness and all the good moments we shared. My last thoughts are for my little angel, Manina, who taught me so much through her extreme strength.

References

1. *© 2004 Allen Institute for Brain Science. Allen Mouse Brain Atlas. Available from http://mouse.brain-map.org/.*
2. *Jax laboratory available from https://www.jax.org/.*
3. *tissue expression database availbable from http://tissues.jensenlab.org/.*
4. Adhikari, A., M.A. Topiwala, and J.A. Gordon, *Synchronized activity between the ventral hippocampus and the medial prefrontal cortex during anxiety.* Neuron, 2010. **65**(2): p. 257-69.
5. Adhikari, A., M.A. Topiwala, and J.A. Gordon, *Single units in the medial prefrontal cortex with anxiety-related firing patterns are preferentially influenced by ventral hippocampal activity.* Neuron, 2011. **71**(5): p. 898-910.
6. Aggleton, J.P., H.S. Blindt, and J.N. Rawlins, *Effects of amygdaloid and amygdaloid-hippocampal lesions on object recognition and spatial working memory in rats.* Behav Neurosci, 1989. **103**(5): p. 962-74.
7. Ambrogi Lorenzini, C., C. Bucherelli, and A. Giachetti, *Passive and active avoidance behavior in the light-dark box test.* Physiol Behav, 1984. **32**(4): p. 687-9.
8. Arora, V., et al., *Increased Grik4 Gene Dosage Causes Imbalanced Circuit Output and Human Disease-Related Behaviors.* Cell Rep, 2018. **23**(13): p. 3827-3838.
9. Atucha, E., et al., *Recognition memory: Cellular evidence of a massive contribution of the LEC to familiarity and a lack of involvement of the hippocampal subfields CA1 and CA3.* Hippocampus, 2017. **27**(10): p. 1083-1092.
10. Balderas, I., et al., *The consolidation of object and context recognition memory involve different regions of the temporal lobe.* Learn Mem, 2008. **15**(9): p. 618-24.
11. Ballesteros-Yanez, I., et al., *Density and morphology of dendritic spines in mouse neocortex.* Neuroscience, 2006. **138**(2): p. 403-9.
12. Balmer, T.S., *Perineuronal Nets Enhance the Excitability of Fast-Spiking Neurons.* eNeuro, 2016. **3**(4).
13. Bandelow, B., S. Michaelis, and D. Wedekind, *Treatment of anxiety disorders.* Dialogues Clin Neurosci, 2017. **19**(2): p. 93-107.
14. Barker, G.R. and E.C. Warburton, *When is the hippocampus involved in recognition memory?* J Neurosci, 2011. **31**(29): p. 10721-31.
15. Beneyto, M., et al., *Abnormal glutamate receptor expression in the medial temporal lobe in schizophrenia and mood disorders.* Neuropsychopharmacology, 2007. **32**(9): p. 1888-902.
16. Benjamini, Y., et al., *Controlling the false discovery rate in behavior genetics research.* Behav Brain Res, 2001. **125**(1-2): p. 279-84.
17. Benjamini, Y. and Y. Hochberg, *Controlling the false discovery rate: a practical and powerful approach to multiple testing. .* J R Stat Soc Series B Stat Methodol 1995. **57**: p. 11.
18. Beurdeley, M., et al., *Otx2 binding to perineuronal nets persistently regulates plasticity in the mature visual cortex.* J Neurosci, 2012. **32**(27): p. 9429-37.
19. Blanchard, R.J. and D.C. Blanchard, *Attack and defense in rodents as ethoexperimental models for the study of emotion.* Prog Neuropsychopharmacol Biol Psychiatry, 1989. **13 Suppl**: p. S3-14.
20. Blechert, J., et al., *Fear conditioning in posttraumatic stress disorder: evidence for delayed extinction of autonomic, experiential, and behavioural responses.* Behav Res Ther, 2007. **45**(9): p. 2019-33.

21. Bloodgood, D.W., et al., *Fear extinction requires infralimbic cortex projections to the basolateral amygdala.* Transl Psychiatry, 2018. **8**(1): p. 60.
22. Borsini, F., J. Podhorna, and D. Marazziti, *Do animal models of anxiety predict anxiolytic-like effects of antidepressants?* Psychopharmacology (Berl), 2002. **163**(2): p. 121-41.
23. Bourne, J. and K.M. Harris, *Do thin spines learn to be mushroom spines that remember?* Curr Opin Neurobiol, 2007. **17**(3): p. 381-6.
24. Bravo-Rivera, C., et al., *Persistent active avoidance correlates with activity in prelimbic cortex and ventral striatum.* Front Behav Neurosci, 2015. **9**: p. 184.
25. Brown, M.W., E.C. Warburton, and J.P. Aggleton, *Recognition memory: material, processes, and substrates.* Hippocampus, 2010. **20**(11): p. 1228-44.
26. Busti, D., et al., *Different fear states engage distinct networks within the intercalated cell clusters of the amygdala.* J Neurosci, 2011. **31**(13): p. 5131-44.
27. Cai, H., et al., *Central amygdala PKC-delta(+) neurons mediate the influence of multiple anorexigenic signals.* Nat Neurosci, 2014. **17**(9): p. 1240-8.
28. Calhoon, G.G. and K.M. Tye, *Resolving the neural circuits of anxiety.* Nat Neurosci, 2015. **18**(10): p. 1394-404.
29. Canteras, N.S., *The medial hypothalamic defensive system: hodological organization and functional implications.* Pharmacol Biochem Behav, 2002. **71**(3): p. 481-91.
30. Catches, J.S., J. Xu, and A. Contractor, *Genetic ablation of the GluK4 kainate receptor subunit causes anxiolytic and antidepressant-like behavior in mice.* Behav Brain Res, 2012. **228**(2): p. 406-14.
31. Celio, M.R. and I. Blumcke, *Perineuronal nets--a specialized form of extracellular matrix in the adult nervous system.* Brain Res Brain Res Rev, 1994. **19**(1): p. 128-45.
32. Chechik, G., I. Meilijson, and E. Ruppin, *Synaptic pruning in development: a computational account.* Neural Comput, 1998. **10**(7): p. 1759-77.
33. Christianson, J.P., et al., *Safety signals mitigate the consequences of uncontrollable stress via a circuit involving the sensory insular cortex and bed nucleus of the stria terminalis.* Biol Psychiatry, 2011. **70**(5): p. 458-64.
34. Christoffel, D.J., S.A. Golden, and S.J. Russo, *Structural and synaptic plasticity in stress-related disorders.* Rev Neurosci, 2011. **22**(5): p. 535-49.
35. Chung, L., *A Brief Introduction to the Transduction of Neural Activity into Fos Signal.* Dev Reprod, 2015. **19**(2): p. 61-7.
36. Ciocchi, S., et al., *Encoding of conditioned fear in central amygdala inhibitory circuits.* Nature, 2010. **468**(7321): p. 277-82.
37. Contractor, A., C. Mulle, and G.T. Swanson, *Kainate receptors coming of age: milestones of two decades of research.* Trends Neurosci, 2011. **34**(3): p. 154-63.
38. Courtin, J., et al., *Prefrontal parvalbumin interneurons shape neuronal activity to drive fear expression.* Nature, 2014. **505**(7481): p. 92-6.
39. Crawley, J. and F.K. Goodwin, *Preliminary report of a simple animal behavior model for the anxiolytic effects of benzodiazepines.* Pharmacol Biochem Behav, 1980. **13**(2): p. 167-70.
40. Cunningham, M.G., S. Bhattacharyya, and F.M. Benes, *Amygdalo-cortical sprouting continues into early adulthood: implications for the development of normal and abnormal function during adolescence.* J Comp Neurol, 2002. **453**(2): p. 116-30.
41. Deacon, R.M., *Digging and marble burying in mice: simple methods for in vivo identification of biological impacts.* Nat Protoc, 2006. **1**(1): p. 122-4.
42. Delaney, A.J. and C.E. Jahr, *Kainate receptors differentially regulate release at two parallel fiber synapses.* Neuron, 2002. **36**(3): p. 475-82.

43. Divac, I., R. Wikmark, and A. Gade, *Spontaneous alternation in rats with lesions in the frontal lobe: An extension of the frontal lobe syndrome.* Physiol Psychol, 1975. **3**: p. 7.
44. Donato, F., et al., *Early- and late-born parvalbumin basket cell subpopulations exhibiting distinct regulation and roles in learning.* Neuron, 2015. **85**(4): p. 770-86.
45. Donato, F., S.B. Rompani, and P. Caroni, *Parvalbumin-expressing basket-cell network plasticity induced by experience regulates adult learning.* Nature, 2013. **504**(7479): p. 272-6.
46. Doron, N.N. and J.E. Ledoux, *Organization of projections to the lateral amygdala from auditory and visual areas of the thalamus in the rat.* J Comp Neurol, 1999. **412**(3): p. 383-409.
47. Dulawa, S.C. and R. Hen, *Recent advances in animal models of chronic antidepressant effects: the novelty-induced hypophagia test.* Neurosci Biobehav Rev, 2005. **29**(4-5): p. 771-83.
48. Duvarci, S. and D. Pare, *Amygdala microcircuits controlling learned fear.* Neuron, 2014. **82**(5): p. 966-80.
49. Eaton, W.W., O.J. Bienvenu, and B. Miloyan, *Specific phobias.* Lancet Psychiatry, 2018. **5**(8): p. 678-686.
50. Ehrlich, I., et al., *Amygdala inhibitory circuits and the control of fear memory.* Neuron, 2009. **62**(6): p. 757-71.
51. Elston, G.N. and J. DeFelipe, *Spine distribution in cortical pyramidal cells: a common organizational principle across species.* Prog Brain Res, 2002. **136**: p. 109-33.
52. Etkin, A. and T.D. Wager, *Functional neuroimaging of anxiety: a meta-analysis of emotional processing in PTSD, social anxiety disorder, and specific phobia.* Am J Psychiatry, 2007. **164**(10): p. 1476-88.
53. Fanselow, M.S., *Conditioned and unconditional components of post-shock freezing.* Pavlov J Biol Sci, 1980. **15**(4): p. 177-82.
54. Fanselow, M.S. and J.E. LeDoux, *Why we think plasticity underlying Pavlovian fear conditioning occurs in the basolateral amygdala.* Neuron, 1999. **23**(2): p. 229-32.
55. Fanselow, M.S. and A.M. Poulos, *The neuroscience of mammalian associative learning.* Annu Rev Psychol, 2005. **56**: p. 207-34.
56. Fanselow, M.S. and T.J. Tighe, *Contextual conditioning with massed versus distributed unconditional stimuli in the absence of explicit conditional stimuli.* J Exp Psychol Anim Behav Process, 1988. **14**(2): p. 187-99.
57. Favuzzi, E., et al., *Activity-Dependent Gating of Parvalbumin Interneuron Function by the Perineuronal Net Protein Brevican.* Neuron, 2017. **95**(3): p. 639-655 e10.
58. Felix-Ortiz, A.C., et al., *BLA to vHPC inputs modulate anxiety-related behaviors.* Neuron, 2013. **79**(4): p. 658-64.
59. File, S.E., et al., *Animal tests of anxiety.* Curr Protoc Neurosci, 2004. **Chapter 8**: p. Unit 8 3.
60. Fitzgerald, P.J., et al., *Durable fear memories require PSD-95.* Mol Psychiatry, 2015. **20**(7): p. 901-12.
61. Foa, E.B. and C.P. McLean, *The Efficacy of Exposure Therapy for Anxiety-Related Disorders and Its Underlying Mechanisms: The Case of OCD and PTSD.* Annu Rev Clin Psychol, 2016. **12**: p. 1-28.
62. Ghosh, S. and S. Chattarji, *Neuronal encoding of the switch from specific to generalized fear.* Nat Neurosci, 2015. **18**(1): p. 112-20.
63. Gogolla, N., et al., *Perineuronal nets protect fear memories from erasure.* Science, 2009. **325**(5945): p. 1258-61.
64. Goo, M.S., et al., *Activity-dependent trafficking of lysosomes in dendrites and dendritic spines.* J Cell Biol, 2017. **216**(8): p. 2499-2513.

65. Gratacos, M., et al., *Identification of new putative susceptibility genes for several psychiatric disorders by association analysis of regulatory and non-synonymous SNPs of 306 genes involved in neurotransmission and neurodevelopment.* Am J Med Genet B Neuropsychiatr Genet, 2009. **150B**(6): p. 808-16.
66. Gray, J. and N. McNaughton, *The Neuropsychology of Anxiety.* Oxford Psychology series, Oxford University Press Inc, New York, 2000.
67. Griebel, G. and A. Holmes, *50 years of hurdles and hope in anxiolytic drug discovery.* Nat Rev Drug Discov, 2013. **12**(9): p. 667-87.
68. Gross, C.T. and N.S. Canteras, *The many paths to fear.* Nat Rev Neurosci, 2012. **13**(9): p. 651-8.
69. Gunduz-Cinar, O., et al., *Identification of a novel gene regulating amygdala-mediated fear extinction.* Mol Psychiatry, 2018.
70. Hall, C. and E.L. Ballachey, *A study of the rat's behavior in a field. A contribution to method in comparative psychology.* Univ. Calif. Publ. Psychol. , 1932. **6**: p. 1-12.
71. Han, S., et al., *Elucidating an Affective Pain Circuit that Creates a Threat Memory.* Cell, 2015. **162**(2): p. 363-374.
72. Handley, S.L. and S. Mithani, *Effects of alpha-adrenoceptor agonists and antagonists in a maze-exploration model of 'fear'-motivated behaviour.* Naunyn Schmiedebergs Arch Pharmacol, 1984. **327**(1): p. 1-5.
73. Haubensak, W., et al., *Genetic dissection of an amygdala microcircuit that gates conditioned fear.* Nature, 2010. **468**(7321): p. 270-6.
74. Hebb, D.O., *The organization of Behavior.* New York: John Wiley and Sons, 1949.
75. Hensch, T.K., *Critical period plasticity in local cortical circuits.* Nat Rev Neurosci, 2005. **6**(11): p. 877-88.
76. Herry, C., et al., *Switching on and off fear by distinct neuronal circuits.* Nature, 2008. **454**(7204): p. 600-6.
77. Herry, C., et al., *Neuronal circuits of fear extinction.* Eur J Neurosci, 2010. **31**(4): p. 599-612.
78. Herry, C. and J.P. Johansen, *Encoding of fear learning and memory in distributed neuronal circuits.* Nat Neurosci, 2014. **17**(12): p. 1644-54.
79. Herry, C. and N. Mons, *Resistance to extinction is associated with impaired immediate early gene induction in medial prefrontal cortex and amygdala.* Eur J Neurosci, 2004. **20**(3): p. 781-90.
80. Hoffman, E.J. and S.J. Mathew, *Anxiety disorders: a comprehensive review of pharmacotherapies.* Mt Sinai J Med, 2008. **75**(3): p. 248-62.
81. Holtmaat, A., et al., *Experience-dependent and cell-type-specific spine growth in the neocortex.* Nature, 2006. **441**(7096): p. 979-83.
82. Holtzman-Assif, O., V. Laurent, and R.F. Westbrook, *Blockade of dopamine activity in the nucleus accumbens impairs learning extinction of conditioned fear.* Learn Mem, 2010. **17**(2): p. 71-5.
83. Hylin, M.J., et al., *Disruption of the perineuronal net in the hippocampus or medial prefrontal cortex impairs fear conditioning.* Learn Mem, 2013. **20**(5): p. 267-73.
84. Ivakine, E.A., et al., *Neto2 is a KCC2 interacting protein required for neuronal Cl- regulation in hippocampal neurons.* Proc Natl Acad Sci U S A, 2013. **110**(9): p. 3561-6.
85. Jarrell, T.W., et al., *Involvement of cortical and thalamic auditory regions in retention of differential bradycardiac conditioning to acoustic conditioned stimuli in rabbits.* Brain Res, 1987. **412**(2): p. 285-94.

86. Jaskolski, F., F. Coussen, and C. Mulle, *Subcellular localization and trafficking of kainate receptors.* Trends Pharmacol Sci, 2005. **26**(1): p. 20-6.
87. Jennings, J.H., et al., *Distinct extended amygdala circuits for divergent motivational states.* Nature, 2013. **496**(7444): p. 224-8.
88. Johansen, J.P., et al., *Molecular mechanisms of fear learning and memory.* Cell, 2011. **147**(3): p. 509-24.
89. Johansen, J.P., et al., *Optical activation of lateral amygdala pyramidal cells instructs associative fear learning.* Proc Natl Acad Sci U S A, 2010. **107**(28): p. 12692-7.
90. Jontes, J.D. and S.J. Smith, *Filopodia, spines, and the generation of synaptic diversity.* Neuron, 2000. **27**(1): p. 11-4.
91. Kalin, N.H., J.E. Sherman, and L.K. Takahashi, *Antagonism of endogenous CRH systems attenuates stress-induced freezing behavior in rats.* Brain Res, 1988. **457**(1): p. 130-5.
92. Kalinichenko, V.V., et al., *Haploinsufficiency of the mouse Forkhead Box f1 gene causes defects in gall bladder development.* J Biol Chem, 2002. **277**(14): p. 12369-74.
93. Kam, A.Y., et al., *Morphine induces AMPA receptor internalization in primary hippocampal neurons via calcineurin-dependent dephosphorylation of GluR1 subunits.* J Neurosci, 2010. **30**(45): p. 15304-16.
94. Karpova, N.N., et al., *Fear erasure in mice requires synergy between antidepressant drugs and extinction training.* Science, 2011. **334**(6063): p. 1731-4.
95. Kasai, H., et al., *Structure-stability-function relationships of dendritic spines.* Trends Neurosci, 2003. **26**(7): p. 360-8.
96. Kennedy, M.J. and M.D. Ehlers, *Organelles and trafficking machinery for postsynaptic plasticity.* Annu Rev Neurosci, 2006. **29**: p. 325-62.
97. Kheirbek, M.A., et al., *Differential control of learning and anxiety along the dorsoventral axis of the dentate gyrus.* Neuron, 2013. **77**(5): p. 955-68.
98. Kidd, F.L., et al., *A presynaptic kainate receptor is involved in regulating the dynamic properties of thalamocortical synapses during development.* Neuron, 2002. **34**(4): p. 635-46.
99. Kim, J.H., A.S. Hamlin, and R. Richardson, *Fear extinction across development: the involvement of the medial prefrontal cortex as assessed by temporary inactivation and immunohistochemistry.* J Neurosci, 2009. **29**(35): p. 10802-8.
100. Kim, J.H., G.P. McNally, and R. Richardson, *Recovery of fear memories in rats: role of gamma-amino butyric acid (GABA) in infantile amnesia.* Behav Neurosci, 2006. **120**(1): p. 40-8.
101. Kim, J.H. and R. Richardson, *A developmental dissociation of context and GABA effects on extinguished fear in rats.* Behav Neurosci, 2007. **121**(1): p. 131-9.
102. Kim, J.H. and R. Richardson, *The effect of temporary amygdala inactivation on extinction and reextinction of fear in the developing rat: unlearning as a potential mechanism for extinction early in development.* J Neurosci, 2008. **28**(6): p. 1282-90.
103. Kim, S.Y., et al., *Diverging neural pathways assemble a behavioural state from separable features in anxiety.* Nature, 2013. **496**(7444): p. 219-23.
104. Kirkby, R.J., et al., *Effects of hippocampal lesions and duration of sensory input on spontaneous alternation.* J Comp Physiol Psychol, 1967. **64**(2): p. 342-5.
105. Ko, S., et al., *Altered behavioral responses to noxious stimuli and fear in glutamate receptor 5 (GluR5)- or GluR6-deficient mice.* J Neurosci, 2005. **25**(4): p. 977-84.
106. Lahti, L., et al., *Differentiation and molecular heterogeneity of inhibitory and excitatory neurons associated with midbrain dopaminergic nuclei.* Development, 2016. **143**(3): p. 516-29.

107. Laine, M.A., et al., *Genetic Control of Myelin Plasticity after Chronic Psychosocial Stress.* eNeuro, 2018. **5**(4).
108. Lauri, S.E., et al., *A critical role of a facilitatory presynaptic kainate receptor in mossy fiber LTP.* Neuron, 2001. **32**(4): p. 697-709.
109. Lauri, S.E., et al., *Endogenous activation of kainate receptors regulates glutamate release and network activity in the developing hippocampus.* J Neurosci, 2005. **25**(18): p. 4473-84.
110. LeDoux, J., *Rethinking the emotional brain.* Neuron, 2012. **73**(4): p. 653-76.
111. LeDoux, J.E., *Brain mechanisms of emotion and emotional learning.* Curr Opin Neurobiol, 1992. **2**(2): p. 191-7.
112. LeDoux, J.E., *Emotion: clues from the brain.* Annu Rev Psychol, 1995. **46**: p. 209-35.
113. LeDoux, J.E., *Emotion circuits in the brain.* Annu Rev Neurosci, 2000. **23**: p. 155-84.
114. LeDoux, J.E., *Anxious.* Vikings, 2015.
115. LeDoux, J.E., et al., *Different projections of the central amygdaloid nucleus mediate autonomic and behavioral correlates of conditioned fear.* J Neurosci, 1988. **8**(7): p. 2517-29.
116. LeDoux, J.E. and D.S. Pine, *Using Neuroscience to Help Understand Fear and Anxiety: A Two-System Framework.* Am J Psychiatry, 2016. **173**(11): p. 1083-1093.
117. Lee, S., et al., *Inhibitory networks of the amygdala for emotional memory.* Front Neural Circuits, 2013. **7**: p. 129.
118. Likhtik, E., et al., *Amygdala intercalated neurons are required for expression of fear extinction.* Nature, 2008. **454**(7204): p. 642-5.
119. Likhtik, E., et al., *Prefrontal entrainment of amygdala activity signals safety in learned fear and innate anxiety.* Nat Neurosci, 2014. **17**(1): p. 106-13.
120. Lissek, S., et al., *Classical fear conditioning in the anxiety disorders: a meta-analysis.* Behav Res Ther, 2005. **43**(11): p. 1391-424.
121. Lissek, S. and B. van Meurs, *Learning models of PTSD: Theoretical accounts and psychobiological evidence.* Int J Psychophysiol, 2015. **98**(3 Pt 2): p. 594-605.
122. Maccarrone, G. and M.D. Filiou, *Protein profiling and phosphoprotein analysis by isoelectric focusing.* Methods Mol Biol, 2015. **1295**: p. 293-303.
123. Mahadevan, V., et al., *Neto2-null mice have impaired GABAergic inhibition and are susceptible to seizures.* Front Cell Neurosci, 2015. **9**: p. 368.
124. Marsicano, G., et al., *The endogenous cannabinoid system controls extinction of aversive memories.* Nature, 2002. **418**(6897): p. 530-4.
125. Mattheisen, M., et al., *Genome-wide association study in obsessive-compulsive disorder: results from the OCGAS.* Mol Psychiatry, 2015. **20**(3): p. 337-44.
126. McDonald, A.J., *Neurons of the lateral and basolateral amygdaloid nuclei: a Golgi study in the rat.* J Comp Neurol, 1982. **212**(3): p. 293-312.
127. McNamara, J.O., 2nd, et al., *Cell type-specific delivery of siRNAs with aptamer-siRNA chimeras.* Nat Biotechnol, 2006. **24**(8): p. 1005-15.
128. Medina, A.M., et al., *Startle reactivity and PTSD symptoms in a community sample of women.* Psychiatry Res, 2001. **101**(2): p. 157-69.
129. Merali, Z., C. Levac, and H. Anisman, *Validation of a simple, ethologically relevant paradigm for assessing anxiety in mice.* Biol Psychiatry, 2003. **54**(5): p. 552-65.
130. Mineka, S. and R. Zinbarg, *Conditioning and ethological models of anxiety disorders: stress-in-dynamic-context anxiety models.* Nebr Symp Motiv, 1996. **43**: p. 135-210.
131. Moses, S.N., et al., *Differential contributions of hippocampus, amygdala and perirhinal cortex to recognition of novel objects, contextual stimuli and stimulus relationships.* Brain Res Bull, 2005. **67**(1-2): p. 62-76.

132. Moses, S.N., R.J. Sutherland, and R.J. McDonald, *Differential involvement of amygdala and hippocampus in responding to novel objects and contexts.* Brain Res Bull, 2002. **58**(5): p. 517-27.
133. Motta, S.C., et al., *Dissecting the brain's fear system reveals the hypothalamus is critical for responding in subordinate conspecific intruders.* Proc Natl Acad Sci U S A, 2009. **106**(12): p. 4870-5.
134. Mouse Genome Sequencing, C., et al., *Initial sequencing and comparative analysis of the mouse genome.* Nature, 2002. **420**(6915): p. 520-62.
135. Mumby, D.G. and J.P. Pinel, *Rhinal cortex lesions and object recognition in rats.* Behav Neurosci, 1994. **108**(1): p. 11-8.
136. Myers, K.M. and M. Davis, *Mechanisms of fear extinction.* Mol Psychiatry, 2007. **12**(2): p. 120-50.
137. Nakamura, K., *Neural circuit for psychological stress-induced hyperthermia.* Temperature (Austin), 2015. **2**(3): p. 352-61.
138. Nestler, E.J. and S.E. Hyman, *Animal models of neuropsychiatric disorders.* Nat Neurosci, 2010. **13**(10): p. 1161-9.
139. Ng, D., et al., *Neto1 is a novel CUB-domain NMDA receptor-interacting protein required for synaptic plasticity and learning.* PLoS Biol, 2009. **7**(2): p. e41.
140. Njung'e, K. and S.L. Handley, *Evaluation of marble-burying behavior as a model of anxiety.* Pharmacol Biochem Behav, 1991. **38**(1): p. 63-7.
141. Orav, E., et al., *NETO1 Guides Development of Glutamatergic Connectivity in the Hippocampus by Regulating Axonal Kainate Receptors.* eNeuro, 2017. **4**(3).
142. Ornitz, E.M. and R.S. Pynoos, *Startle modulation in children with posttraumatic stress disorder.* Am J Psychiatry, 1989. **146**(7): p. 866-70.
143. Orr, S.P., et al., *De novo conditioning in trauma-exposed individuals with and without posttraumatic stress disorder.* J Abnorm Psychol, 2000. **109**(2): p. 290-8.
144. Orr, S.P., L.J. Metzger, and R.K. Pitman, *Psychophysiology of post-traumatic stress disorder.* Psychiatr Clin North Am, 2002. **25**(2): p. 271-93.
145. Ottersen, O.P. and Y. Ben-Ari, *Afferent connections to the amygdaloid complex of the rat and cat. I. Projections from the thalamus.* J Comp Neurol, 1979. **187**(2): p. 401-24.
146. Pape, H.C. and D. Pare, *Plastic synaptic networks of the amygdala for the acquisition, expression, and extinction of conditioned fear.* Physiol Rev, 2010. **90**(2): p. 419-63.
147. Paternain, A.V., et al., *GluR5 and GluR6 kainate receptor subunits coexist in hippocampal neurons and coassemble to form functional receptors.* J Neurosci, 2000. **20**(1): p. 196-205.
148. Pattwell, S.S., et al., *Selective early-acquired fear memories undergo temporary suppression during adolescence.* Proc Natl Acad Sci U S A, 2011. **108**(3): p. 1182-7.
149. Pattwell, S.S., et al., *Altered fear learning across development in both mouse and human.* Proc Natl Acad Sci U S A, 2012. **109**(40): p. 16318-23.
150. Pavlov, I., *Conditional Reflexes.* New York: Dover Publications, 1960.
151. Pellow, S., et al., *Validation of open:closed arm entries in an elevated plus-maze as a measure of anxiety in the rat.* J Neurosci Methods, 1985. **14**(3): p. 149-67.
152. Perugini, A., et al., *Synaptic plasticity from amygdala to perirhinal cortex: a possible mechanism for emotional enhancement of visual recognition memory?* Eur J Neurosci, 2012. **36**(4): p. 2421-7.
153. Phillips, R.G. and J.E. LeDoux, *Differential contribution of amygdala and hippocampus to cued and contextual fear conditioning.* Behav Neurosci, 1992. **106**(2): p. 274-85.

154. Pinheiro, P.S., et al., *GluR7 is an essential subunit of presynaptic kainate autoreceptors at hippocampal mossy fiber synapses.* Proc Natl Acad Sci U S A, 2007. **104**(29): p. 12181-6.
155. Pizzorusso, T., et al., *Reactivation of ocular dominance plasticity in the adult visual cortex.* Science, 2002. **298**(5596): p. 1248-51.
156. Qiu, S., et al., *GluA1 phosphorylation contributes to postsynaptic amplification of neuropathic pain in the insular cortex.* J Neurosci, 2014. **34**(40): p. 13505-15.
157. Ray, W.J., et al., *Startle response in generalized anxiety disorder.* Depress Anxiety, 2009. **26**(2): p. 147-54.
158. Reijmers, L.G., et al., *Localization of a stable neural correlate of associative memory.* Science, 2007. **317**(5842): p. 1230-3.
159. Rice, D.P. and L.S. Miller, *Health economics and cost implications of anxiety and other mental disorders in the United States.* Br J Psychiatry Suppl, 1998(34): p. 4-9.
160. Risold, P.Y. and L.W. Swanson, *Structural evidence for functional domains in the rat hippocampus.* Science, 1996. **272**(5267): p. 1484-6.
161. Risold, P.Y. and L.W. Swanson, *Connections of the rat lateral septal complex.* Brain Res Brain Res Rev, 1997. **24**(2-3): p. 115-95.
162. Rodriguez-Romaguera, J., F.H. Do Monte, and G.J. Quirk, *Deep brain stimulation of the ventral striatum enhances extinction of conditioned fear.* Proc Natl Acad Sci U S A, 2012. **109**(22): p. 8764-9.
163. Romanski, L.M. and J.E. LeDoux, *Equipotentiality of thalamo-amygdala and thalamo-cortico-amygdala circuits in auditory fear conditioning.* J Neurosci, 1992. **12**(11): p. 4501-9.
164. Romberg, C., et al., *Depletion of perineuronal nets enhances recognition memory and long-term depression in the perirhinal cortex.* J Neurosci, 2013. **33**(16): p. 7057-65.
165. Roozendaal, B., et al., *Noradrenergic activation of the basolateral amygdala modulates consolidation of object recognition memory.* Neurobiol Learn Mem, 2008. **90**(3): p. 576-9.
166. Roozendaal, B., B.S. McEwen, and S. Chattarji, *Stress, memory and the amygdala.* Nat Rev Neurosci, 2009. **10**(6): p. 423-33.
167. Ruediger, S., et al., *Learning-related feedforward inhibitory connectivity growth required for memory precision.* Nature, 2011. **473**(7348): p. 514-8.
168. Ruiz, A., et al., *Distinct subunits in heteromeric kainate receptors mediate ionotropic and metabotropic function at hippocampal mossy fiber synapses.* J Neurosci, 2005. **25**(50): p. 11710-8.
169. Saito, Y., et al., *Developing corticorubral axons of the cat form synapses on filopodial dendritic protrusions.* Neurosci Lett, 1992. **147**(1): p. 81-4.
170. Samson, R.D., S. Duvarci, and D. Pare, *Synaptic plasticity in the central nucleus of the amygdala.* Rev Neurosci, 2005. **16**(4): p. 287-302.
171. Sato, M., et al., *The lateral parabrachial nucleus is actively involved in the acquisition of fear memory in mice.* Mol Brain, 2015. **8**: p. 22.
172. Sejnowski, T.J., *The book of Hebb.* Neuron, 1999. **24**(4): p. 773-6.
173. Senn, V., et al., *Long-range connectivity defines behavioral specificity of amygdala neurons.* Neuron, 2014. **81**(2): p. 428-37.
174. Shaltiel, G., et al., *Evidence for the involvement of the kainate receptor subunit GluR6 (GRIK2) in mediating behavioral displays related to behavioral symptoms of mania.* Mol Psychiatry, 2008. **13**(9): p. 858-72.
175. Shepherd, J.K., et al., *Behavioural and pharmacological characterisation of the elevated "zero-maze" as an animal model of anxiety.* Psychopharmacology (Berl), 1994. **116**(1): p. 56-64.

176. Shi, C. and M. Davis, *Pain pathways involved in fear conditioning measured with fear-potentiated startle: lesion studies.* J Neurosci, 1999. **19**(1): p. 420-30.
177. Shin, L.M., S.L. Rauch, and R.K. Pitman, *Amygdala, medial prefrontal cortex, and hippocampal function in PTSD.* Ann N Y Acad Sci, 2006. **1071**: p. 67-79.
178. Silva, B.A., C.T. Gross, and J. Graff, *The neural circuits of innate fear: detection, integration, action, and memorization.* Learn Mem, 2016. **23**(10): p. 544-55.
179. Slaker, M., et al., *Removal of perineuronal nets in the medial prefrontal cortex impairs the acquisition and reconsolidation of a cocaine-induced conditioned place preference memory.* J Neurosci, 2015. **35**(10): p. 4190-202.
180. Sparta, D.R., et al., *Inhibition of projections from the basolateral amygdala to the entorhinal cortex disrupts the acquisition of contextual fear.* Front Behav Neurosci, 2014. **8**: p. 129.
181. Spruston, N., *Pyramidal neurons: dendritic structure and synaptic integration.* Nat Rev Neurosci, 2008. **9**(3): p. 206-21.
182. Straub, C., et al., *Distinct functions of kainate receptors in the brain are determined by the auxiliary subunit Neto1.* Nat Neurosci, 2011. **14**(7): p. 866-73.
183. Straub, C., et al., *Distinct Subunit Domains Govern Synaptic Stability and Specificity of the Kainate Receptor.* Cell Rep, 2016. **16**(2): p. 531-544.
184. Tang, M., et al., *Neto2 interacts with the scaffolding protein GRIP and regulates synaptic abundance of kainate receptors.* PLoS One, 2012. **7**(12): p. e51433.
185. Tang, M., et al., *Neto1 is an auxiliary subunit of native synaptic kainate receptors.* J Neurosci, 2011. **31**(27): p. 10009-18.
186. Taniguchi, H., *Genetic dissection of GABAergic neural circuits in mouse neocortex.* Front Cell Neurosci, 2014. **8**: p. 8.
187. Taylor, G.T., S. Lerch, and S. Chourbaji, *Marble burying as compulsive behaviors in male and female mice.* Acta Neurobiol Exp (Wars), 2017. **77**(3): p. 254-260.
188. Thibaut, F., *Anxiety disorders: a review of current literature.* Dialogues Clin Neurosci, 2017. **19**(2): p. 87-88.
189. Thomas, A., et al., *Marble burying reflects a repetitive and perseverative behavior more than novelty-induced anxiety.* Psychopharmacology (Berl), 2009. **204**(2): p. 361-73.
190. Tovote, P., et al., *Midbrain circuits for defensive behaviour.* Nature, 2016. **534**(7606): p. 206-12.
191. Tovote, P., J.P. Fadok, and A. Luthi, *Neuronal circuits for fear and anxiety.* Nat Rev Neurosci, 2015. **16**(6): p. 317-31.
192. Treit, D., J.P. Pinel, and H.C. Fibiger, *Conditioned defensive burying: a new paradigm for the study of anxiolytic agents.* Pharmacol Biochem Behav, 1981. **15**(4): p. 619-26.
193. Turner, B.H. and M. Herkenham, *Thalamoamygdaloid projections in the rat: a test of the amygdala's role in sensory processing.* J Comp Neurol, 1991. **313**(2): p. 295-325.
194. Tye, K.M., et al., *Amygdala circuitry mediating reversible and bidirectional control of anxiety.* Nature, 2011. **471**(7338): p. 358-62.
195. Ueno, H., et al., *Postnatal development of GABAergic interneurons and perineuronal nets in mouse temporal cortex subregions.* Int J Dev Neurosci, 2017. **63**: p. 27-37.
196. Umemori, J., et al., *Distinct effects of perinatal exposure to fluoxetine or methylmercury on parvalbumin and perineuronal nets, the markers of critical periods in brain development.* Int J Dev Neurosci, 2015. **44**: p. 55-64.
197. Umemori, J., et al., *iPlasticity: Induced juvenile-like plasticity in the adult brain as a mechanism of antidepressants.* Psychiatry Clin Neurosci, 2018. **72**(9): p. 633-653.

198. Wang, D. and J. Fawcett, *The perineuronal net and the control of CNS plasticity.* Cell Tissue Res, 2012. **349**(1): p. 147-60.
199. Wang, D.V., et al., *Neurons in the amygdala with response-selectivity for anxiety in two ethologically based tests.* PLoS One, 2011. **6**(4): p. e18739.
200. Warburton, E.C. and M.W. Brown, *Neural circuitry for rat recognition memory.* Behav Brain Res, 2015. **285**: p. 131-9.
201. Watanabe-Iida, I., et al., *Determination of kainate receptor subunit ratios in mouse brain using novel chimeric protein standards.* J Neurochem, 2016. **136**(2): p. 295-305.
202. Wehner, J.M. and R.A. Radcliffe, *Cued and contextual fear conditioning in mice.* Curr Protoc Neurosci, 2004. **Chapter 8**: p. Unit 8 5C.
203. Wilensky, A.E., et al., *Rethinking the fear circuit: the central nucleus of the amygdala is required for the acquisition, consolidation, and expression of Pavlovian fear conditioning.* J Neurosci, 2006. **26**(48): p. 12387-96.
204. Wisden, W. and P.H. Seeburg, *A complex mosaic of high-affinity kainate receptors in rat brain.* J Neurosci, 1993. **13**(8): p. 3582-98.
205. Wittchen, H.U., et al., *The size and burden of mental disorders and other disorders of the brain in Europe 2010.* Eur Neuropsychopharmacol, 2011. **21**(9): p. 655-79.
206. Vogel-Ciernia, A. and M.A. Wood, *Examining object location and object recognition memory in mice.* Curr Protoc Neurosci, 2014. **69**: p. 8 31 1-17.
207. Vogel, E., et al., *Projection-Specific Dynamic Regulation of Inhibition in Amygdala Micro-Circuits.* Neuron, 2016. **91**(3): p. 644-51.
208. Wolff, S.B., et al., *Amygdala interneuron subtypes control fear learning through disinhibition.* Nature, 2014. **509**(7501): p. 453-8.
209. Wondolowski, J. and M. Frerking, *Subunit-dependent postsynaptic expression of kainate receptors on hippocampal interneurons in area CA1.* J Neurosci, 2009. **29**(2): p. 563-74.
210. Vorhees, C.V. and M.T. Williams, *Assessing spatial learning and memory in rodents.* ILAR J, 2014. **55**(2): p. 310-32.
211. Wu, L.J., et al., *Increased anxiety-like behavior and enhanced synaptic efficacy in the amygdala of GluR5 knockout mice.* PLoS One, 2007. **2**(1): p. e167.
212. Wyeth, M.S., et al., *Neto auxiliary protein interactions regulate kainate and NMDA receptor subunit localization at mossy fiber-CA3 pyramidal cell synapses.* J Neurosci, 2014. **34**(2): p. 622-8.
213. Wyeth, M.S., et al., *Neto Auxiliary Subunits Regulate Interneuron Somatodendritic and Presynaptic Kainate Receptors to Control Network Inhibition.* Cell Rep, 2017. **20**(9): p. 2156-2168.
214. Xu, C., et al., *Distinct Hippocampal Pathways Mediate Dissociable Roles of Context in Memory Retrieval.* Cell, 2016. **167**(4): p. 961-972 e16.
215. Yamada, J., T. Ohgomori, and S. Jinno, *Perineuronal nets affect parvalbumin expression in GABAergic neurons of the mouse hippocampus.* Eur J Neurosci, 2015. **41**(3): p. 368-78.
216. Yu, K., et al., *The central amygdala controls learning in the lateral amygdala.* Nat Neurosci, 2017. **20**(12): p. 1680-1685.
217. Zhang, W., et al., *A transmembrane accessory subunit that modulates kainate-type glutamate receptors.* Neuron, 2009. **61**(3): p. 385-96.